Role of Platelet Tyrosine Kinases in Atherosclerosis

By

Tony J. Zheng

A DISSERTATION

Presented to the Department of Biomedical Engineering

Of the Oregon Health & Science University

School of Medicine

In partial fulfillment of the requirements for the degree of

Doctor of Philosophy

In Biomedical Engineering

May 2022

CERTIFCATE OF APPROVAL

This is to certify that the Ph.D. dissertation of

Tony J. Zheng

Role of Platelet Tyrosine Kinases in Atherosclerosis

Has been approved by

_____

Mentor: Owen J. T. McCarty, Ph.D.

_____

Mentor: Joseph E. Aslan Ph.D.

_____

Member: Summer L. Gibbs Ph.D.

_____

Member: Julia E. Maxson Ph.D.

_____

Member: Bill D. Rooney Ph.D.

_____

Member: Cristina Puy Garcia Ph.D.

Table of Contents

List of Figures

Chapter 1: Introduction to Platelet Biology and Anti-Platelet Agents

Chapter 2: General Methods and Materials

Chapter 3: Assessment of the effects of Syk and BTK inhibitors on GPVI-mediated platelet signaling and function

Chapter 4: Effects of antiplatelet agents and tyrosine kinase inhibitors on oxLDL-mediated platelet procoagulant activity

Chapter 5: Conclusions & Future Directions

List of Tables

List of Abbreviations

AA	arachidonic acid
ACD	acid citrate dextrose
ADP	adenosine diphosphate
AMP	adenosine monophosphate
Akt	protein kinase B
APC	activated protein C or allophycocyanin
ATP	adenosine triphosphate
AU	arbitrary unit
BSA	bovine serum albumin
BTK	Bruton's tyrosine kinase
BV	brilliant violet
CD	cluster of differentiation
CLEC-2	C-type lectin receptor-2
COX-1	cycooxygenase-1
CRP-XL	crosslinked collagen related peptide
CSK	C-terminus Src kinase
DAG	diacylglycerol
DIC	differential interference contrast
DMSO	dimethyl sulfoxide
ECM	extracellular matrix
ERK	extracellular signal-regulated kinase
FAK	focal adhesion kinase

FcRγ	Fc receptor γ
FITC	fluorescein
FSC	forward scatter
FVIII	factor VIII
FXIII	factor XIII
GDP	guanosine diphosphate
GP	glycoprotein
GPCR	G-protein coupled receptor
GPIb	glycoprotein Ib
GPIIb/IIIa	glycoprotein IIb/IIIa or integrin $\alpha_{IIb}\beta_3$
GPVI	glycoprotein VI
GTP	guanosine triphosphate
HBS	HEPES buffered saline
HDL	high density lipoprotein
IP	immunoprecipitation
IP_3	inositol trisphosphate
IRB	Internal Review Board
ITAM	immunoreceptor tyrosine-based activation motif
JAK	Janus kinase
JNK	c-Jun N-terminal kinase
kDa	kilodalton
LAT	linker for activation of T cells
LDL	low-density lipoprotein

MAPK	mitogen-activated protein kinase
MFI	mean fluorescence intensity
MW	molecular weight
NA	numerical aperture
NaCit	sodium citrate
NHP	non-human primate
NO	nitric oxide
oxLDL	oxidized low density lipoprotein
PAR	protease activated receptor
PBS	phosphate buffer saline
PDGF(R)	platelet derived growth factor (receptor)
PE	phycoerythrin
PFA	paraformaldehyde
PGI_2	prostaglandin I2 or prostacyclin
PI	phosphatidylinositol
PIP_2	phosphatidylinositol 4, 5-bisphosphate
PI3K	phosphoinositide 3-kinase
PKA	protein kinase A
PKB	protein kinase B
PKC	protein kinase C
PLA	phospholipase A
PLCβ	phospholipase C-β
PLCγ2	phospholipase C-γ2

PPP	platelet poor plasma
PRP	platelet rich plasma
PS	phosphatidylserine
RBC	red blood cell
RPM	rotations per minute
RT	room temperature
SEM	standard error of means
SFK	Src family kinases
SLP-76	lymphocyte cytosolic protein 2
STAT	signal transducers and activators of transcription
Syk	Spleen tyrosine kinase
TKI	tyrosine kinase inhibitor
TLR	toll-like receptor
TSP-1	thrombospondin-1
TSP-2	thrombospondin-2
TxA_2	thromboxane A_2
TxB_2	thromboxane B_2
VCAM-1	vascular cell adhesion molecule 1
VEGF(R)	vascular endothelial growth factor (receptor)
vWF	von Willebrand factor
WB	Western blot
WT	wild type

Acknowledgments

I would like to start by expressing my deepest thanks to my two mentors, Drs. Owen McCarty and Joseph Aslan. Thank you, Joe, for everything you taught me about platelets. I enjoy and cherish all our discussions about science, data, experimental design, writing, and working alongside you in the lab. Thank you, Owen, for guiding me and pushing me in the lab, in the gym, on the trail, and in life.

Thank you to my dissertation advisory committee (DAC): Drs. Julia Maxson, Summer Gibbs, Bill Rooney, Cristina Puy, Owen McCarty, and Joe Aslan for all the great and insightful feedback on my projects during every DAC meeting and keeping me on track with my progress.

One of Owen's many phrases was "standing on the shoulders of giants." I would like to thank all the current and past lab members who I worked with and who came before me that provided the foundation for all this work and research to be possible and to be built upon. To my lab mates, thank you, Anh, Stephanie, Novella, and Hari, for teaching me, for all your help, discussions, and expertise, and paving the road for me to follow. Thank you, Ivan, for all your experimental help, scientific discussions, and conversations about basketball. Thank you, JP, for all the Western blots and technical support. Thank you, Cristina for all the science talks. Thank you, Tia for sharing these same steps of grad school, helping each other, and showing me how to tour. Thank you, Shatzel, for your clinical knowledge and expertise and feedback. Thank you, Paul, for all your help with

the mice studies. Thank you to the Oregon primate center, Paul, Melissa, and others for all your help with the NHP studies. Thank you, Nhu and Helen, for your assistance with experiments. Thank you, Liz, for letting me be a mentor and jumpstarting my project with all your experimental help. Lastly, thank you to Alex Melrose for teaching me all the assays when I joined the lab and becoming a great friend, gym partner, and housemate.

Thank you to the MD/PhD program, to Dr. Jacoby, Alexis Young, and to all my fellow classmates especially my cohort Caroline, Gavin, Jackie, and Burcu for continuously supporting each other.

Thank you to the BME administration for all your help and support. Thank you to Catherine Hogan for all your help with my grant applications. Thank you to Angelyn Kimball for all your help with finances and budget.

Thank you to Jackie Wirz, Amy Garcia, Min Lee Booth, Monica Hinds, Allison Fryer, David Jacoby, Owen McCarty, and Peter Georges for being there for me in a time where I needed it the most.

Thank you to all my friends that I have made along the way, in college, medical school, graduate schools, and in life. You all bring balance and joy outside of work, much love.

Most importantly, none of this would be possible without the love and support from my family. I am beyond grateful to my parents for all the *sacrifices* they made in *their lives* in order to raise me and place me in the environments for opportunities and growth.

Abstract

Role of Platelet Tyrosine Kinases in Atherosclerosis

Tony J. Zheng

Department of Biomedical Engineering

School of Medicine

Oregon Health & Science University

May 2022

Dissertation Advisors: Drs. Owen J. T. McCarty, Ph.D. & Joseph E. Aslan, Ph.D.

Atherosclerosis is the leading cause of cardiovascular disease, accounting for nearly 30% of deaths in the United States. Patients with late-stage atherosclerosis suffer from life-threatening complications, such as myocardial infarctions, ischemic strokes, aneurysms, and multi-organ failure. Many current treatment options, including anti-platelet and anti-coagulant therapies, although moderately effective at alleviating or preventing thrombotic events of atherosclerosis, carry a risk for bleeding and hemorrhagic complications. Thus, there remains a need to further understand the molecular basis of hemostasis and thrombosis in order develop safer and more effective therapies.

To this end, one recent therapeutic group of interest is tyrosine kinase inhibitors (TKIs). TKIs have traditionally been used with great success in treating hematological

malignancies and inflammatory conditions. Due to the central role of tyrosine kinases also seen in platelet activation, TKIs have recently been studied as potential anti-platelet agents, demonstrating effects against atherosclerotic plaque-triggered thrombus formation. However, the mechanism by which tyrosine kinases are activated in platelets and effects of tyrosine kinase inhibitors on platelet functional responses are ill-defined. Thus, the goal of this thesis is to investigate mechanisms in which tyrosine kinase inhibitors reduce thrombotic events, while maintaining hemostasis processes in atherosclerosis, to guide therapeutic interventions for future patients.

In particular, spleen tyrosine kinase (Syk) and Bruton's tyrosine kinase (BTK) play critical roles in platelet physiology, facilitating ITAM-mediated signaling downstream of platelet glycoprotein VI (GPVI) and GPIIb/IIIa receptors. In this thesis, we first investigate the effects of 12 different Syk and BTK inhibitors on GPVI-mediated platelet signaling and function. We demonstrate that TKIs targeting Syk or BTK inhibit central platelet functional responses but may differentially affect protein activities and organization in critical systems downstream of Syk and BTK in platelets. As these TKIs targeting Syk, BTK and other kinases are further developed and implemented for an increasing number of inflammatory, oncogenic and other conditions, studies such as our work herein will help to address a growing need to better understand the effects of such compounds on essential molecular machinery around Syk-BTK signaling in platelets and other physiologically relevant cell types.

At the site of atherogenesis and atherosclerotic lesions, oxidized low density lipoprotein (oxLDL) contributes to disease progression through interactions with peripheral blood cells, especially platelets. However, mechanisms by which oxLDL affect platelet activation and atherothrombosis, and how to best therapeutically target and safely prevent such responses remains unclear. Here, we next investigate how oxLDL upregulates GPVI mediated platelet hemostatic and procoagulant responses, and how traditional antiplatelet therapies and tyrosine kinase inhibitors affect such oxLDL-enhanced platelet activity *ex vivo*. In this chapter, we demonstrate that oxLDL enhances platelet functional responses and procoagulant activity downstream of GPVI signaling. Therapeutically, we demonstrate that P2Y antagonists such as ticagrelor and tyrosine kinase inhibitors targeting BTK and Syk such as ibrutinib and fostamatinib, respectively, reduce such oxLDL-enhanced platelet responses, but COX inhibitors like aspirin do not. In future studies, we will test murine and nonhuman primate models to extend our study of tyrosine kinase inhibitors on oxLDL-platelet interactions to *in vivo* models.

Overall, the studies presented in this dissertation help characterize the role of tyrosine kinases in platelet activation and platelet functional responses and provide insight on the potential use and development of tyrosine kinase inhibitors as safer antiplatelet agents in the setting of atherosclerosis.

Chapter 1: Introduction to Platelet Biology and Tyrosine Kinase Inhibitors

1.1 Overview

Atherosclerosis is the leading cause of cardiovascular disease, accounting for over 600,000 deaths and over $300 billion in health care cost in the United States every year. Terminal complications of atherosclerosis, including myocardial infarctions, ischemic strokes, and multi-organ failure, result from late-stage endothelial dysfunction, vessel rupture, and thrombosis. In this process, platelets play a pivotal role in hemostatic plug formation to repair the ruptured vessel and reduce bleeding. However, the same process leads to thrombus formation, subsequent stenosis, and terminal complications. Therefore, there is a pressing need to understand the (patho)mechanism of hemostasis and thrombosis in atherosclerosis, which could help guide therapeutic interventions for future patients.

In hemostasis and thrombosis, tyrosine kinases are known to regulate platelet activity. During atherosclerotic plaque rupture, newly exposed extracellular membrane (ECM) proteins including collagen bind to platelets to initiate hemostatic plug formation. In this process, tyrosine kinases play a pivotal role in facilitating platelet activation to further

thrombus formation. Due to the role of platelet tyrosine kinases in hemostasis and thrombosis, characterizing the mechanisms of select tyrosine kinases is of particular interest for developing therapeutics to treat thrombotic complications without causing bleeding. In this dissertation, we will explore the role of platelet tyrosine kinases in atherosclerosis by evaluating tyrosine kinase inhibitors as tools for mechanistic studies and their potential as antiplatelet agents to reduce thrombosis, while minimally affecting hemostatic processes. Overall, we will assess tyrosine kinases as potential targets for safe and effective treatment in atherosclerosis.

In this chapter, we will first introduce atherosclerosis, the role of platelets in hemostasis and thrombosis, and extracellular matrix (ECM) proteins that bind to initiate platelet activation, namely von Willebrand factor (vWF), collagen, fibrinogen, and fibrin, as well as other adhesive proteins such as fibronectin, laminin, nidogen, thrombospondin, and vitronectin that support platelet activation. Next, we will introduce the main signaling pathways that transduce the signals from ECM protein binding, such as GPVI/ITAM-mediated pathways, integrin receptor signaling, and PAR signaling. Lastly, we will introduce prominent tyrosine kinases that mediate these signaling pathways, most notably Bruton's tyrosine kinase (BTK) and Spleen tyrosine kinase (Syk). We will overview the current landscape of tyrosine kinase inhibitors (TKIs) targeting BTK and Syk and their effects on platelet functional responses and procoagulant activity.

1.2 Atherosclerosis

Atherosclerosis is a chronic inflammatory disease characterized by early-stage formation of fatty streaks, lesions, and plaques in the intima layer of arteries followed by progressive inflammation and lipid accumulation, resulting in late-stage plaque rupture, thrombosis and terminal complications (1, 2) (**Figure 1.1**). In early-stage atherosclerosis, the oxidation of low-density lipoprotein (LDL) drives the initial formation of fatty streaks, leading to the recruitment of monocytes, differentiation into macrophages, and formation of foam cells underlying the arterial endothelium (1, 2). In late-stage atherosclerosis, the progressive plaque expansion can lead to narrowing of the vessel lumen, resulting in ischemia, plaque rupture, and thrombosis (1, 2).

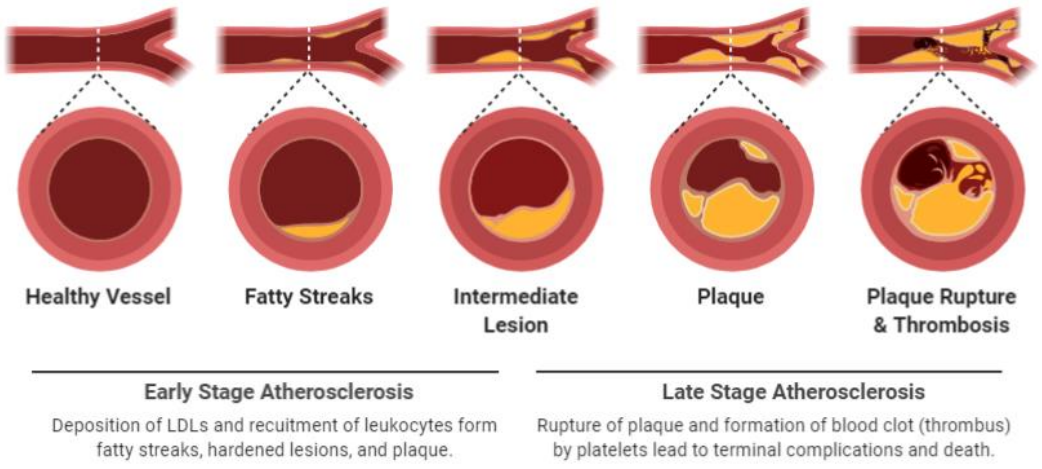

Figure 1.1. Progression of Atherosclerosis. Atherosclerosis is a chronic inflammatory disease. In early-stage atherosclerosis, the deposition and oxidation of low-density lipoprotein (LDL) and recruitment of leukocytes lead to the formation of fatty streaks, harden lesions, and plaques in the arterial endothelium. In late-stage atherosclerosis, the rupture of plaque and formation of a thrombus by platelets can lead to terminal complications and death. Figure created with BioRender.com by Tony J. Zheng.

1.3 Platelets in Hemostasis and Thrombosis

Platelets are discoid, anucleate fragments derived from the cytoplasm of bone marrow megakaryocytes and are the smallest circulating element in the bloodstream, roughly 1 – 3 microns in diameter (3, 4). The lifespan of a single platelet is 7-10 days and 150,000 – 450,000 platelets circulate in every microliter of blood before being cleared by the spleen. The primary function of platelets is to survey and respond to vascular damage by repairing the vascular leak in a process called hemostasis. Hemostasis is achieved through the combination of platelet adhesion and activation and the coagulation cascade to generate a hemostatic plug or thrombus that seals the vascular leak. The end product thrombus is an aggregate consisting primarily of red blood cells, activated platelets, and fibrin. On the other hand, thrombosis is a pathological response that occurs when the thrombus growth becomes excessive and uncontrollable and obstructs the normal blood flow of the intact blood vessel, leading to myocardial infarctions and ischemic events.

Thus, platelets play a pivotal role in hemostasis and thrombosis. Specifically, platelets initiate the formation of a thrombus through 1) platelet adhesion, 2) platelet activation, and 3) platelet aggregation. In the following sections, we will describe in detail the extracellular matrix (ECM) proteins that support platelet adhesion, the main signaling pathways that transduce the signals from ECM protein binding and lead to platelet activation, and the platelet functional responses that drive platelet aggregation.

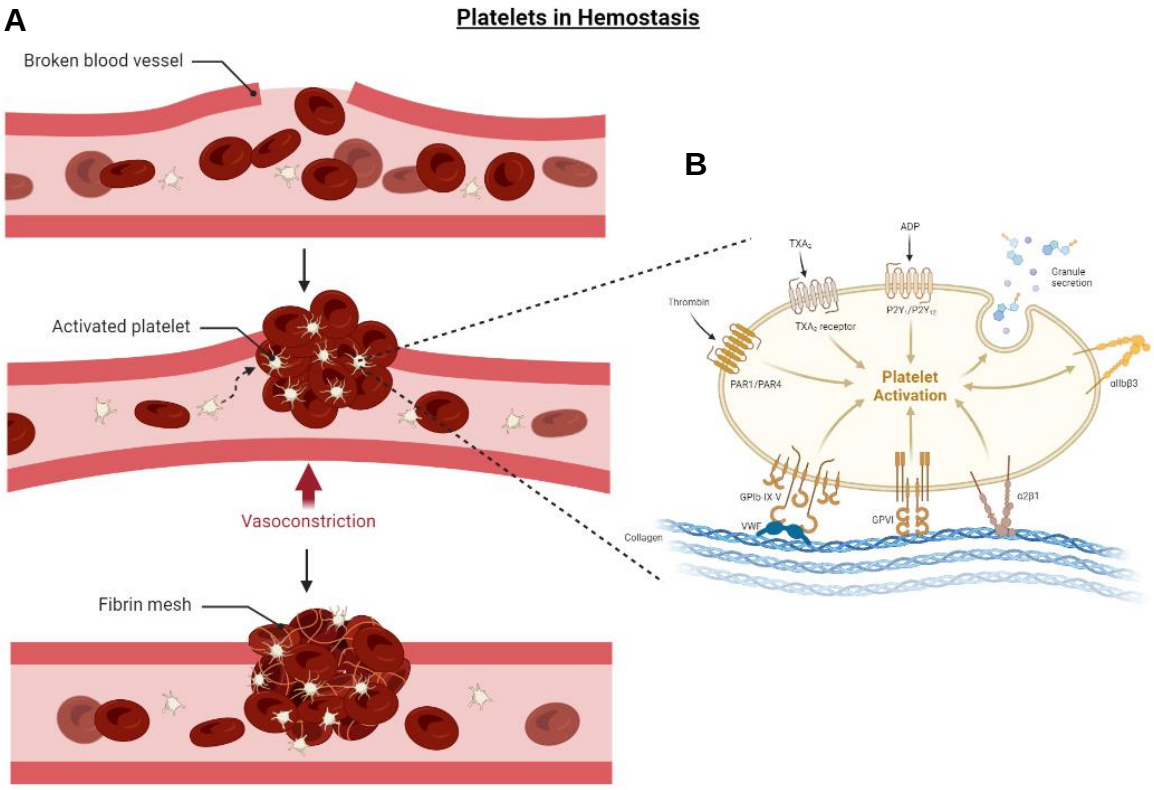

Figure 1.2. Platelets in Hemostasis. A) The primary function of platelets is to survey and respond to vascular damage by repairing the vascular leak in a process called hemostasis. Hemostasis is achieved through the combination of platelet adhesion and activation and the coagulation cascade to generate a hemostatic plug or thrombus that seals the vascular leak. The end product thrombus is an aggregate consisting primarily of red blood cells, activated platelets, and fibrin mesh. **B)** Platelets are activated via a number of ligands such as collagen binding to GPVI and integrin receptors, thrombin on PAR1/4 receptors, TXA_2 on TXA_2 receptors, and ADP on P2Y receptors, activating platelets and secreting granules. Figure created with BioRender.com.

1.4 Extracellular Matrix Proteins

Platelet adhesion to exposed extracellular matrix (ECM) proteins at the site of vascular injury is a critical initial step in hemostasis and thrombosis, as well as in inflammatory and immunopathological responses. In particular, these ECM proteins include collagen and fibrinogen in limited amounts, as well as other adhesive proteins such as von Willebrand factor (vWF), fibronectin, laminin and nidogen that are synthesized by vascular wall cells and are activated or immobilized onto the ECM upon vascular injury. These ECM and adhesive proteins will be described in the following subsections.

1.4.1. von Willebrand Factor

Platelets are initially recruited to a site of vascular injury and damage mediated by von Willebrand factor (vWF). vWF is a multimeric glycoprotein present in ECM, in Weibel-Palade bodies of endothelial cells, in platelet alpha granules, and in circulation as a complex with Factor VIII (FVIII) (5). vWF is produced by megakaryocytes as a propeptide of 2813 amino acids and each mature vWF monomer domain is 2050 amino acids after secretion. Each vWF domain provides structural support and unique functions. The D'-D3 domain binds to FVIII, the A1 domain binds to platelets via glycoprotein Ib (GPIb) receptor and collagen type IV, the A2 domain is the cleaving site for the plasma metalloprotease "a disintegrin and metalloprotease with thrombospondin type motifs 13" known as ADAMST13 which inactivates vWF, the A3 domain binds to collagen types I and III, and the C2 domain binds to platelet integrin receptors (6). The structure and domains of vWF is shown in **Figure 1.3**.

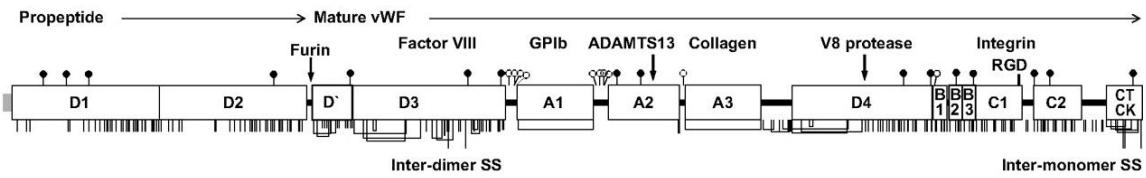

Figure 1.3. Von Willebrand factor (vWF) structure and domains. vWF (2813 amino acids) consist of a propeptide and a mature vWF (2050 amino acids). The D'-D3 domain binds to FVIII, the A1 domain binds to platelets via glycoprotein Ib (GPIb) receptor and collagen type IV, the A2 domain is the cleaving site for ADAMST13, the A3 domain binds to collagen types I and III, and the C2 domain binds to platelet integrin receptors. Figure adapted from Zhou et al., *Blood* 2012: 788:91-100. Reprinted with permission.

In particular, platelets bind and adhere to vWF by tethering of glycoprotein Ib (GPIb) receptor as part of the platelet membrane GPIb-IX-V complex at the A1 domain of immobilized vWF but not to soluble vWF. In addition, subendothelial vWF in the ECM supports platelet adhesion by associating with collage type VI (7-9). It is important to note that hemostasis remains preserved in the absence of endogenous endothelial vWF if plasma vWF is present. Under static flow conditions, vWF is irregularly coiled. However, under flow conditions, vWF extends and exposes its binding domains. The cleaving of vWF by ADAMST13 releases vWF into the plasma, ranging from 40 to 200 monomers in length and is a crucial mechanism in preventing microvascular thrombi formation (10, 11).

Deficiency or defects in vWF results in von Willebrand disease (VWD), the most common hereditary bleeding disorder affecting up to 1% of the population in the United States. Type 1 and 2 VWD are inherited as autosomal dominant traits, while type 3 VWD is inherited as autosomal recessive. Patients with VWD typically presents with varying degrees of bleeding tendency, from nosebleeds, easy bruising, bleeding gums, and

heavier menstrual periods to severe internal bleeding and bleeding into joints. On the other hand, a deficiency in the platelet GPIb-V-IX complex results in Bernard-Soulier Syndrome. Bernard-Soulier Syndrome is an autosomal recessive disorder and is characterized by abnormally large platelets.

1.4.2. Collagen

Collagen is a triple helical protein and the most abundant structural protein in the extracellular matrix (ECM) (12). A single collagen molecule, tropocollagen, is roughly 300 nm long and 1.5 nm in diameter, Fibrillar collagen type I, III, and V are found in the deep layers of the ECM (13). Fibrillar collagen type IV, VIII, and XVIII are found in the basement membrane closer to the endothelial layer (13). At the site of vascular injury and following tethering and rolling on vWF at the A1 domain (collagen type IV) or A3 domain (collagen type I and III), platelets bind to the exposed collagen via glycoprotein VI (GPVI) receptor (13). In addition to GPVI, integrin $\alpha_2\beta_1$ also supports platelet-collagen interactions to reinforce collagen binding and enhance GPVI signaling. Cross-linked collagen related peptide (CRP-XL) is a synthetic specific GPVI agonist commonly used for platelet functional tests and will be used in the studies discussed in the following chapters.

1.4.3. Fibrinogen and Fibrin

Fibrinogen is a soluble glycoprotein complex, composed of two trimers, with each trimer made up of three different polypeptide chains (α chain, β chain, and γ chain) joined at the N-terminus by five disulfide bonds (14-17). Fibrinogen circulates in the blood stream at a

concentration of 1500-400 mg/dl. During vascular injury, fibrinogen binds to platelets GpIIb/IIIa surface membrane receptor to support platelet to platelet binding and platelet aggregation. Platelet spreading on a fibrinogen surface is shown in **Figure 1.4** over the time course In addition, fibrinogen is cleaved into fibrin by thrombin at the N-terminus of the α and β chains to form a fibrin-based blood clot in coagulation.

Fibrin is a fibrous, non-globular protein formed from the cleavage of fibrinogen by thrombin in coagulation. The polymerization and crosslinking of fibrin by FXIII hardens and contracts the fibrin-platelet plug, playing a key step in clot formation at the site of vascular injury. Deficiency or dysfunctional fibrin or premature lysis of fibrin is often linked with defects in its precursor fibrinogen and presents with bleeding disorders or hemorrhages in patients. Excessive generation of fibrin due to over activation of the coagulation cascade or platelets lead to thrombosis.

Deficiency in and/or dysfunctional plasma fibrinogen results in a number of congenital or acquired diseases, including congenital afibrinogenemia, congenital hypofibrinogenemia, fibrinogen storage disease, congenital dysfibrinogenemia, acquired dysfibrinogenemia, congenital hypodysfibrinogenmia, and cryofibrinogenemia. Patients with fibrinogen disorders typically present with pathological episodes of bleeding and/or blood clotting and/or abnormal deposition of fibrinogen in the kidneys, liver, and other tissues.

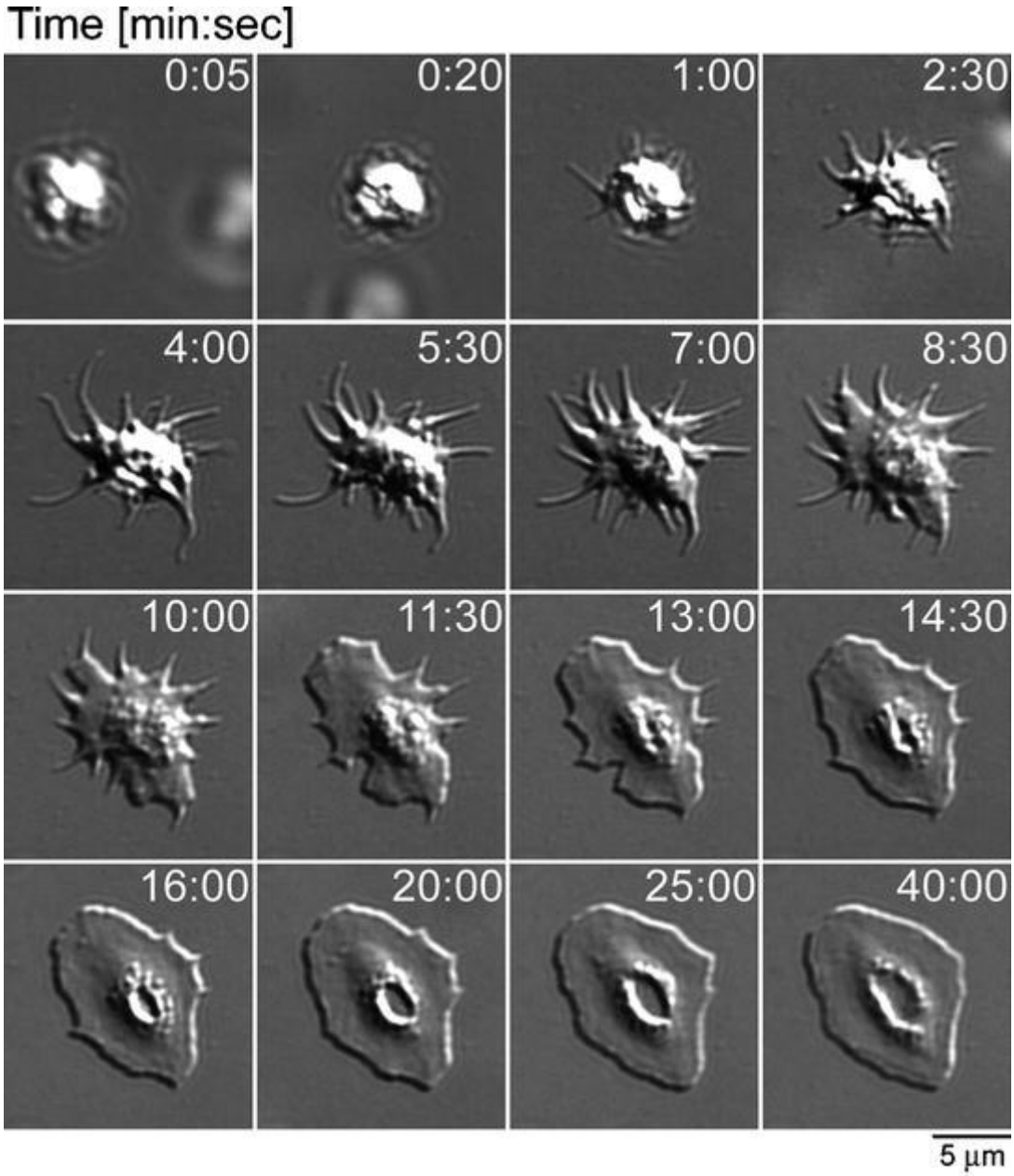

Figure 1.4. Platelets spreading on fibrinogen in real-time. Imaging of platelets over a time course of 40 minutes. When platelets come into initial contact with immobilized fibrinogen, the platelet rounds and generates short filopodial protrusions before generating sheet-like lamellipodia before fully spreading. Scale bar is 5 µm. Figure adapted from Aslan et al., *Methods in Molecular Biology: Platelets and Megakaryocytes* 2012: 788:91-100. Reprinted with permission.

1.4.4. Fibronectin, Laminin, Nidogen, and other adhesive proteins

Laminin is a heterotrimeric glycoprotein composed of an α chain, β chain, and γ chain. It is approximately 400-900 kDa and functions as structural support in the basal lamina of the basement membrane. Currently, 15 laminin trimers have been discovered as different combinations of the three chains. In particular, laminin associates with collagen type IV and bind to platelet integrin receptors and was the first non-collagenous protein found to bind and stimulate platelet GPVI receptor.

Nidogen is a sulfated monomeric glycoprotein composed of three globular domains that binds to collagen, perlecan, and laminin in the basal lamina of the basement membrane to provide structural support for the extracellular matrix. Two types of nidogens, nidogen-1 and nidogen-2, have been identified, with nidogen-1 demonstrating capabilities to activate platelets and support platelet adhesion (18).

Other adhesive proteins that have been identified as ligands for platelet receptors include fibronectin, thrombospondin, and vitronectin. Fibronectin is a glycoprotein dimer linked by a pair of disulfide bonds, approximately 500-600 kDa, that bind to platelet integrins αIIbβ3 and α5β1 receptors, existing as soluble fibronectin in the plasma or insoluble fibronectin in the ECM (19). Similarly, vitronectin is a 54 kDa glycoprotein found in plasma, the ECM, and platelets. Vitronectin has also been shown to bind to integrin $\alpha_V\beta_3$ and plays a role in clot formation and thrombi stabilization (20, 21). Thrombospondins are a family of secreted glycoproteins. Thrombospondin-1 (TSP-1) is a glycoprotein

found in platelet α granules and secreted upon platelet activation by thrombin. In turn, TSP-1 binds to platelets and mediates platelet adhesion. TSP-1 is found at higher levels in atherosclerotic plaques, however its role in thrombus formation remains unclear. In contrast, thrombospondin-2 (TSP-2) is not found in platelets but rather in the ECM. Deficiency in TSP-2 has been associated with hemostatic defects in mice (22).

1.5 Platelet Receptors and Signaling Pathways

Extracellular matrix and adhesive proteins bind to platelets via specific platelet surface receptors that activate platelets through a cascade of signaling events that drive platelet activation. Platelets exhibit a host of surface receptors

1.5.1. GPVI/ITAM-Mediated Signaling

On platelets, glycoprotein VI (GPVI) is a 62 kDa, ITAM-containing membrane protein that serves as the main physiological signaling receptor for extracellular matrix proteins including collagen, laminin, and nidogen. GPVI belongs to the Ig receptor superfamily, with two extracellular Ig domains D1 and D2, a mucin-rich stalk that contains a site for O-glycosylation, a transmembrane helix domain of a 19 amino acids, and 51 amino acid cytoplasmic tail. GPVI is coupled to a disulfide-linked Fc receptor γ-chain (FcRγ) close to the extracellular domain, which contains the ITAM signaling motif (18, 23-29). The GPVI structure is shown in **Figure 1.6.** At the site of vascular injury, the exposed subendothelial matrix proteins as well as polymerized fibrin bind to and activate GPVI by Src family kinases (SFKs), namely Lyn and Fyn (30-35). Phosphorylated ITAMs on GPVI-associated FcRγ then serve as a platform to recruit and activate Spleen tyrosine

kinase (Syk) (36). Syk phosphorylates a number of substrates associated with the linker for activation of T cells (LAT) at the LAT signalosome, including Bruton's tyrosine kinase (BTK), Tec family kinases, phosphoinositide 3-kinase (PI3K), and phospholipase C γ2 (PLCγ2) (36-38). This protein complex promotes protein kinase C (PKC) activation, intracellular mobilization of Ca^{2+}, granule secretion, "inside-out" integrin activation, and platelet hemostatic and thrombotic responses (36, 38). The GPVI/ITAM-mediated signaling pathway is shown in **Figure 1.7.** Phosphoproteomic studies and causal analyses identify over 3000 significant phosphorylation events and over 300 signaling relations in platelet GPVI-mediated responses (39, 40).

Platelets from GPVI knockout mice exhibits normal adhesion onto collagen, however activation-dependent platelet spreading and platelet aggregation is inhibited (41). It is hypothesized that adhesion is maintained through integrin receptors and vWF, however, GPVI remains crucial for platelet activation. Defects in the GPVI receptor in humans are rare and are associated with a mild bleeding disorder presentation in patients (42).

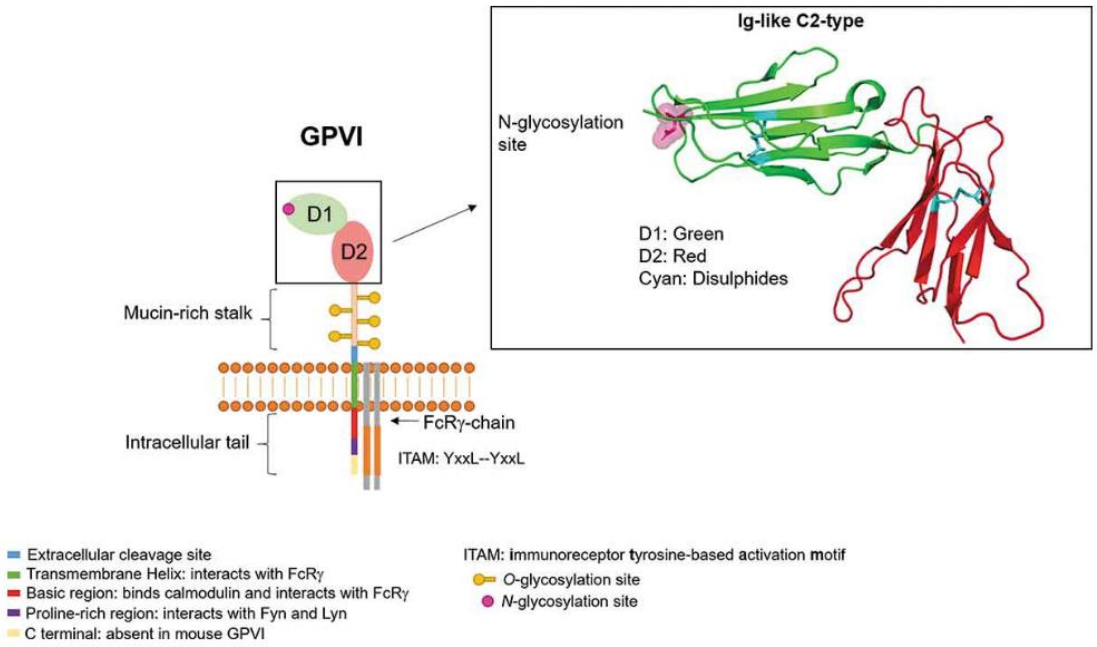

Figure 1.5. Glycoprotein VI (GVPI) structure. GPVI contains two extracellular Ig domains D1 and D2, a mucin-rich stalk that contains a site for O-glycosylation, a transmembrane helix domain, and a cytoplasmic tail. GPVI is coupled to a disulfide linked FcRγ close to the extracellular domain, which contains the ITAM signaling motif. Figure adapted from Clark et al., *Platelets* 2021; 32:6:724-732. Reprinted with permission.

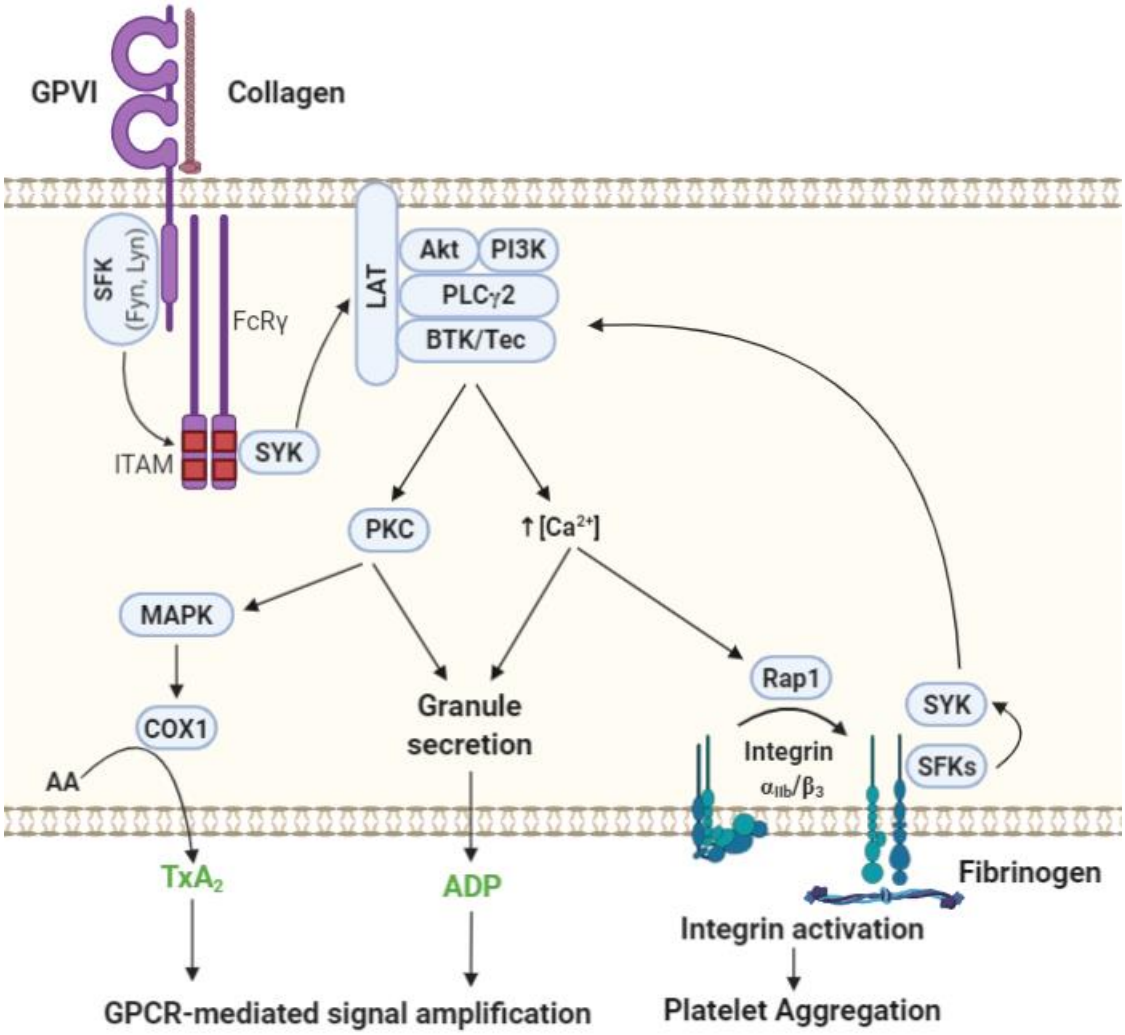

Figure 1.6. Platelet GPVI/ITAM and integrin signaling. Glycoprotein VI (GPVI) serves as the main physiological signaling receptor for extracellular matrix proteins including collagen, laminin, and nidogen. GPVI is coupled to a disulfide-linked Fc receptor γ-chain (FcRγ). Activated GPVI becomes phosphorylated by Src family kinases (SFK), namely Lyn and Fyn, on intracellular immunoreceptor tyrosine-based activation motifs (ITAMs). Phosphorylated ITAMs then serve as a platform to recruit and activate Spleen tyrosine kinase (Syk). Syk phosphorylates a number of substrates associated with the linker for activation of T cells (LAT) at the LAT signalosome, including Bruton's tyrosine kinase (BTK), Tec family kinases, phosphoinositide 3-kinase (PI3K), and phospholipase C γ2 (PLCγ2). This protein complex promotes protein kinase C (PKC) activation, intracellular mobilization of Ca^{2+}, granule secretion, "inside-out" integrin $\alpha_{IIb}\beta_3$ activation, and platelet hemostatic and thrombotic responses. Activated integrin $\alpha_{IIb}\beta_3$ binds to fibrinogen, triggering "outside-in" activation of platelets via the LAT signalosome**.** Figure created in BioRender.com by Tony J. Zheng.

1.5.2. Integrin Receptor Signaling

Integrins consist of noncovalently-bound α and β subunits that regulate and respond to the binding of soluble, cell-surface, and extracellular matrix ligands. Platelets express a repertoire of major and minor integrins, ranging from the highly expressed megakaryocyte- and platelet-specific integrin $\alpha_{IIb}\beta_3$ (also known as GPIIb/IIIa) to less abundant family members including $\alpha_v\beta_3$ (vitronectin receptor), $\alpha_2\beta_1$ (collagen receptor) (43), $\alpha_5\beta_1$ (fibronectin receptor) (19), and $\alpha_6\beta_1$ (laminin receptor) (28).

Despite platelets possessing a wide array of integrins, platelet biology is largely dominated by the activation and activity of the integrin $\alpha_{IIb}\beta_3$ due to the >10-fold excess in copy number of this integrin relative to the other minor integrins on the cell surface. Integrin $\alpha_{IIb}\beta_3$ proteins are ubiquitous transmembrane α/β heterodimers that reside on the resting platelet surface in a low affinity, closed conformational state (44-46). When platelets are activated, "inside-out" signaling triggers integrin $\alpha_{IIb}\beta_3$ to undergo a conformation change unfolding into a high affinity, opened state. "Inside-out" signaling can be initiated by various soluble platelet agonists, such as epinephrine, ADP, and thromboxane A2 (TxA2) or by immobilized agonists, such as collagen and von Willebrand factor (vWF), from other platelet receptors, such as GPVI and G-protein coupled receptors (GPCRs) (47-49). These pathways activate PLC, generating diacylglycerol (DAG) and inositol trisphosphate (IP_3) activation, triggering calcium release. In turn, DAG and calcium activates PKC, Rap1 and subsequently integrins, including GPIIb/IIIa. Once activated, integrin $\alpha_{IIb}\beta_3$ binds adhesive proteins including

fibrinogen and vWF and induces integrin clustering and subsequently promotes "outside-in" signaling that initiates cellular events to drive platelet spreading, aggregation, clot retraction, and thrombus consolidation (44-47). Clustering of $\alpha_{IIb}\beta_3$ leads to activation of Src through autophosphorylation and recruitment of Syk mediated by the SH2 domain and interdomain A region of the β_3 tail (50, 51). "Outside-in" activation of integrin $\alpha_{IIb}\beta_3$ has also been shown to induce Fcγ-RIIa phosphorylation and downstream tyrosine phosphorylation of PLCγ2 (52, 53). The structure, confirmation change and clustering of integrin $\alpha_{IIb}\beta_3$ is shown in **Figure 1.7**. Integrin "inside-out" signaling is shown in **Figure 1.8** and "outside-in" signaling pathway in platelets is shown in **Figure 1.9**.

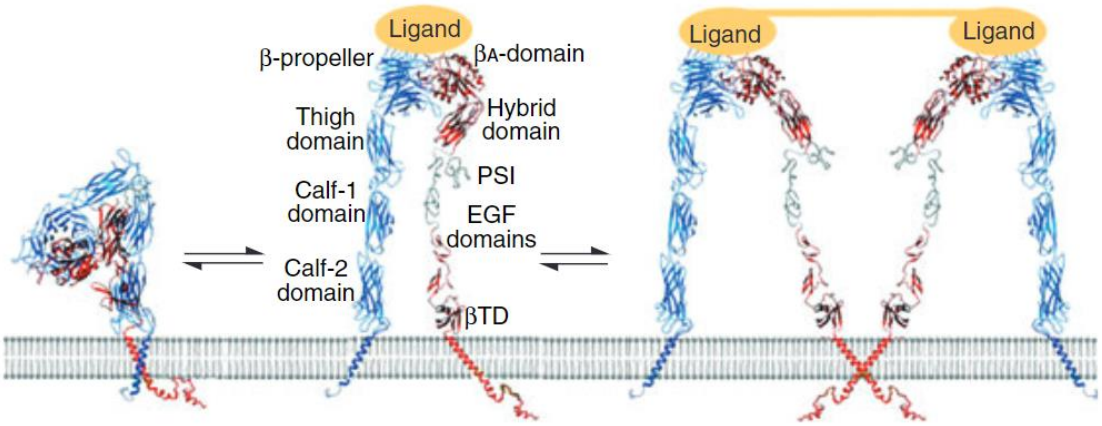

Figure 1.7. Integrin $\alpha_{IIb}\beta_3$ (GPIIb/IIIa) receptor structure, conformational shape change, and clustering. The inactivated form is shown on the left. Binding of ligand to the receptor activates and extends the molecule into an active state (middle) and clustering with other integrin receptors (right). Figure adapted from Ma et al., *Journal of Thrombosis and Hemostasis* 2007: 5:1345-1352. Reprinted with permission.

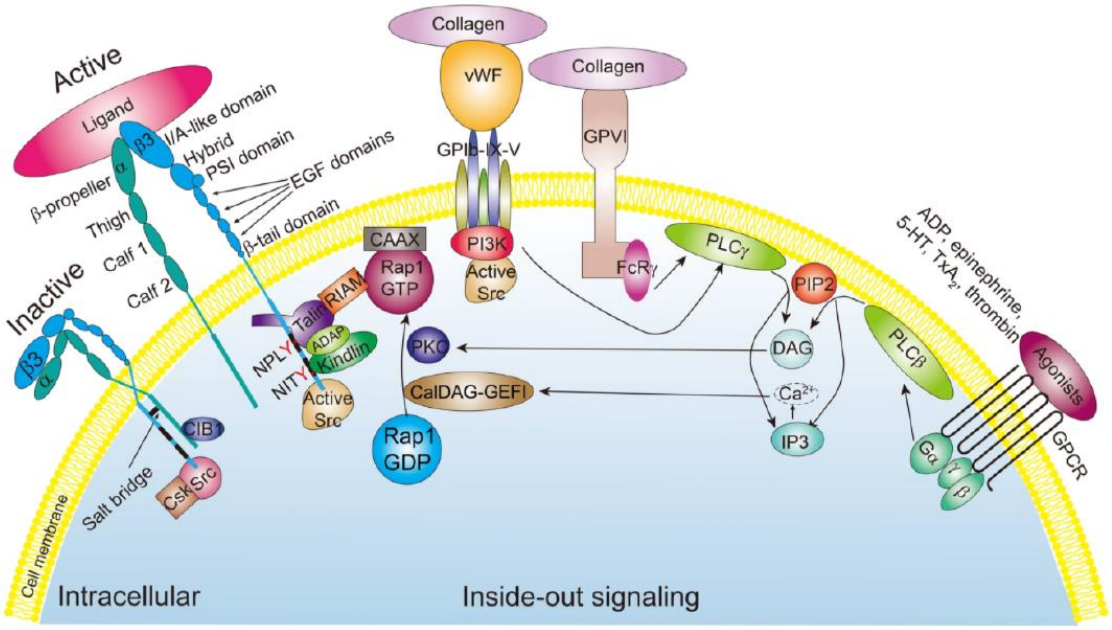

Figure 1.8. Integrin $\alpha_{IIb}\beta_3$ (GPIIb/IIIa) "inside-out" signaling. "Inside-out" signaling can be initiated by various soluble platelet agonists, such as epinephrine, ADP, and TxA2 or by immobilized agonists, such as collagen and vWF, from other platelet receptors, such as GPVI and GPCRs. These pathways activate PLC, generating DAG and IP_3 triggering to calcium release. DAG and calcium activate PKC, which allows activation of Rap1, Rap1 complexes, and subsequently integrin activation. Figure adapted from Huang et al., *Journal of Hematology & Oncology* 2019;12, 26. Reprinted with permission.

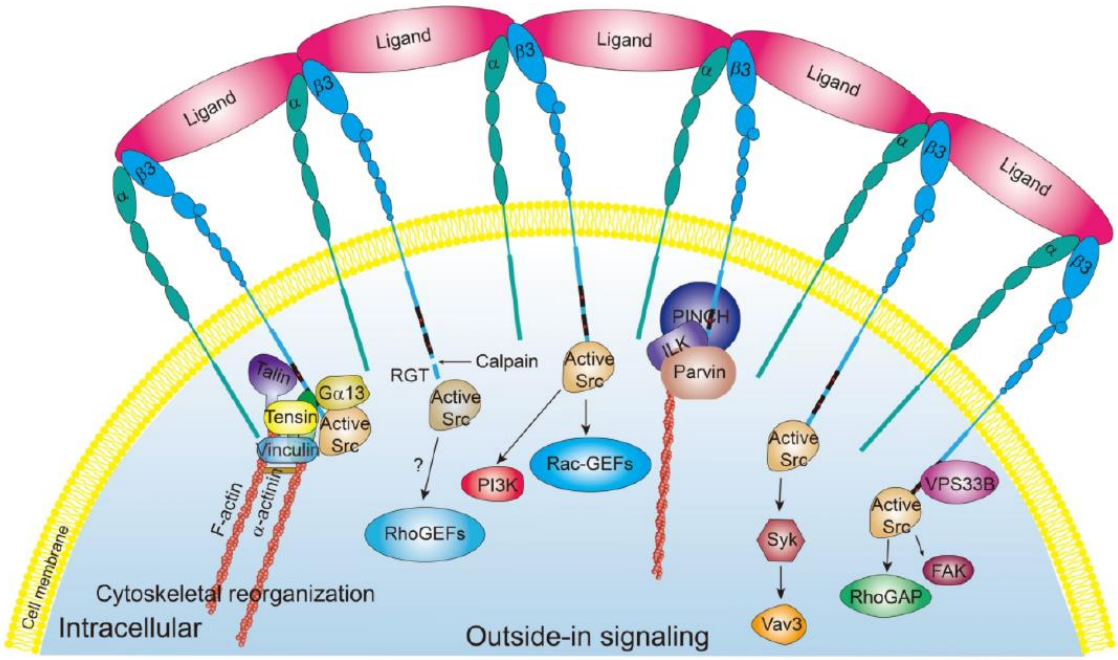

Figure 1.9. Integrin $\alpha_{IIb}\beta_3$ (GPIIb/IIIa) "outside-in" signaling. Activation and clustering of $\alpha_{IIb}\beta_3$ leads to activation of Src through autophosphorylation and recruitment of Syk mediated by the SH2 domain and interdomain A region of the β_3 tail and supports the activation of multiple signaling proteins including FAK, Syk, RhoGAPs and GEFs and PI3K. Talin, kindlin, tensin and vinculin drives cytoskeletal reorganization. Figure adapted from Huang et al., *Journal of Hematology & Oncology* 2019; 12, 26. Reprinted with permission.

1.5.3. GPCR Signaling

G-protein coupled receptors (GPCRs) are seven-transmembrane domain serpentine proteins, with an extracellular N-terminus and an intracellular C-terminus that convey signals through heterotrimeric G proteins (54, 55). GPCRs bind to soluble factors released during platelet activation such as ADP, thromboxane A2 (TxA2), and thrombin (generated during coagulation) that furthers platelet activation (56, 57). Ligands interact with the GPCRs with a high affinity and each occupied receptor has the ability to activate multiple downstream G proteins for amplification of the initial signal that will lead to rapid platelet activation (54). Platelets express a number of different GPCRs on their surface such as the purinergic ADP receptors P2Y1 and P2Y12, as well as the thrombin interactive GPCRs protease activated receptor 1 (PAR1) and 4 (PAR4) (54, 58, 59). Uniquely, PARs are activated by N-terminal proteolytic cleavage by thrombin that results in the generation of a tethered ligand important for irreversible receptor activation (55, 60-62).

GPCR signaling is initiated by the activation of the intracellular Gα-subunit, in which a guanine is exchanged from GDP to GTP, resulting in a dissociation of the Gβγ-dimer subunits and subsequent downstream activation signal propagation (60). This includes platelet PARs signaling through RhoA via ERK1/2 kinases activation that is crucial for platelet shape change (63). The main downstream target of the $G\alpha_q$ subunit is PLCβ enzymes that hydrolyze the membrane PIP_2 into IP_3 and DAG, which leads to PKC activation and MAPK pathways that results in increasing calcium levels and granule secretion (64). Tyrosine phosphorylation events are also necessary for GPCR-mediated

platelet signaling transduction and granule secretion. PAR signaling results in tyrosine phosphorylation of the PKC isoform PKCδ as well as certain SFK members. However, PAR-induced phosphorylation is a lower extent compared to GPVI/ITAM signaling (65). The tyrosine kinase FER, downstream of Syk, was found to be phosphorylated at the Y714 region in platelets stimulated with either thrombin or a PAR4-activating peptide, suggesting a role in signaling downstream from the G protein-coupled PAR4 (66).

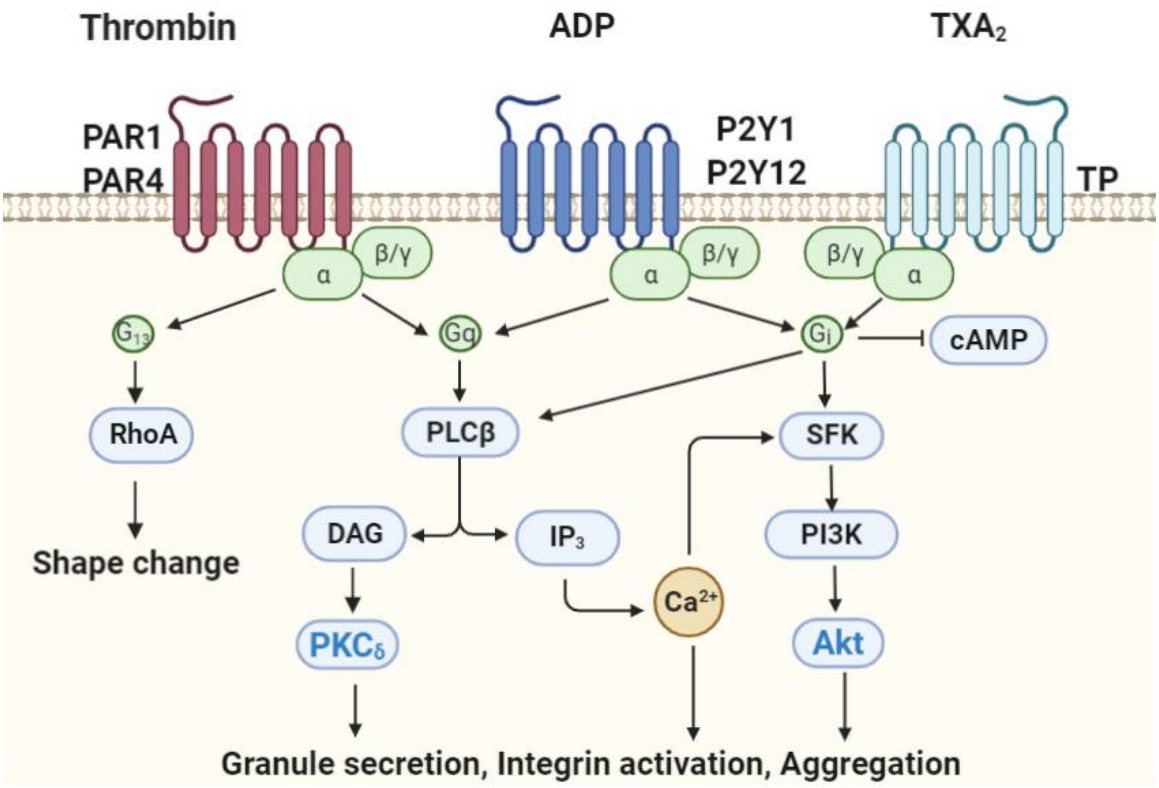

Figure 1.10. Platelet GPCR signaling. G protein-coupled receptors (GPCR) are activated by soluble agents such as thrombin, adenosine diphosphate (ADP) and thromboxane A_2 (TxA_2). Downstream GPCR signaling initiates the recruitment of the G protein complex leading to the activation of different types of Gα proteins; $G\alpha_{13}$, $G\alpha_q$ and $G\alpha_i$. Protease activated receptor (PAR) 1 and 4 stimulated by thrombin will lead to platelet shape change via RhoA, platelet granule secretion and integrin activation via PLCß and increased intracellular Ca^{2+} concentrations. Figure created in BioRender.com by Dr. Stephanie E. Reitsma.

1.6 Tyrosine Kinases & Tyrosine Kinase Inhibitors

1.6.1 Bruton's Tyrosine Kinase

Bruton's tyrosine kinase (BTK), a Tec family kinase, is a non-receptor tyrosine kinase consisting of an amino terminal pleckstrin homology (PH) domain, a proline-rich TEC homology (TH) domain, SRC homology (SH) domains SH2 and SH3, and a kinase domain with enzymatic activity. BTK was originally found to be defective in inherited immunodeficiency disease X-linked agammaglobulinemia (XLA), playing a critical role in B-cell signaling, differentiation, and survival. In platelets, BTK plays a central role in signaling downstream of GPVI as well as the hemITAM receptor CLEC-2.

1.6.2. BTK Inhibitors

Inhibitors targeting BTK have been developed to treat hematological malignancies and autoimmune diseases and were clinically observed to exhibit antiplatelet effects in patients (67-69). The following BTK inhibitors discussed are summarized in **Table 1.1**. Ibrutinib (PCI-32765) is a first-generation, orally available, small molecule BTK inhibitor (68, 70) used as a first-line treatment of relapsed chronic lymphocytic leukemia (CLL) and Waldenstrom's macroglobulinemia and second-line treatment of mantle cell lymphoma, graft vs. host disease, and other B-cell malignancies (68, 71, 72). Ibrutinib selectively binds to the Cys-481 residue of BTK, irreversibly blocks BTK enzymatic activity, and inhibits BTK phosphorylation (68, 70). While efficacious, the use of ibrutinib comes with a risk of bleeding and atrial fibrillation (73-75). Although mild,

there is an unmet clinical need to improve the hemostatic safety profile of next-generation BTK inhibitors.

1.6.3. Spleen Tyrosine Kinase

Spleen tyrosine kinase (Syk) is a 72kDa non-receptor tyrosine kinase that contains two SRC homology 2 (SH2) domains and a carboxyl-terminal tyrosine kinase domain (76). The two SH2 domains are linked by interdomain A and the SH2 domains and kinase domain is linked by interdomain B (76). Syk is ubiquitously expressed in hematopoietic cells and plays a central role in cell signaling (76, 77). In platelets, Syk plays a well-established role in the GPVI signaling cascade. Specifically, phosphorylated ITAMs on GPVI-associated FcRγ serve as a platform to recruit Syk, in which the two SH2 domains bind to two phosphorylated tyrosine residues on the receptor complex, facilitated by Src family kinase phosphorylation. Activated Syk directly binds to members of the Vav and PLCγ families (78), the p85α subunit of PI3K, and SH2 domain-containing leukocyte protein 76 (SLP76) and SLP65 (76), and then phosphorylates a number of downstream substrates including BTK, Tec, PLCγ2, and PI3K at the LAT signalosome (**Figure 1**). Inhibitors targeting Syk have been developed to treat hematological malignancies such as B-cell lymphomas, and allergic, inflammatory, and autoimmune diseases (76, 77, 79-81) and have recently been shown to have antiplatelet effects (82-85). The following Syk inhibitors discussed are summarized in **Table 1.2**.

1.6.4. Syk Inhibitors

Fostamatinib (prodrug of R406) was the first clinically available oral Syk inhibitor developed and approved for the treatment of chronic immune thrombocytopenia (ITP). Fostamatinib is also being trialed for rheumatoid arthritis and recurrent B-cell non-Hodgkin lymphoma (B-NHL) (86-88). In platelets, R406 abrogated shape change and aggregation and reduced the tyrosine phosphorylation of Syk, SLP-76, LAT, BTK, Akt, PKC, and PLCγ2 induced by GPVI activation (84). In addition, R406 also effectively reduced platelet adhesion on collagen under both static and flow conditions, granule secretion, and "inside-out" integrin activation . However, R406 is non-specific for Syk, and targets 25 kinases with a $K_d < 15$ nM and an 50 additional kinases with a $K_d < 100$ nM (89). To limit adverse side effects and off-target kinase activities, entospletinib (GS-9973) was developed as an oral, selective inhibitor of Syk and is currently in phase 2 trials for treatment of relapsed or refractory chronic lymphocytic leukemia (CLL) and other hematological malignancies (89-93). Entospletinib is Syk selective, with a $K_d = 7.6$ nM and affects only one other kinase with a $K_d < 100$ nM (89). When combined with BTK inhibitor tirabrutinib, entospletinib induced a significant decrease in platelet response to collagen *in vitro* and *ex vivo* compared to each agent alone (94). Using microfluidics to study platelet interactions with ECM proteins under a shear rate of 200 s^{-1}, entospletinib pretreated platelets inhibited deposition on collagen surfaces. In addition, when entospletinib was introduced 90 s after clot initiation, further platelet deposition and clot propagation was inhibited (95). Entospletinib pre-treated platelets also reduced the volume of platelet aggregate formation under flow (48). Perfusion of the Syk inhibitor PRT-060318 across a preformed thrombus enhanced thrombus breakdown and platelet

detachment, while ibrutinib only caused a minor decrease in thrombus contractile score (96).

Other second- and third- generation Syk inhibitors currently in clinical trials include cevidoplenib (SKI-O-703), lanraplenib (GS-9876), MK-8457, and BI1002494; minimal bleeding side effects have thus far been reported (97). Lanraplenib (GS-9876) inhibited GPVI-induced phosphorylation of LAT and PLCγ2, platelet aggregation in human whole blood, platelet binding to collagen under arterial flow conditions, and GPVI-stimulated platelet aggregation *ex vivo* of GS-9876 treated monkeys without an increase in bleeding time (98). However, the effect of the rest of these second- and third-generation Syk inhibitors on GPVI-mediated platelet functional responses and signaling events still remains undefined. Lastly, it has been shown that glycosylation of anti-SARS-CoV-2 spike IgG immune complexes increases platelet thrombus formation on vWF in COVID-19 and that inhibition of Syk and BTK reverses the enhancement of such thrombus formation (99). It is speculated there may be added benefit to using Syk and BTK inhibitors to reduce thrombotic events in COVID-19 that can be used alongside anticoagulants and immunosuppressants to further reduce thrombosis and inflammation (39, 99, 100). Overall, Syk inhibitors show promise in preventing specific signaling events along the GPVI pathway and reducing platelet thrombotic responses without affecting or compromising hemostasis.

1.6.5. Src Family Kinases

Src family kinases (SFK) are non-receptor tyrosine kinases present in nearly all cells that function to regulate cellular activation and signaling in response to external stimuli (101, 102). The nine SFKs include Src, Lck, Hck, Fyn, Blk, Fgr, Yes, and Yrk (101). All SFKs share a conserved domain structure, consisting of consecutive SH3, SH2, and tyrosine kinase (SH1) domains, followed by a SH4 region with a unique section of 50-70 residues that differentiates the different family kinases (101, 102). In platelets, SFKs, namely Lyn and Fyn, play a key role in the initial phosphorylation of ITAM upon GPVI activation (103).

1.6.6. SFK Inhibitors

The SFK inhibitor pyrozolopyrimidine (PP2) abrogated phosphorylation of LAT Tyr 191, p-Akt, Syk Tyr 525/526, Syk Tyr 352, and PLCγ2 Tyr 759 (104-106). In addition, PP2 inhibited Ca^{2+} mobilization (107) and reduced dense granule secretion, alpha granule secretion, alpha granule secretion, and aggregation in response to collagen stimulation (105). PP2 inhibited platelet shape change and aggregate formation when stimulated with CRP-XL and collagen fibrils (106). Following the success of imatinib, dasatinib was developed as an imatinib-resistant BCR-ABL inhibitor that also targets SFKs for patients with CML and acute lymphoblastic leukemia (ALL) (108, 109). In platelets, dasatinib abolished shape change, inhibited alpha granule secretion, ATP secretion, and aggregation, and reduced tyrosine phosphorylation in a dose-dependent manner in response to collagen stimulation (110). In addition, dasatinib inhibited phosphatidic acid production by PLCγ2 and the production of D3-phosphoinositides by PI3K in response to

collagen (110). Platelets collected from patients with CML receiving dasatinib treatment demonstrated reduced thrombi formation on collagen matrix surfaces under arterial shear rate conditions in comparison to platelets from untreated patients (110, 111). In support of this, another group also demonstrated that dasatinib inhibited platelet deposition under shear on collagen and subsequent deposition when dasatinib was introduced 90 s after clot initiation (95). Dasatinib also reduced convulxin-induced phosphatidylserine exposure and attenuated thrombin generation in a dose-dependent manner (112). Go6976, a PKC isoform inhibitor, reduced platelet aggregation upon convulxin, CRP-XL, or collagen stimulation (all activators of GPVI) and reduced intracellular calcium release upon convulxin stimulation, but had limited effect on platelet aggregation or intracellular calcium upon PAR4 and P2Y12 stimulation (104). Platelets activated with convulxin in the presence of Go6976 elicited a concentration-dependent inhibition of LAT Tyr 191 and Syk Tyr 525/526 phosphorylation, while Syk Tyr 352 phosphorylation was unaffected (104).

1.6.7. JAK/STAT Pathway

Janus activated kinases (JAKs) and signal transducers and activators of transcription (STAT) proteins control pleiotropic pathways that transduce signaling events in response to more than 50 cytokines and growth factors (113, 114). The JAK family of tyrosine kinases is comprised of four different members, namely JAK1, JAK2, JAK3, and TYK2. JAKs are proteins with a molecular mass of 120-140 kDa composed of a FERM amino terminus domain, a SH2-like domain, and a pseudokinase and kinase domain in the carboxyl terminus. The pseudokinase domains lacks catalytic activity but has key

regulatory functions (115). Following ligand binding to the receptor, JAKs are autophosphorylated and in turn phosphorylate the cytoplasmic tail of the membrane receptor, which facilitates the recruitment of downstream mediators such as STATs (116) (**Figure 1.11**).

1.6.8. JAK Inhibitors

The JAK family members have emerged as druggable targets for diseases involving dysregulated immune response or hematological malignancies. Over the last decades, TKIs targeting different JAK members, commonly known as "jakinibs," have been approved by the FDA (117). Ruxolitinib (Jakafi/Jakavi) was first approved in 2011 to treat polycythemia vera (118) and myelofibrosis (119) in patients with deficient response to hydroxyurea treatment. Tofacitinib was approved a year later for use in rheumatoid arthritis (RA) patients (120). Upadactinib and baricitinib have also been approved for the treatment of RA (121, 122). Due to JAK's key role in regulating immune function, jakinibs have moderate side effects related with immune dysfunction and increased risk of infection in some patients. More recently, jakinibs have also been associated with impairments in hemostasis and cardiovascular function. Jakinib therapy seems to trigger thrombotic complications (123-125) and bleeding events (126) in a manner that may involve dysregulated platelet and megakaryocyte function (127). Tofacitinib, a selective JAK3 inhibitor, increases the risk of blood clots and heart problems (128, 129). Baricitinib and ruxolitinib, which show more potency towards JAK2 compared to other jakinibs, have been related to increases in the incidence of venous thromboembolisms in rheumatoid arthritis and myeloproliferative neoplasms patients (130). In addition,

individuals with the bone marrow somatic gain-of-function JAK2-V617F mutation develop MPNs that are associated with an increased risk of venous and arterial thrombosis. This mutation triggers constitutive JAK2 activity and has been directly related to thrombotic effects in both human patients and mice models (131-133).

Platelets express several cytokine receptors and downstream JAK/STAT proteins that play a role in platelet function *in vitro* and *in vivo*. One of the most important molecules signaling through JAK/STAT is thrombopoietin (TPO), a primary regulator of platelet production (134, 135). Platelets and megakaryocytes express the TPO receptor, whose activation triggers downstream tyrosine phosphorylation events involving PI3K and JAK2 (136, 137). In addition to playing roles on cytokine and growth factor signaling, JAK/STAT pathways also modulate platelet function following activation by classical agonists. For example, the JAK2/STAT3 axis plays a significant role in collagen-mediated platelet activation (138, 139). A recent report from our group showed that pretreatment of platelets with the JAK1 and JAK2 inhibitors ruxolitinib and baricitinib impairs ITAM-mediated platelet granule secretion and aggregation (140). However, upadacitinib, oclacitinib, and tofacitinib exhibited more limited effects on platelet function *in vitro* (141). It is noteworthy that none of the inhibitors tested affected platelet function mediated by thrombin stimulation (141), suggesting that JAKs regulate ITAM signaling but not PAR-mediated platelet activation.

Despite the abovementioned phenomena, it remains unclear how JAK and ITAM singaling pathways are interconnected in platelets. As a potential explanation, Houck and

colleagues demonstrated that JAK members are located in close proximity to GPVI, which allows the cross-activation of ITAM and JAK pathways, and subsequent activation of STATs (132). A greater understanding of the effect of JAK/STAT inhibitors on hemostatic function is critical, as many novel, specific second-generation inhibitors specific to JAK isoforms are currently under development and have the potential to be approved for clinical use in the upcoming years (142).

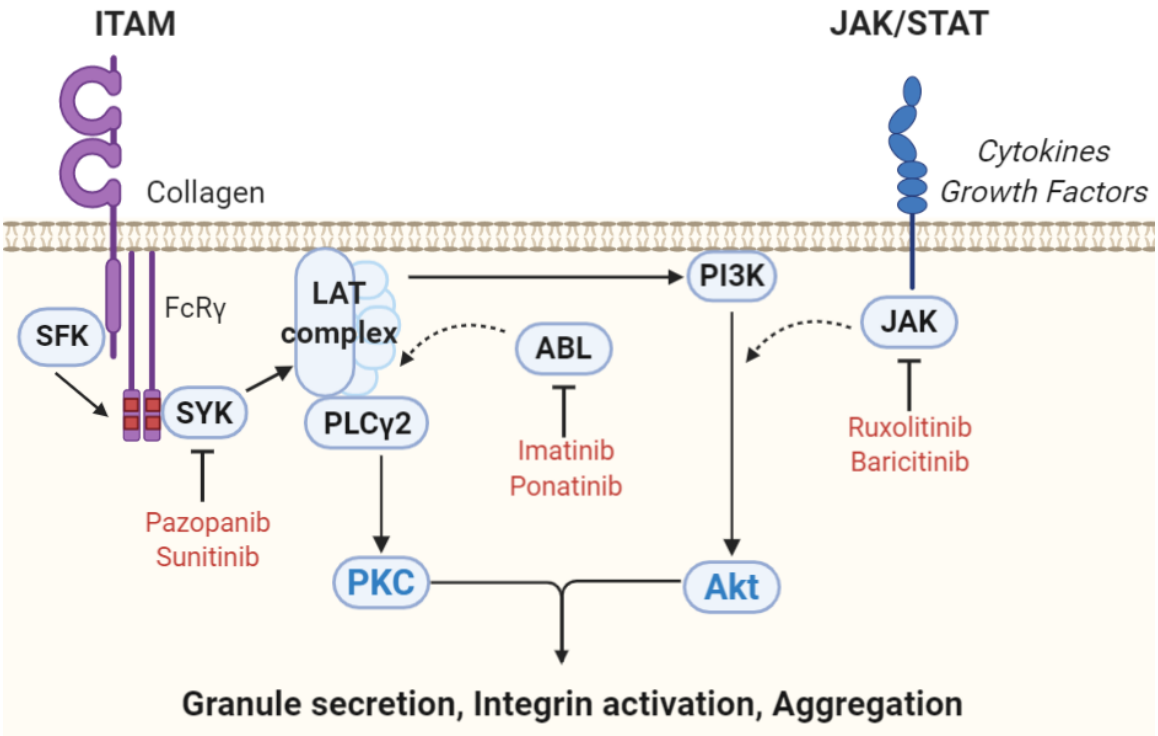

Figure 1.11. Platelet JAK/STAT signaling and role of JAK, ABL, and VEGFR inhibitors. Janus kinases (JAK) and signal transducers and activators of transcription (STAT) control pleiotropic pathways that transduce signaling events in response to more than 50 cytokines and growth factors. For instance, thrombopoietin (TPO) is a primary regulator platelet production that triggers downstream tyrosine phosphorylation events involving PI3K and JAK2. JAK inhibitors baricitinib and ruxolitinib have shown more potency towards JAK2 compared to other jakinibs, as well as impairing ITAM-mediated platelet granule secretion and platelet aggregation. Other TKIs targeting ABL tyrosine kinase such as imatinib and ponatinib have been shown to inhibit key nodes at the LAT signalosome, impairing collagen-induced platelet aggregation and reducing granule secretion upon GPVI stimulation. TKIs targeting VEGFR and PDGFR such as pazopanib and sunitinib inhibits platelet GPVI-mediated Syk phosphorylation and Ca^{+2} elevation as well as integrin activation, secretion, and platelet aggregation. Figure created in BioRender.com by Dr. Ivan Parra-Izquierdo.

1.6.9. Other Platelet Tyrosine Kinase Families, Receptors, and Inhibitors

ABL Family Kinases and Inhibitors

The ABL family of non-receptor tyrosine kinases is one of the most conserved subgroup of tyrosine kinases. ABL proteins are composed of a SH2, a SH3, and a tyrosine kinase domain that bind to cytoskeletal proteins acting as a bridge between early signaling phosphorylation events and cellular cytoskeletal reorganization (143).

Over the past decade, several TKIs targeting the ABL family of kinases have been approved for the treatment of chronic myeloid leukemia (CML) (**Table 1.3**). Imatinib was the first small-molecule TKI approved by the FDA in 2001 (144). The FDA later approved the use of second generation BCR-ABL inhibitors including bosutinib, nilotinib, dasatinib, and ponatinib for the treatment of CML. In addition, novel BCR-ABL1 inhibitors are currently under development and aim to overcome drug resistance commonly associated with imatinib and second-generation inhibitors (145). Despite the efficacy of ABL inhibitors in CML, several adverse effects related to impaired hemostasis are common in these patients, with up to 40% of patients under dasatinib therapy showing grade 3 bleeding events in a comparative study (111).

The effects of ABL inhibitors on hemostasis may be explained by their ability to target key nodes of platelet signaling. ABL proteins are expressed by human platelets and regulate platelet function in response to select agonists. Imatinib reversibly impairs

arachidonic acid (AA)-induced aggregation in CML patients (111), which is supported by an additional case report showing defective platelet aggregation in response to AA in a patient receiving imatinib for 5 years. However, epinephrine, ADP, and ristocetin-mediated aggregation were not affected by imatinib (146). Imatinib inhibited platelet spreading on fibrillar collagen and fibrinogen surfaces and aggregation on collagen surfaces under shear (147). Ponatinib has been related to cardiovascular ischemic events and inhibits ITAM-mediated platelet function *ex vivo* (147). However, a similar concentration of nilotinib and imatinib did not promote the same inhibitory effects on platelet function *ex vivo* (147). The inhibitory effects of ponatinib in platelets may also be explained by ponatinib's ability to nonspecifically target other key tyrosine kinases such as the SFKs (148). Ponatinib impaired collagen-induced platelet aggregation and decreased integrin activation upon GPVI stimulation from healthy patients and patients on ponatinib therapy (149). Another comparative study using different ABL inhibitors demonstrated that dasatinib inhibits platelet activation and thrombin generation in a more consistent manner compared to nilotinib, ponatinib, and bosutinib (150). Bosutinib increased phosphatidylserine exposure on platelet surfaces and alpha granule secretion upon GPVI and PAR1/4 stimulation, whereas dasatinib had a strong inhibitory effect (150). Yet, countering any potential antiplatelet effect that ponatinib might exhibit, we found in mice a new form of vascular toxicity for the ponatinib that involves vWF-mediated platelet adhesion and a secondary microvascular angiopathy that produces ischemic wall motion abnormalities (151). This may explain in part why ponatinib use has been associated with high rates of acute ischemic events (152, 153). Dasatinib,

bosutinib, nilotinib decreased alpha granule secretion and lysosomal granule secretion in response to GPVI and PAR1/4 stimulation (150).

Focal Adhesion Kinase (FAK) Family and FAK Inhibitors

The focal adhesion kinase (FAK) family of non-receptor tyrosine kinases, composed of FAK and proline-rich tyrosine kinase 2 (PYK2) proteins, represents another promising target for treatment of cancer and hematologic malignancies. FAK proteins play prominent roles in regulating signaling events downstream of integrins and PAR receptors (154). Moreover, FAK plays a role in megakaryopoiesis by regulating key signaling pathways downstream of TPO, which in turn affects platelet function (155). Human platelets express FAK (156), which is phosphorylated upon stimulation with LDL in a different fashion compared to stimulation with thrombin (157). A mechanistic study aiming to understand the role of FAK in platelets showed that PF-573,228, a FAK inhibitor, abrogated platelet spreading on fibrinogen and CRP-XL, as well as granule secretion, aggregation, and calcium signaling (158). Pharmacologic studies using PF-573,228 and the PYK2 inhibitor Tyrphostin A9 demonstrated that FAK, but not PYK2, inhibits granule secretion, integrin activation, and the procoagulant phenotype induced by GPVI agonists (159). However, a recent study using FAK-deficient mice showed that the effects of FAK inhibitors PF-573,228 and PF-573,271 are not mediated by FAK inhibition and are more likely mediated by off-target effects on other tyrosine kinases in platelets (160).

VEGFR and PDGFR family and Inhibitors

Vascular endothelial growth factor (VEGF), platelet-derived growth factor (PDGF), and their corresponding receptors (VEGFR and PDGFR respectively), are key regulators of angiogenesis, migration, cell growth, and cell differentiation. Pharmacologic agents targeting the VEGF/PDGF axis have shown promising antitumor activity in clinical studies (161) (**Table 1.3**).

Human platelets express VEGFRs and PDGFRs on their membranes and contain VEGF and PDGF in their granules (162, 163). Upon activation, platelet-released PDGF triggers a negative feedback loop in platelets in a PDGFR-dependent manner (163). Pazopanib (GW786034) is a TKI targeting VEGFR and PDGFR tyrosine kinases that has been associated with bleeding effects in kidney cancer patients (164). Mechanistic studies showed that pazopanib inhibits platelet GPVI-mediated Syk phosphorylation and Ca^{+2} elevation, resulting in reduced platelet procoagulant activity of phospholipid phosphatidylserine exposure in platelets isolated from healthy volunteers. Similarly, pazopanib dose-dependently reduced collagen-induced integrin activation, granule secretion, and platelet aggregation (165). Pazopanib also reduced thrombus size over collagen under physiologically relevant flow conditions (166). Recent studies on other TKIs targeting VEGFR include sunitinib, axitinib, and cabozantinib. Sunitinib dose-dependently reduced collagen-induced aggregation in PRP and washed platelets, while cabozantinib and vatalanib inhibited this response in washed platelets only (167). Sunitinib, axitinib, and vatalanib reduced thrombus formation on collagen by 10–50% (167). Intracellular calcium responses in isolated platelets were inhibited by

sunitinib (77%) and pazopanib (82%) (167). Overall, pharmacologic agents targeting the VEGF/PDGF axis have shown antiplatelet effects.

C-terminal Src Kinase (CSK) Family and Inhibitors

The C-terminal Src kinase (CSK) family of non-receptors tyrosine kinases is comprised of CSK and CSK-homologous kinase (CHK) proteins and regulates key cellular processes such as differentiation, migration, and cell growth (168). These proteins are known to be endogenous negative regulators of the Src family of kinases (169), which suggests that they may play key roles in regulating platelet function downstream of ITAM receptors. Supporting this idea, studies using murine CSK-null platelets have revealed that CSK and CHK are critical regulators of Src kinases in a manner that affects platelet function downstream of ITAM-dependent receptors (170, 171). Small-molecule inhibitors of CSK are currently under development and have the potential to reach the clinical stage over the next years as potential agents for cancer therapy (172).

FES Family Kinases and Inhibitors

Tyrosine kinase proteins FES/FPS play important roles in hematopoiesis (173), which has prompted researchers to develop novel FER inhibitors with potential utility for cancer treatment (174). Murine and human platelets express the FES family members FPS/FES and FER. Mice lacking FPS and FES kinases show increased erythrocyte, platelet, and neutrophil counts, as well as qualitative defects in myeloid colony formation (66). In addition, *ex vivo* studies with platelets demonstrated that FES plays a role in platelet aggregation following stimulation with collagen and ADP, suggesting that both ITAM

and GPCR signaling are regulated by FES kinases. Signaling studies demonstrated that FES regulate platelet function independent of Syk, PLCγ2, MAPKs, and Akt and therefore the specific signaling nodes regulated by FES remain to be determined (66).

1.7. Thesis Overview

In this thesis, we examine the role of platelet tyrosine kinases in hemostatic and thrombotic processes in the setting of atherosclerosis. The following studies in part define the effects of tyrosine kinase inhibitors (TKIs) targeting Bruton's tyrosine kinase (BTK) and Spleen tyrosine kinase (Syk) on glycoprotein VI (GPVI) mediated signaling pathways and oxidized low-density lipoprotein (oxLDL) enhanced platelet procoagulant activity.

In Chapter 3, we study the effects of Syk and BTK inhibitors on GPVI-mediated platelet signaling and function. Specifically, we investigate the effects of 12 TKIs, including four Syk inhibitors, Bay 61-3606, R406 (fostamatinib), entospletinib, TAK-659, four irreversible BTK inhibitors, ibrutinib, acalabrutinib, ONO-4059 (tirabrutinib), AVL-292 (spebrutinib), and four reversible BTK inhibitors, CG-806, BMS-935177, BMS-986195, and fenebrutinib. We find that TKIs targeting Syk or BTK reduced platelet adhesion to collagen and fibrinogen, dense granule secretion, alpha granule secretion, and integrin $\alpha_{IIb}\beta_3$ receptor activation in response to the GPVI agonist CRP-XL, however, differentially affected downstream signaling events and protein organization around PI3K and PKC. Overall, the data presented in this chapter elucidates in part the mechanism surrounding the Syk-BTK-PI3K signaling axis and suggests that TKIs targeting Syk or

BTK inhibit central platelet functional responses but may differentially affect protein activities and organization in critical systems downstream of Syk and BTK in platelets. This knowledge may be helpful in the identification of specific druggable targets in platelets that can potentially reduce thrombosis while minimally affecting hemostasis.

In Chapter 4, we expand our investigation of the role of platelet tyrosine kinases to the disease setting of atherosclerosis. In the development of atherosclerosis, the oxidation of lipoproteins is one of several main driving factors of disease progression. Thus, in this chapter, we investigate how oxLDL upregulates GPVI-mediated platelet hemostatic and procoagulant responses, and how traditional and emerging antiplatelet therapies affect oxLDL-enhanced platelet activity *ex vivo*. We find that oxLDL enhanced GPVI-mediated platelet dense granule secretion, alpha granule secretion, integrin activation, and aggregation, as well as procoagulant phosphatidylserine exposure and fibrin generation. Moreover, the data presented in this chapter suggest that P2Y antagonists (e.g., ticagrelor), and TKIs targeting BTK (e.g., ibrutinib) and Syk (e.g., fostamatinib) reduced oxLDL-mediated platelet responses and procoagulant activity, whereas COX inhibitors (e.g., aspirin) had no significant effect. Overall, our results demonstrate that oxLDL enhances *ex vivo* platelet responses and procoagulant activity downstream of GPVI signaling in a manner that may be reduced by P2Y antagonists and tyrosine kinase inhibitors, but not significantly affected by COX inhibitors.

Lastly, in Chapter 5, we summarize the findings presented in Chapters 3-4, discuss the conclusions drawn from these studies, and propose ongoing and future studies that will

continue to investigate the role of platelet tyrosine kinases in atherosclerosis. As a direct extension to the *ex vivo* work presented in Chapter 4, ongoing studies focus on *in vivo* murine and non-human primate (NHP) models to further investigate the effects of antiplatelet agents (e.g., ticagrelor, aspirin) and tyrosine kinase inhibitors (e.g., ibrutinib) on oxLDL-enhanced platelet procoagulant activity. Lastly, future studies will extend this work to examine the interactions between platelets and trans-aortic valve replacements (TAVRs) and assess the effects of tyrosine kinase inhibitors on such interactions that underlie the associated thrombosis complications on these biomaterials. Overall, the work presented in this thesis aims to help elucidate the role and mechanisms of tyrosine kinases in platelets to support hemostatic processes and help identify potential druggable targets in platelets that may be effective and safe in the setting of thrombosis and atherosclerosis.

Table 1.1. Bruton's Tyrosine Kinase (BTK) Inhibitors

Name	FDA Approval	Clinical Indication(s)	Effect on Platelets & Key Characteristics
BTK Inhibitors			
Ibrutinib	Yes	Mantle cell lymphoma Chronic lymphocytic leukemia Small lymphocytic leukemia Waldenstrom's macroglobulinemia Graft vs. host disease	Irreversible, IC_{50} = 0.2 – 2.0 nM ↓ platelet adhesion on collagen and fibrinogen, integrin activation, P-selectin exposure, dense granule secretion ↓ platelet aggregation from murine, baboon, and patient samples receiving ibrutinib treatment ↓ thrombus formation on human atherosclerotic plaque homogenate and plaque tissue ↓ phosphorylation of BTK, PLCγ2, and Akt downstream of GPVI in platelets, but not Syk or SLP-76
Acalabrutinib	Yes	Mantle cell lymphoma	Irreversible, IC_{50} = 2 – 20 nM ↓ adhesion on collagen and fibrinogen, integrin activation, P-selectin exposure, dense granule secretion ↓ phosphorylation of ERK, IKB, PLCγ2, and Akt, but does not inhibit the phosphorylation of EGFR, SFKs (Src, Lyn, Fyn, Yes, Lck), and Tec family kinases
Zanubrutinib	Yes	Mantle cell lymphoma	Irreversible ↓ platelet dense and alpha granule secretion, but not integrin activation, platelet aggregation
Tirabrutinib	No	Clinical Trials – Phase 2	Irreversible ↓ adhesion on collagen and fibrinogen, integrin activation, P-selectin exposure, dense granule secretion ↓ platelet aggregation ↑ closure/bleeding time
Remibrutinib	No	Clinical Trials – Phase 3	Irreversible Highly selective for BTK over Tec
Evobrutinib	No	Clinical Trials – Phase 3	Crosses blood-brain barrier ↓ platelet aggregation

Table 1.1. Bruton's Tyrosine Kinase (BTK) Inhibitors (cont.)

Tolebrutinib	No	Clinical Trial – Phase 2	Crosses blood-brain barrier
Fenebrutinib	No	Clinical Trials – Phase 2	Reversible ↓ adhesion on collagen and fibrinogen, integrin activation, P-selectin exposure, dense granule secretion ↓ platelet aggregation in response to low, but not high collagen concentrations ↓ phosphorylation of PLCγ2, Akt, BTK Tyr551, and PKC substrates
BMS-935177	No	Pre-clinical	Reversible ↓ adhesion on collagen and fibrinogen, integrin activation, P-selectin exposure, dense granule secretion ↓ phosphorylation of PLCγ2, Akt, BTK Tyr551, and PKC substrates ↓ PI3K localization with tubulin
BMS-986195	No	Pre-clinical	Reversible ↓ adhesion on collagen and fibrinogen, integrin activation, P-selectin exposure, dense granule secretion ↓ phosphorylation of PLCγ2, Akt, BTK Tyr551, and PKC substrates ↓ PI3K localization with tubulin
CG-806	No	Pre-clinical	Reversible ↓ adhesion on collagen and fibrinogen, integrin activation, P-selectin exposure, dense granule secretion ↓ phosphorylation of PLCγ2, Akt, BTK Tyr551, and PKC substrates
Rilzabrutinib	No	Clinical Trials – Phase 3	Reversible ↓ BTK and Tec ↓ platelet aggregation stimulated by atherosclerotic plaque material and collagen in a dose-dependent manner
Vecabrutinib	No	Clinical Trials – Phase 2	Reversible
LOXO-305	No	Clinical Trials – Phase 3	Reversible

Table 1.2. Spleen tyrosine kinase (Syk) and Janus kinase (JAK) inhibitors

Name	FDA Approval	Clinical Indication(s)	Effect on Platelets & Key Characteristics
Syk Inhibitors			
Fostamatinib (R406)	Yes	Immune thrombocytopenia	↓ adhesion on collagen and fibrinogen, integrin activation, P-selectin exposure, dense granule secretion ↓ platelet aggregation ↓ phosphorylation of Syk, SLP-76, LAT, BTK, Akt, PKC, and PLCγ2
Entospletinib	No	Clinical Trials – Phase 3	↓ adhesion on collagen and fibrinogen, integrin activation, P-selectin exposure, dense granule secretion ↓ adhesion on collagen under shear
Lanraplenib	No	Clinical Trials – Phase 2	Minimal bleeding observed ↓ phosphorylation of LAT and PLCγ2 ↓ platelet aggregation in human whole blood and monkey
Cevidoplenib	No	Clinical Trials – Phase 2	Minimal bleeding observed
MK-8457	No	Clinical Trials – Phase 2	Minimal bleeding observed
BI1002494	No	Pre-clinical	↓ outside-in signaling of integrin $\alpha_{IIb}\beta_3$
JAK Inhibitor(s)			
Ruxolitinib	Yes	Myelofibrosis	More potency towards JAK2 ↓ ITAM-mediated platelet granule secretion and aggregation
Tofacitinib	Yes	Rheumatoid arthritis	Selective JAK3 inhibitor
Upadacitinib	Yes	Rheumatoid arthritis	n/a
Baricitinib	Yes	Rheumatoid arthritis	More potency towards JAK2 ↓ ITAM-mediated platelet granule secretion and aggregation
Oclacitinib	Yes	Dermatitis (dogs)	n/a

Table 1.3. ABL, VEGFR/PDGFR, SFK, and PKC Inhibitors

Name	FDA Approval	Clinical Indication(s)	Effect on Platelets & Key Characteristics
ABL Inhibitor(s)			
Imatinib	Yes	Chronic myeloid leukemia Acute lymphoblastic leukemia Gastrointestinal stromal tumor	↓ arachidonic acid and collagen induced aggregation ↓ ADP induced aggregation ↓ platelet spreading on collagen and fibrinogen and platelet aggregation on collagen under shear
Bosutinib	Yes	Rheumatoid arthritis	↑ phosphatidylserine exposure and alpha granule secretion
Nilotinib	Yes	Chronic myeloid leukemia	↓ alpha granule secretion and lysosomal granule release
Dasatinib	Yes	Chronic myeloid leukemia Acute lymphoblastic leukemia	↓ alpha granule secretion, ATP secretion, aggregation, and tyrosine phosphorylation ↓ phosphatidic acid production and production of D3-phosphoinositides ↓ thrombi formation on collagen matrix surfaces under arterial shear rate conditions from CML patients receiving dasatinib ↓ platelet deposition under shear on collagen ↓ convulxin-induced phosphatidylserine exposure and thrombin generation ↓ phosphatidylserine exposure ↓ integrin activation upon GPVI stimulation, but ↑ integrin activation upon GPVI + PAR stimulation
Ponatinib	Yes	Chronic myeloid leukemia	↓ ITAM-mediated platelet function *ex vivo* ↓ platelet aggregation and integrin activation upon GPVI stimulation from healthy patients and patients receiving ponatinib

Table 1.3. ABL, VEGFR/PDGFR, SFK, and PKC Inhibitors (cont.)

VEGFR/PDGFR Inhibitor(s)			
Pazopanib	Yes	Renal cell carcinoma Soft tissue sarcoma	↓ GPVI-mediated Syk phosphorylation, Ca^{+2} elevation, and phosphatidylserine exposure ↓ collagen-induced integrin activation, granule secretion, and platelet aggregation ↓ platelet responses to ADP, AA, and a TxA2 analog
Sunitinib	Yes	Gastrointestinal stromal tumor Renal cell carcinoma Pancreatic neuroendocrine tumors	↓ collagen-induced aggregation in PRP and washed platelets ↓ intracellular calcium responses
Axitinib	Yes	Renal cell carcinoma	↓ thrombus formation collagen
Cabozantinib	Yes	Renal cell carcinoma Hepatocellular carcinoma	↓ platelet aggregation
Vatalanib	No	Clinical Trials – Phase III	↓ platelet aggregation
SFK Inhibitors			
PP2	Yes	Pre-clinical	↓ phosphorylation of LAT Tyr 191, p-Akt, Syk Tyr 525/526, Syk Tyr 352, and PLCγ2 Tyr 759 ↓ Ca^{2+} mobilization ↓ dense granule secretion, alpha granule secretion, P-selectin expression, and aggregation
PKC Inhibitor(s)			
Go6976	Yes	Pre-clinical	↓ platelet aggregation upon convulxin, CRP-XL, or collagen stimulation ↓ intracellular calcium release upon convulxin stimulation ↓ phosphorylation of LAT Tyr 191 and Syk Tyr 525/526

Chapter 2: General Materials and Methods

2.1 Ethical Considerations

Human venous blood was drawn from healthy adult male and female volunteers in accordance with Oregon Health & Science University (OHSU) Institutional Review Board (IRB) approved protocol. All human donors provided full informed and written consent in accordance with the Declaration of Helsinki. All donated blood samples were deidentified prior to platelet isolation and preparation. For all studies using Rhesus macaques (*Macaca mulatta*), protocols, procedures, and experiments were approved by OHSU and Oregon National Primate Research Center (ONPRC) in accordance with the regulations of the Institutional Animal Care and Usage Committee (IACUC).

2.2 Common Reagents & Antibodies

Collagen was obtained from Chrono-Log (Havertown, PA), crosslinked collagen related peptide (CRP-XL) from R. Farndale (Cambridge University, Cambridge, UK), human fibrinogen from Enzyme Research (South Bend, IN), prostacyclin (PGI_2) from Cayman Chemical (Ann Arbor, MI), and integrilin from Merck & Co. (Whitehouse Station, NJ). Bovine thrombin, fatty acid-free bovine serum albumin (BSA), and all other reagents were obtained from Sigma-Aldrich (St. Louis, MO) unless specified otherwise.

Primary antisera against phosphorylated Akt substrates (#9614S), PLCγ2 Y_{1217} (##3871S), DAPP1 Y_{139} (#13703S), phosphorylated MAPK substrates (#2325), and phosphorylated PKC substrates (#2261) were obtained from Cell Signaling Technology

(Danvers, MA). Anti-α tubulin antibody (#T6199) was obtained from Sigma-Aldrich (St. Louis, Missouri, USA) and PI 3-kinase p85α antibody (#sc-376112) was obtained from Santa Cruz Biotechnology (Dallas, Texas, USA). Flow cytometry antibodies APC anti-human CD62P (#304910) was obtained from BioLegend (San Diego, California, USA), FITC mouse anti-human PAC-1 (#340507) was obtained from BD Biosciences (Franklin Lakes, New Jersey, USA), and FITC bovine lactadherin was obtained from Haematologic Technologies (Essex Junction, Vermont, USA). 4G10 (#05-321) was obtained from Sigma Millipore (St. Louis, Missouri, USA).

2.3 Human Blood Collection

Human venous blood was drawn from healthy adult male and female volunteers by venipuncture into 1:10 sodium citrate (NaCit, 3.8% w/v) and warmed 1:10 acid citrate dextrose (ACD, 30 °C; 85 mM sodium citrate, 100 mM glucose, 71 mM citric acid).

2.4 Platelet Preparation

The drawn blood was centrifuged at 200 *g* for 20 min to isolate and obtain the platelet rich plasma (PRP). Prostacyclin (PGI_2, 0.1 µg/ml) was added to the PRP, and the mixture was centrifuged at 1,000 *g* for 10 min. The platelet poor plasma (PPP) was removed to isolate and obtain platelets. The collected platelets were re-suspended in 25 ml modified HEPES/Tyrode buffer (129 mM NaCl, 0.34 mM Na_2HPO_4, 2.9 mM KCl, 12 mM $NaHCO_3$, 20 mM HEPES, 5 mM glucose, 1 mM $MgCl_2$, pH 7.3) and 3 ml ACD and centrifuged at 1,000 *g* for 10 min to further wash the platelets. The supernatant is

removed and the washed, platelet sample is resuspended in HEPES/Tyrode buffer to the desired concentration for experimental use.

2.5 Plasma Preparation

Plasma was isolated by centrifuging whole blood (mixed with sodium citrate, 0.32% w/v) at 2,000 *g* for 10 min at room temperature (RT) and stored at -80 ^{o}C.

2.6 Static Adhesion Assay

Circular glass coverslips (12 mm diameter, #1.5 glass coverslips; Fisher Scientific) were coated with human fibrinogen (100 µg/ml) or soluble collagen (50 µg/ml). The coated surfaces were then treated and blocked with filtered, denatured fatty acid-free BSA (5 mg/ml). Selected inhibitors of interest or vehicle (0.1% DMSO) were added to platelets (2×10^7/ml) in solution for 10 min. The inhibitor-treated platelets were then seeded onto the immobilized fibrinogen- or collagen-coated coverslip surfaces and incubated at 37 °C for 45 min and 30 min, respectively. The glass coverslips were then washed three times with PBS to remove non-adherent platelets. Adherent platelets were fixed in 4% paraformaldehyde (PFA) for 10 min and washed three times with PBS. Platelets are stained with phalloidin to detect actin filaments and with fluorescent antibodies for proteins of interest. Coverslips were mounted on pre-cleaned microscope slides (25 × 75 × 1 mm) using Fluoromount G (Southern Biotech) and stored at -4 ^{o}C for microscopy and fluorescence imaging.

2.7 Microscopy and Image Analysis

Immobilized platelets from static adhesion assays are imaged using Kohler-illuminated Nomarski differential interference contrast (DIC) optics with a Zeiss 63 × oil immersion 1.40 numerical aperture (NA) plan-apochromat lens on a Zeiss Axio Imager M2 microscope using Slidebook 5.5 image acquisition software (Intelligent Imaging Innovations, Denver, CO). Three images for each treatment condition were taken. Individual platelet surface areas, total surface area covered by platelets, and average number of platelets per imaged field adherent on collagen were measured and analyzed using Image J (NIH). Similarly, the average platelet surface area of platelets spread on fibrinogen were measured and calculated using Image J (NIH). The total area of the field of view was 14, 587 μm^2.

2.8 Dense Granule Secretion Assay

Washed, purified platelets were prepared to a concentration of 2×10^8/ml. Platelets were incubated with the selected inhibitors of interest or vehicle (0.1% DMSO) for 10 min in a clear flat bottom 96-well plate (Corning Costar, Tewksbury, MA) and then stimulated with agonists of interest. The 96-well plate was placed in an Infinite M200 spectrophotometer (TECAN, Mannderdorf, Switzerland) and shook for 20 s. Detection reagent Chrono-Lume (Chrono-Log) was added to each well to detect for ATP released, measured as the light output generated by an ATP-luciferin-luciferase reaction. An automated protocol is carried out to shake for 10 s, and sample luminescence was measured and recorded at 30 s intervals for 5 min. Four kinetic profiles were recorded for each treatment condition and the average luminescence measured at 4 min was

calculated. Graphical depiction of the dense granule secretion assay workflow is shown in **Figure 2.1**.

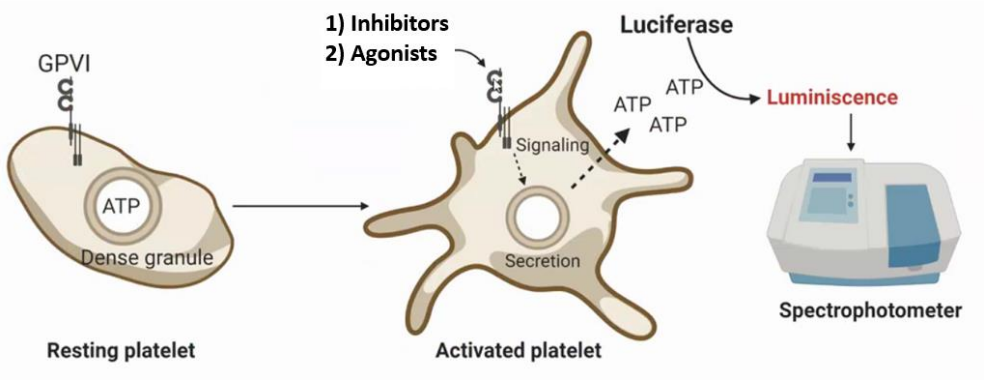

Figure 2.1. Dense Granule Secretion Assay Workflow. Washed, purified platelets were prepared to a concentration of 2×10^8/ml, incubated with the selected inhibitors of interest or vehicle (0.1% DMSO) for 10 min, and then stimulated with agonists of interest. Detection reagent Chrono-Lume (Chrono-Log) was used to detect for ATP released, which is measured as the light output generated by an ATP-luciferin-luciferase reaction. An automated protocol is carried out to shake for 10 s, and sample luminescence was measured and recorded at 30 s intervals for 5 min. Created in BioRender.com by Dr. Ivan Parra-Izquierdo, modified by Tony J. Zheng.

2.9 Flow Cytometry

Washed, purified platelets were prepared to a concentration of 2×10^7/ml and incubated with the selected inhibitors of interest or vehicle (0.1% DMSO) for 10 mins. FITC PAC-1 (1:50) and APC CD62P (1:50) were added to stain for activated integrin $\alpha_{IIb}\beta_3$ and P-selectin, respectively. FITC lactadherin (1:25) was added to stain for phosphatidylserine exposure. All other fluorescent antibodies of interest are noted in each corresponding chapter. Each platelet mixture was stimulated with agonists of interest and incubated for

20 min at 37 °C. Untreated platelets (vehicle, 0.1% DMSO) and platelets stimulated with thrombin (1 U) served as the negative and positive controls, respectively. Each sample was analyzed using flow cytometry on a BD FACSCantoII flow cytometer. Platelet populations were identified and gated by logarithmic signaling amplification for forward and side scatter. Graphical depiction of the flow cytometry workflow is shown in **Figure 2.2**.

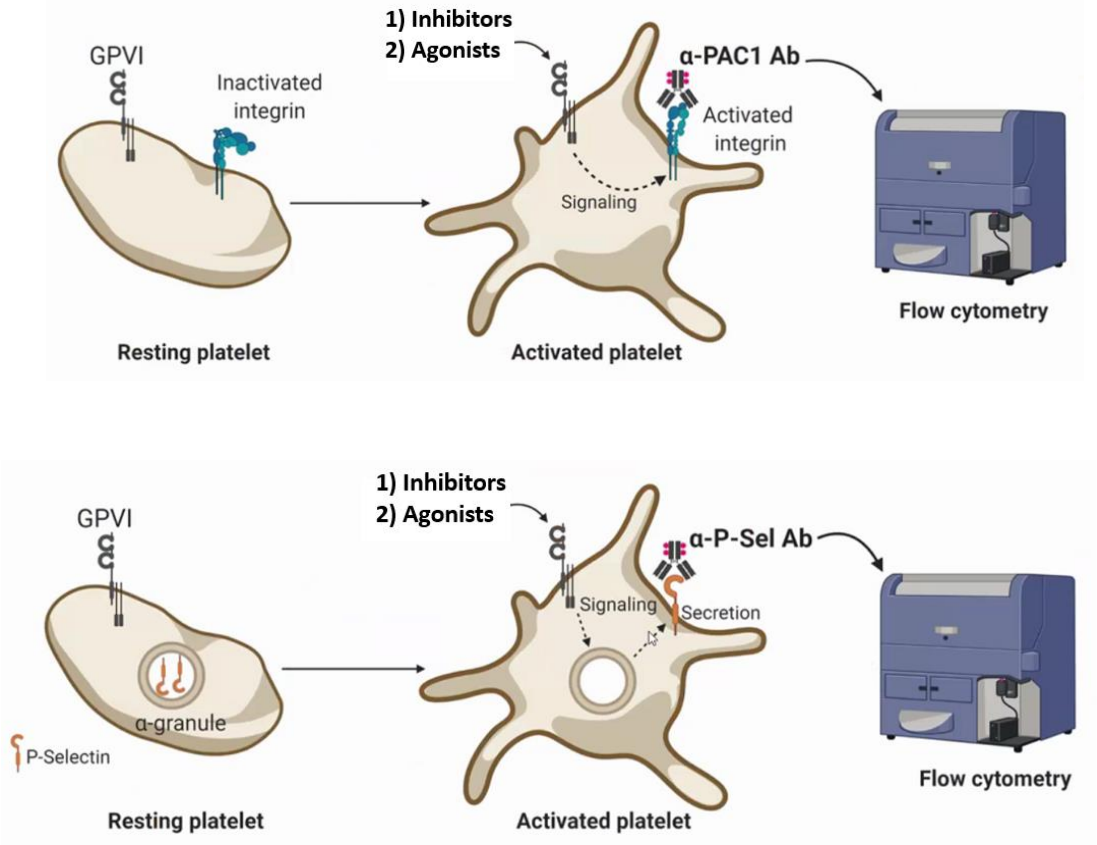

Figure 2.2. Flow Cytometry Workflow. Washed, purified platelets were prepared to a concentration of 2×10^7/ml, incubated with the selected inhibitors of interest or vehicle (0.1% DMSO), stained with **A)** FITC PAC-1 (1:50) and **B)** APC CD62P (1:50) activated integrin $\alpha_{IIb}\beta_3$ and P-selectin, respectively, and stimulated with agonists of interest and incubated for 20 min at 37 °C. Each sample was analyzed using flow cytometry on a BD FACSCantoII flow cytometer. Platelet populations were identified and gated by logarithmic signaling amplification for forward and side scatter. Created in BioRender.com by Dr. Ivan Parra-Izquierdo, modified by Tony J. Zheng.

2.10 Platelet Aggregation

Washed, purified platelets were prepared to a concentration of 3×10^8/ml (300 µl) and were incubated with the selected inhibitors of interest or vehicle (0.1% DMSO) for 10 mins at room temperature in glass cuvettes. Each platelet mixture was stimulated with agonists of interest and monitored under continuous stirring at 1200 rpm. The change in light transmission was measured using a 490 + 4 + 4 aggregometer for 5 mins (Chrono Log Corporation).

2.11 Western Blotting

Washed, purified platelets were prepared to a concentration of 1×10^9/ml and incubated with glycoprotein (GP) IIb/IIIa inhibitor Integrilin (20 µg/ml). The platelets were then incubated with selected inhibitors of interest or vehicle (0.1% DMSO) for 10 min. Agonists of interest were added to stimulate each platelet mixture and then incubated in at 37 °C on a shaker at 200 RPM for 10 min. Laemmli Sample Buffer was added at a 1:1 volume ratio in dithiothreitol (DTT, 200 mM). The platelet samples were separated by SDS-PAGE and then transferred to nitrocellulose membranes, which were then blocked in 5% milk + PBS prior to antibody staining for Western blot. Antibody staining was performed in 5% BSA + PBS. Each platelet sample was blotted and stained using the antibodies of interest.

2.12 Statistical Analysis

All experimental data was analyzed using GraphPad Prism 9 software (San Diego, California, USA) and represented as the mean ± standard error of the mean (SEM). Samples were analyzed using a one- or two-way ANOVA with Dunnett's multiple comparison's test, where a p-value of < 0.05 was used to test for significance. The p-values are denoted. For all the experiments, *n* indicates the number of independent experiments conducted from platelets isolated from different donors. Experiments were repeated at least three times for each condition. For image analysis, three random fields of view were captured, analyzed, and average for each condition per experiment.

Chapter 3: Assessment of the effects of Syk and BTK inhibitors on GPVI-mediated platelet signaling and function

Tony J. Zheng, Elizabeth R. Lofurno, Alexander R. Melrose, Hari Hara Sudhan Lakshmanan, Jiaqing Pang, Kevin G. Phillips, Meghan E. Fallon, Tia C. L. Kohs, Anh T. P. Ngo, Joseph J. Shatzel, Monica T. Hinds, Owen J. T. McCarty, and Joseph E. Aslan

This work was originally published by the *American Journal of Physiology: Cell Physiology* 2021 320:5, C902-915.

3.1 Abstract

Spleen tyrosine kinase (Syk) and Bruton's tyrosine kinase (BTK) play critical roles in platelet physiology, facilitating ITAM-mediated signaling downstream of platelet glycoprotein VI (GPVI) and GPIIb/IIIa receptors. Small molecule tyrosine kinase inhibitors (TKIs) targeting Syk and BTK have been developed as anti-neoplastic and anti-inflammatory therapeutics and have also gained interest as anti-platelet agents. Here, we investigate the effects of 12 different Syk and BTK inhibitors on GPVI-mediated platelet signaling and function. These inhibitors include, four Syk inhibitors, Bay 61-3606, R406 (fostamatinib), entospletinib, TAK-659, four irreversible BTK inhibitors, ibrutinib, acalabrutinib, ONO-4059 (tirabrutinib), AVL-292 (spebrutinib), and four reversible BTK inhibitors, CG-806, BMS-935177, BMS-986195, and fenebrutinib. *In vitro*, TKIs targeting Syk or BTK reduced platelet adhesion to collagen, dense granule secretion, and alpha granule secretion in response to the GPVI agonist CRP-XL. Similarly, these TKIs

reduced the percentage of activated integrin $\alpha_{IIb}\beta_3$ on the platelet surface in response to CRP-XL, as determined by PAC-1 binding. While all TKIs tested inhibited PLCγ2 phosphorylation following GPVI-mediated activation, other downstream signaling events proximal to PI3K and PKC were differentially affected. In addition, reversible BTK inhibitors had less pronounced effects on GPIIb/IIIa-mediated platelet spreading on fibrinogen and differentially altered the organization of PI3K around microtubules during platelets spreading on fibrinogen. Select TKIs also inhibited platelet aggregate formation on collagen under physiological flow conditions. Together, our results suggest that TKIs targeting Syk or BTK inhibit central platelet functional responses but may differentially affect protein activities and organization in critical systems downstream of Syk and BTK in platelets.

3.2 Introduction

Spleen tyrosine kinase (Syk) and Bruton's tyrosine kinase (BTK) play central roles in the physiology of immune and hematological cells (76, 175). In platelets, Syk and BTK mediate hemostasis, vascular repair, and a range of inflammatory and pathological responses (176). For example, Syk and BTK transduce signals from collagen receptor glycoprotein VI (GPVI) to drive thrombo-inflammatory platelet responses (177). When activated, GPVI associates with Fc receptor γ-chain (FcRγ) and becomes phosphorylated by Src family kinases (SFKs, namely Lyn and Fyn) on intracellular immunoreceptor tyrosine-based activation motifs (ITAMs) (36). Phosphorylated ITAMs on GPVI-associated FcRγ then serve as a platform to recruit, phosphorylate, and activate Syk (36). Then, Syk phosphorylates and activates a number of substrates associated with the linker

for activation of T cells (LAT) at the LAT signalosome, including BTK, phospholipase C γ2 (PLCγ2), phosphoinositide 3-kinase (PI3K) (36, 177, 178) and protein kinase C (PKC) to support platelet hemostatic as well as inflammatory and thrombotic responses (36, 177).

Given their roles in thrombo-inflammatory and other hematological diseases, Syk and BTK have emerged as targets of interest in pathologies driven by platelets and other immune cells (179-181). For instance, small molecule tyrosine kinase inhibitors (TKIs) targeting BTK, such as ibrutinib, have already proved as highly effective, first-line therapeutics used in the treatment of hematologic malignancies and offer promise against a range of immunological and inflammatory disorders (73, 182-184). However, while Syk and BTK are not absolutely required for hemostatic responses of platelets, TKIs with high potency for BTK, such as ibrutinib, are associated with undesirable effects on platelets and bleeding (73). Interestingly, despite key roles as an upstream activator of BTK, inhibition of Syk with broad-spectrum immunomodulatory agents such as fostamatinib are not associated with platelet toxicities and bleeding (185). Overall, several questions remain regarding how Syk and BTK as well as TKIs targeting these kinases affect platelet function.

Studies over the past decade have determined that a number of Syk and BTK inhibitors have effects on platelets *in vivo* as well as *in vitro* (186, 187). However, no studies to date have examined multiple Syk and BTK inhibitors simultaneously to compare as well as to uncover the physiological mechanisms, both the commonalities and disparities, by which

these agents interfere with platelet signaling and function. In this chapter, we investigate the effects of a panel of 12 different clinically relevant Syk and BTK inhibitors on platelet adhesion, granule secretion, activation, aggregation, and protein phosphorylation. Our findings characterize the effects of these inhibitors on GPVI- and GPIIb/IIIa integrin-mediated platelet activation pathways and the interplay of Syk-BTK-PI3K organization to better elucidate how Syk and BTK inhibitors target signaling events central in platelet hemostasis, inflammation, and thrombosis.

3.3 Materials and Methods

3.3.1 Reagents

Collagen was obtained from Chrono-Log (Havertown, PA), CRP-XL from R. Farndale (Cambridge University, Cambridge, UK), human fibrinogen from Enzyme Research (South Bend, IN), prostacyclin (PGI_2) from Cayman Chemical (Ann Arbor, MI), and integrilin from Merck & Co. (Whitehouse Station, NJ). Bovine thrombin, fatty acid-free bovine serum albumin (BSA), and all other reagents were obtained from Sigma-Aldrich (St. Louis, MO) or as previously mentioned (58).

3.3.2 Tyrosine Kinase Inhibitors

Ro 31-8220 and PP2 were obtained from Tocris (Bristol, UK). Bay 61-3606 was from Sigma-Aldrich (St. Louis, MO). R406/fostamatinib, entospletinib, TAK-659, ibrutinib, acalabrutinib, ONO-4059, AVL-292/spebrutinib, BMS-935177, BMS-986195, and

fenebrutinib were obtained from Selleck (Houston, TX). CG-806 was from MedChemExpress (Monmouth Junction, NJ).

3.3.3 Antibodies

Primary antisera against phosphorylated Syk Y_{525} (#2711S), BTK Y_{551} (#MAB7659), AKT T_{308} (#4056S), AKT S_{473} (#4060S), phosphorylated Akt substrates (#9614S), PLCγ2 Y_{1217} (##3871S), DAPP1 Y_{139} (#13703S), and phosphorylated PKC substrates (#2261) were obtained from Cell Signaling Technology (Danvers, MA). Anti-α tubulin antibody (#T6199) was obtained from Sigma-Aldrich (St. Louis, MO) and PI 3-kinase p85α antibody (#sc-376112) was obtained from Santa Cruz Biotechnology (Dallas, TX). APC anti-human CD62P (P-selectin) (#304910) was obtained from BioLegend (San Diego, CA) and FITC mouse anti-human PAC-1 (#340507) was obtained from BD Biosciences (San Jose, CA). Alexa Fluor secondary antibodies: goat anti-mouse IgG1 488 (#A-21121), goat anti-mouse IgG (H + L) 488 (#A-11029), goat anti-mouse IgG2b 546 (#A-21143), and goat anti-rabbit IgG (H + L) 546 (#A-21143) was obtained from Thermo Fisher Scientific (Waltham, MA).

3.3.4 Platelet Preparation

Human venous blood was drawn from healthy adult male and female volunteers into 1:10 sodium citrate (3.8% w/v) and warmed 1:10 acid citrate dextrose (ACD, 30 °C), as previously described (188-190). Written consent was obtained prior to the blood draw and procedure was conducted according to a protocol approved by the Institutional Review Board of Oregon Health & Science University. The drawn blood was centrifuged

at 200 *g* for 20 min to isolate and obtain the platelet rich plasma (PRP). Prostacyclin (0.1 µg/ml) was added to the PRP, and the mixture was centrifuged at 1,000 *g* for 10 min to isolate and obtain platelets. The collected platelets were re-suspended in modified HEPES/Tyrode buffer (129 mM NaCl, 0.34 mM Na_2HPO_4, 2.9 mM KCl, 12 mM $NaHCO_3$, 20 mM HEPES, 5 mM glucose, 1 mM $MgCl_2$, pH 7.3) and ACD to the desired concentration for experimental use.

3.3.5 Static Adhesion Assays

For platelet spreading experiments on fibrinogen or collagen, 12-mm no. 1.5 glass coverslips (Fisher Scientific) were coated with human fibrinogen (100 µg/ml) or soluble collagen (50 µg/ml), respectively. The coated surfaces were then treated and blocked with filtered, denatured fatty acid-free BSA (5 mg/ml). The selected Syk and BTK inhibitors (10 µM) or vehicle (0.1% DMSO) were added to platelets (2×10^7/ml) in solution for 10 min. The inhibitor-treated platelets were then seeded onto the immobilized fibrinogen- or collagen-coated coverslip surfaces and incubated at 37 °C for 45 min and 30 min, respectively. The glass coverslips were then washed three times with PBS to remove non-adherent platelets. Adherent platelets were fixed in 4% paraformaldehyde (PFA) for 10 min and washed three times with PBS. Coverslips were mounted on pre-cleaned microscope slides (25 × 75 × 1 mm) using Fluoromount G (Southern Biotech). Platelets are imaged using Kohler-illuminated Nomarski differential interference contrast (DIC) optics with a Zeiss 63 × oil immersion 1.40 numerical aperture (NA) plan-apochromat lens on a Zeiss Axio Imager M2 microscope using Slidebook 5.5 image acquisition software (Intelligent Imaging Innovations, Denver, CO),

as previously described (189). Three images for each treatment condition were taken. Individual platelet surface areas, total surface area covered by platelets, and average number of platelets per imaged field adherent on collagen were measured and analyzed using Image J (NIH). Similarly, the average platelet surface area of platelets spread on fibrinogen were measured and calculated using Image J (NIH). Data is shown as mean ± SEM; statistical analysis were conducted using a one-way ANOVA test on GraphPad PRISM, where a P value < 0.05 was considered significant.

3.3.6 Fluorescence Microscopy and Quantification

Washed, purified platelets were prepared to a concentration of 2×10^7/ml, incubated on fibrinogen coated glass coverslips, and fixed using 4% PFA, as described above. To fluorescently visualize platelet tubulin, PI3K, and PKC, the adherent platelets were first permeabilized with blocking solution (1% BSA and 1% SDS in PBS, 1:100) and then stained with anti-α-tubulin, anti-p85 PI3K, and anti-PKC primary antibodies in blocking buffer overnight at 4 °C. Coverslips were washed with PBS and adherent platelets were stained using Alexa Fluor secondary antibodies (1:500) and mounted on pre-cleaned microscope slides (25 × 75 × 1 mm) using Fluoromount G (Southern Biotech). Adherent platelets were imaged using a Zeiss Axio Imager M2 microscope, as described above. Three images for each treatment condition were taken. Colocalization analyses of α-tubulin with either p85 PI3K or PKC were performed using a custom FIJI script (SciJava, NIH) incorporating Just Another Co-localization Plugin (JACoP, ver. 2.1.1) (191). Images were pre-processed by smoothing using a median filter with radius = 2 pixels (px) to remove noise outliers and background subtracted with rolling radius = 50 px. Each

image was then automatically quantified using the Mander's colocalization method within JACoP. The Mander's overlap coefficient (MOC) is reported as the percentage of overlap of tubulin signal in channel 1 with PI3K or PKC signal in channel 2, as previously described (192, 193). Each image was then automatically quantified using the Pearson's correlation method within a custom MATLAB script. The Pearson's correlation coefficient (PCC) is reported as the degree of fluorescence intensity correlation between the two channels, as previously described (190, 194).

3.3.7 Platelet Secretion Assay

Washed, purified platelets were prepared to a concentration of 2×10^8/ml. Platelets were incubated with the selected panel of Syk and BTK inhibitors (10 µM) or vehicle (0.1% DMSO) for 10 min in a clear flat bottom 96-well plate (Corning Costar, Tewksbury, MA) and then stimulated with CRP-XL (10 µg/ml) or thrombin (1 U/ml). The 96-well plate was placed in an Infinite M200 spectrophotometer (TECAN, Mannderdorf, Switzerland) and shook for 20 s. Detection reagent Chrono-Lume (Chrono-Log) was added to each well to detect for ATP released, measured as the light output generated by an ATP-luciferin-luciferase reaction. An automated protocol is carried out to shake for 10 s, and sample luminescence was measured and recorded at 30 s intervals for 5 min. Four kinetic profiles were recorded for each treatment condition and the average luminescence measured at 4 min was calculated and normalized by the average luminescence of untreated platelets stimulated with CRP-XL or thrombin. Statistical analysis was performed using a one-way ANOVA test on GraphPad PRISM, where a P value < 0.05 was considered significant.

3.3.8 Flow Cytometry Analysis

Washed, purified platelets were prepared to a concentration of 2×10^7/ml and incubated with the selected panel of Syk and BTK inhibitors (10 µM) or vehicle (0.1% DMSO) for 10 mins. FITC PAC-1 (3:100) and APC CD62P (3:100) were added to stain for activated integrin $\alpha_{IIb}\beta_3$ and P-selectin, respectively. Each platelet mixture was stimulated with CRP-XL (10 µg/ml) and incubated for 20 min. Untreated platelets (vehicle, 0.1% DMSO) unstimulated and stimulated with CRP-XL (10 µg/ml) served as the negative and positive controls, respectively. Each sample was analyzed using flow cytometry on a BD FACSCantoII flow cytometer. Platelet populations were identified and gated by logarithmic signaling amplification for forward and side scatter as well as $CD41^+$ staining, as previously described (195). Statistical analysis was performed using a one-way ANOVA test on GraphPad PRISM, where a P value < 0.05 was considered significant.

3.3.9 Western Blotting

Washed, purified platelets were prepared to a concentration of 1×10^9/ml and incubated with glycoprotein (GP) IIb/IIIa inhibitor Integrilin (20 µg/ml). The platelets were then incubated with the selected panel of Syk and BTK inhibitors (10 µM) or vehicle (0.1% DMSO) for 10 min. CRP-XL (10 µg/ml) was added to stimulate each platelet mixture and then incubated in a 25 °C water bath for 10 min. Laemmli Sample Buffer was added at a 1:1 volume ratio in dithiothreitol (DTT, 200 mM). The platelet samples were separated by SDS-PAGE and then transferred to nitrocellulose for western blotting. The

platelet samples were separated by SDS-PAGE and then transferred to nitrocellulose membranes, which were then blocked in 5% milk + PBS prior to antibody staining for Western blot. Antibody staining was performed in 5% BSA + PBS. Each platelet/inhibitor sample was blotted and stained using the antibodies for phospho-Syk (Tyr525/526), phospho-BTK (Y551) antibody, phospho-DAPP1 (Tyr139), phospho-PLCγ2 (Tyr1217), phospho-Akt (Thr308), phospho-Akt (Ser473), phospho-Akt substrate, phospho-(Ser) PKC substrate, and α tubulin, as previously described (196).

3.3.10 Flow Adhesion and Analysis

Glass capillary tubes (0.2 × 2 × 200 mm; Vitrocom, Mountain Lakes, NJ, USA) were coated with fibrillar type I collagen (100 µg/ml) for one hour at room temperature, as previously described (197). Glass capillaries were then washed with PBS and blocked with 5 mg/ml denatured BSA for one hour at room temperature before connecting to a syringe pump system. Human venous blood was drawn into syringe containing sodium citrate (3.8% w/v) in 1:9 sodium citrate:whole blood and pre-treated with a subset of inhibitors, including entospletinib, ibrutinib, and fenebrutinib (10 µM), before perfusion through the glass capillary tube at a venous shear rate of 300 s^{-1} for 10 min. After 10 minutes of whole blood perfusion, glass capillary tubes were washed with PBS, fixed with 4% paraformaldehyde, and sealed with Fluoromount G. Z-stack images of platelet aggregates in three random fields of view were captured using a 63 × Zeiss Axio Imager M2 microscope with Slidebook 5.5 image acquisition software, as previously described (198, 199). The surface area and volume of each platelet aggregate were determined using a custom MATLAB script (198, 199). Data is shown as mean ± SEM; statistical

analysis were conducted using a one-way ANOVA test on GraphPad PRISM, where a P value < 0.05 was considered significant.

3.4 Results

3.4.1 Effects of TKIs targeting Syk and BTK on Platelet Adhesion to Collagen

We first examined the effects of 12 Syk and BTK inhibitors on GPVI-mediated platelet adhesion to immobilized collagen. Washed platelets were prepared from citrate-anticoagulated whole blood collected from a pool of healthy adult human donors. Purified platelets (2×10^7/ml) were treated with the selected Syk and BTK inhibitors (10 μM) or vehicle (0.1% DMSO) in solution, prior to incubation on collagen-coated coverslips. As seen in **Figure 3.1A**, platelets readily adhered to collagen-coated surfaces. Following 30 min incubation, 104 ± 5 platelets readily adhered onto collagen-coated glass in an imaged area of 14,587 μm^2 under control conditions (**Figure 3.1A**), with an average platelet surface area of 41.2 ± 1.54 μm^2 per platelet (**Figure 3.1C**) and a total surface area of 2,827.3 ± 232.6 μm^2 covered by all platelets in each imaged field of view (**Figure 3.1D**). Pre-incubation of platelets with the Syk and BTK inhibitors significantly decreased the number of platelets adherent to collagen and the average platelet surface area relative to control. The Syk inhibitor Bay 61-3606 reduced the number of platelets adherent to collagen by 31% ± 2.9% and average platelet surface area by 33.3% ± 3.1% similar to other Syk inhibitors, including R406 (27% ± 3.8% reduction in number, 28% ± 7.6% reduction in surface area) and entospletinib (34% ± 2.9% reduction in number,

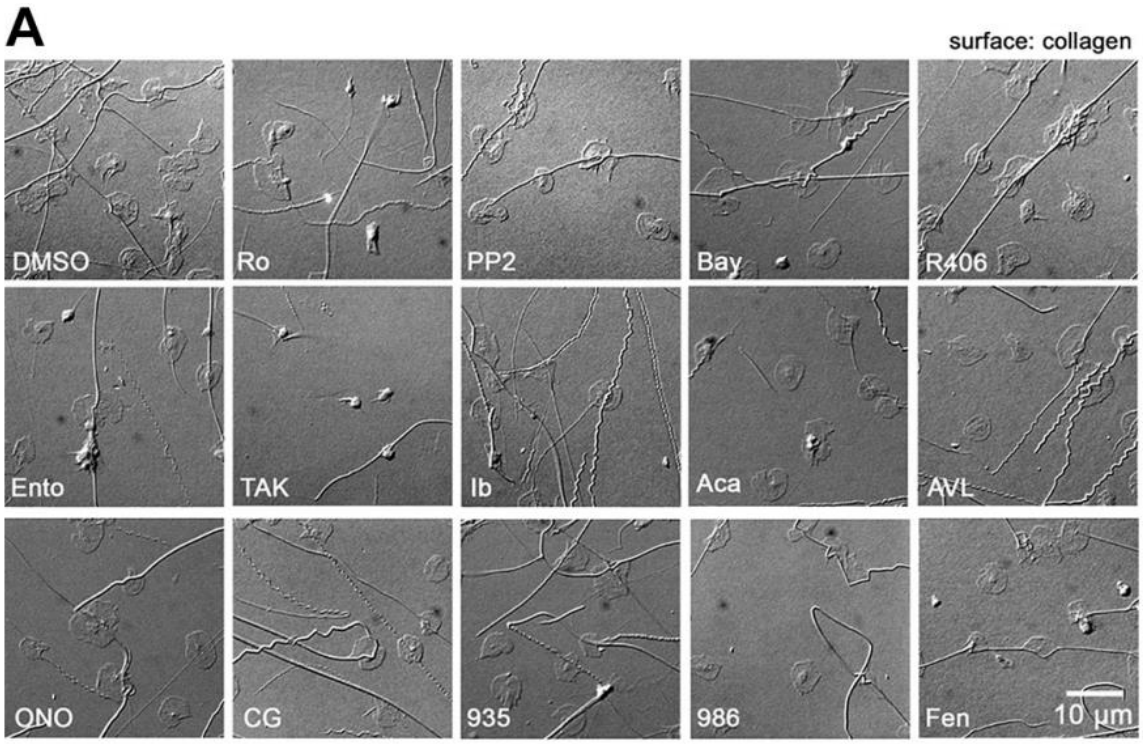

Figure 3.1. Effects of Syk and BTK inhibitors on platelet adhesion to collagen.
(A) Replicate samples (n = 3) of washed human platelets (2×10^7/ml) were treated with the selected Syk and BTK inhibitors (10 μM) or vehicle (0.1 % DMSO) in solution for 10 min and incubated on immobilized collagen-coated (100 μg/ml) glass coverslips for 30 min at 37 °C. After fixation, coverslips were mounted on microscope slides (25 × 75 × 1 mm). Adherent platelets were visualized using Nomarski differential interference contrast (DIC) microscopy at 63,000 × magnification. Images representative of each replicate sample is shown. Scale bar = 10 μm.

21.6% ± 1.9% reduction in surface area); TAK-659 (70% ± 7.5% reduction in number, 91.6% ± 11.5% reduction in surface area) had more pronounced effects (**Figure 3.1B-C**). In an analogous manner, the BTK inhibitor, ibrutinib (52% ± 5.8% reduction in number, 33.5% ± 10% reduction in surface area) reduced platelet adhesion to collagen more than the other BTK inhibitors tested (**Figure 3.1B-C**). Similarly, pre-incubation of platelets with the Syk and BTK inhibitors significantly decreased the total surface area covered by the adherent platelets on collagen (**Figure 3.1D**). Inhibitors of platelet GPVI targeting SFKs (PP2) and protein kinase C (Ro 31-8220)

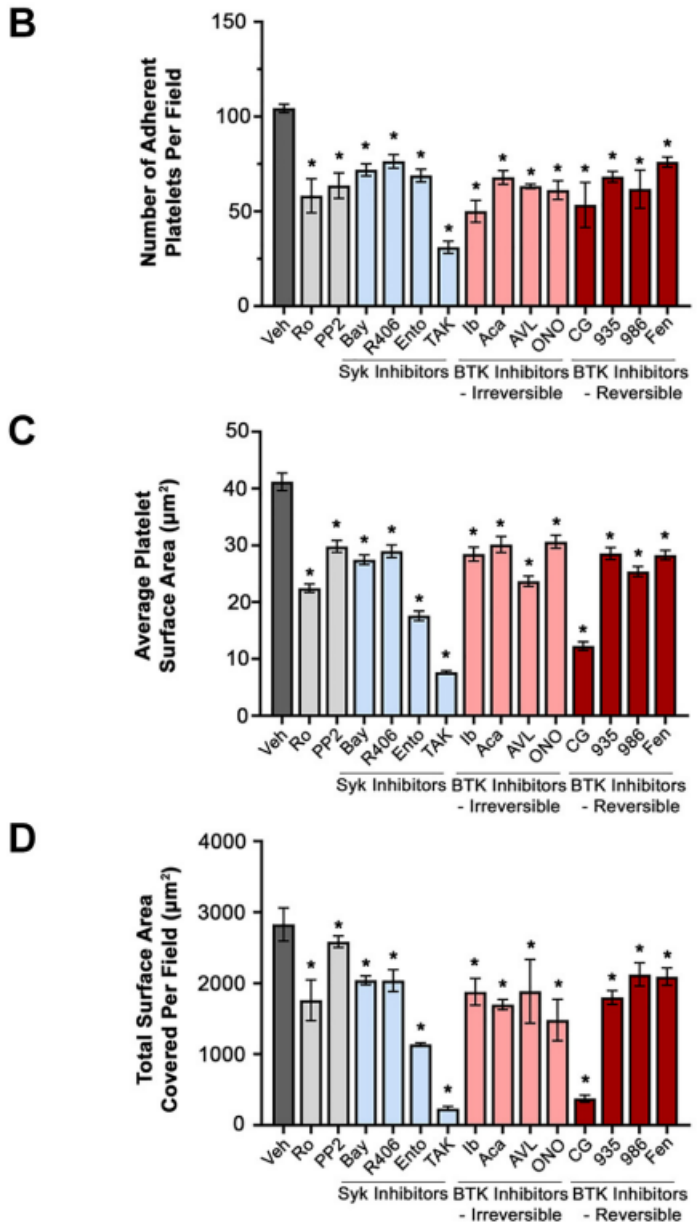

Figure 3.1. Effects of Syk and BTK inhibitors on platelet adhesion to collagen.
(B) Three images of platelets under each TKIs treatment condition were captured and the number of platelets adherent to collagen per field of view (14,587 μm^2) were counted. **(C)** The average surface area of platelets and **(D)** the total surface area covered per imaged field of view were determined using Image J. Data is shown as mean ± SEM; statistical analysis was conducted using a one-way ANOVA test on GraphPad PRISM, where a P value < 0.05 was considered significant, indicated by *.

served as controls and likewise inhibited platelet adhesion to collagen. Together, these results demonstrate that different inhibitors targeting Syk and BTK signaling similarly inhibit the adhesion of platelets to collagen *in vitro*.

3.4.2 Effects of Syk and BTK Inhibitors on GPVI-mediated Granule Secretion and Integrin Activation

Following GPVI activation, platelets secrete adenosine diphosphate (ADP) from dense granules as an autocrine and paracrine activator of platelet purinergic receptors (P2Y1, P2Y12) to progress platelet activation and hemostatic plug formation. We next assessed for platelet dense granule secretion to determine the effects of Syk and BTK inhibitors on GPVI-mediated platelet activation. Following stimulation of platelets with the GPVI-specific agonist CRP-XL in the presence of Chrono-Lume reagent, luminescence was measured over a time course to record the kinetic profile of ATP release as a marker of dense granule secretion. As seen in **Figure 3.2A**, platelets stimulated with CRP-XL secreted dense granule contents (normalized as 1.0 luminescence intensity). Pre-incubation of platelets with Syk and BTK inhibitors prior to stimulation with CRP-XL significantly decreased dense granule release to baseline levels, with the exception of CG-806 which had a less pronounced although still significant effect on platelet ATP release (**Figure 3.2A**). In comparison, pre-incubation of platelets with Syk and BTK inhibitors prior to stimulation with thrombin did not significantly decrease dense granule secretion (**Figure 3.2B**), with the exception of the Syk inhibitor entospletinib, which appeared to interfere with assay luciferase activity for reasons to be determined.(200)

Together, these results suggests that Syk and BTK inhibitors tested selectively block GPVI-mediated dense granule secretion without effects on PAR-mediated platelet activation in response to thrombin.

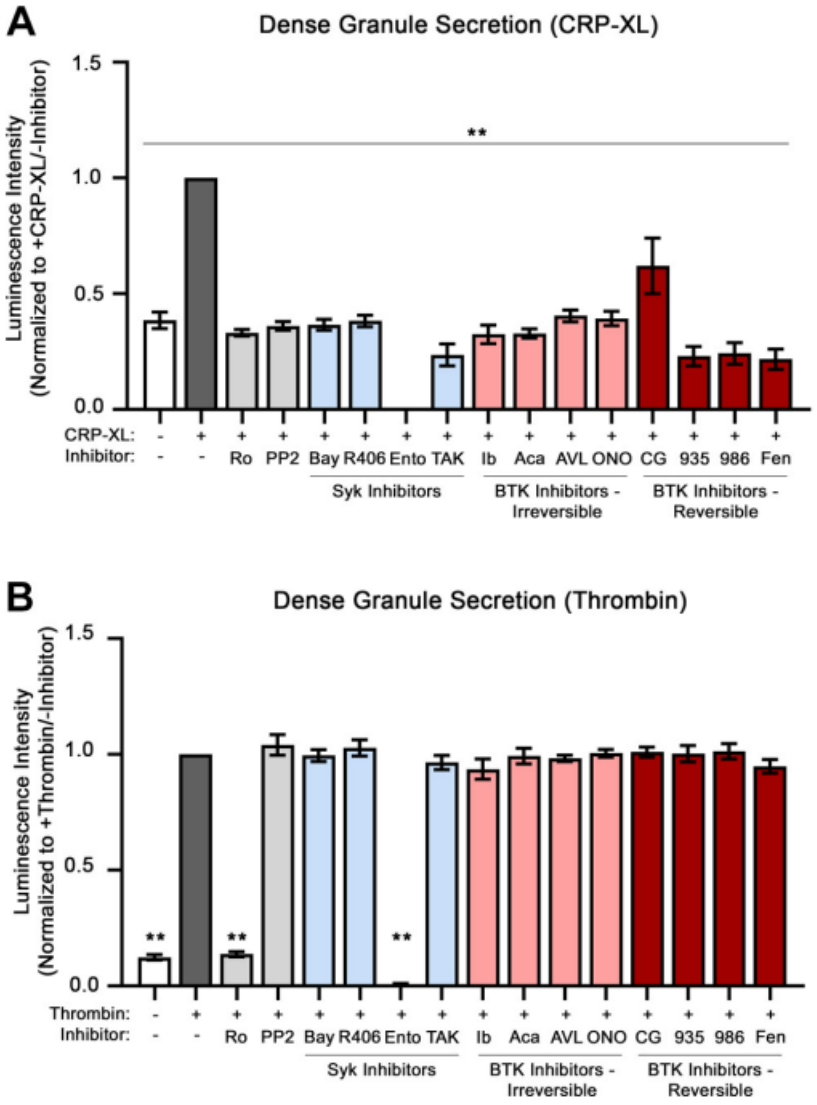

Figure 3.2. Effects of Syk and BTK inhibitors on platelet dense granule secretion. Replicate samples (n = 3) of washed human platelets (2×10^8/ml) were treated with the selected Syk and BTK inhibitors or vehicle (0.1% DMSO) and then stimulated with CRP-XL (10 μg/ml) or thrombin (1 Unit/ml). Platelet samples were monitored using ChromoLume (luciferase enzyme) to measure and record the luminescence kinetics of the dense granule ATP release profile of platelets, at 30 seconds intervals over the course of five minutes. Four kinetic profiles were recorded per platelet sample (n = 3). The average luminescence measured at 240 seconds was calculated and normalized by the average luminescence of the untreated platelets stimulated with CRP-XL or thrombin (+CRP-XL/-inhibitor or +thrombin/-inhibitor). Statistical analysis was performed using one-way ANOVA test on GraphPad PRISM, where a P value < 0.05 was considered significant, indicated by *.

Complementary to ADP secretion from dense granules, activated platelets also mobilize proteins through α-granule secretion, including P-selectin (CD62P). We therefore quantified P-selectin expression via flow cytometry as another marker of GPVI-mediated platelet activation. As seen in **Figure 3.3A** and **Figure 3.4**, stimulation with the GPVI-agonist, CRP-XL, upregulated the percentage of platelets with surface P-selectin from 2.05 ± 0.1% to 19.2 ± 3.4%. Pre-incubation of platelets with the majority of Syk and BTK inhibitors prior to stimulation with CRP-XL significantly decreased platelet surface P-selectin levels relative to control. For instance, the Syk inhibitors, Bay 61-3606 (1.97 ± 0.5%), R406 (3.73 ± 0.5%), entospletinib (2.02 ± 0.5%), and TAK-659 (1.63 ± 0.3%), all significantly reduced the percentage of platelets with P-selectin surface expression following stimulation with CRP-XL. Similarly, BTK inhibitors, including ibrutinib (1.98 ± 0.1%), acalabrutinib (2.17% ± 0.2%), BMS-986195 (1.69 ± 0.1%), and fenebrutinib (1.37 ± 0.1%), all significantly reduced the percentage platelets with surface P-selectin in response to CRP-XL stimulation. Pre-treatment of platelets with the BTK inhibitor CG-806 (19.7 ± 5.7%) did not significantly decrease the exposure of platelet P-selectin following CRP-XL stimulation (**Figure 3.3A**).

As platelets activate in response to GPVI stimulation and feedback from ADP secretion and other factors, downstream pathways promote the "inside-out" activation of the platelet surface integrin $\alpha_{IIb}\beta_3$ to support fibrinogen binding and platelet-platelet aggregation. Resting and CRP-XL stimulated platelets were incubated in solution with FITC-conjugated PAC-1 antibody, which recognizes specifically open active

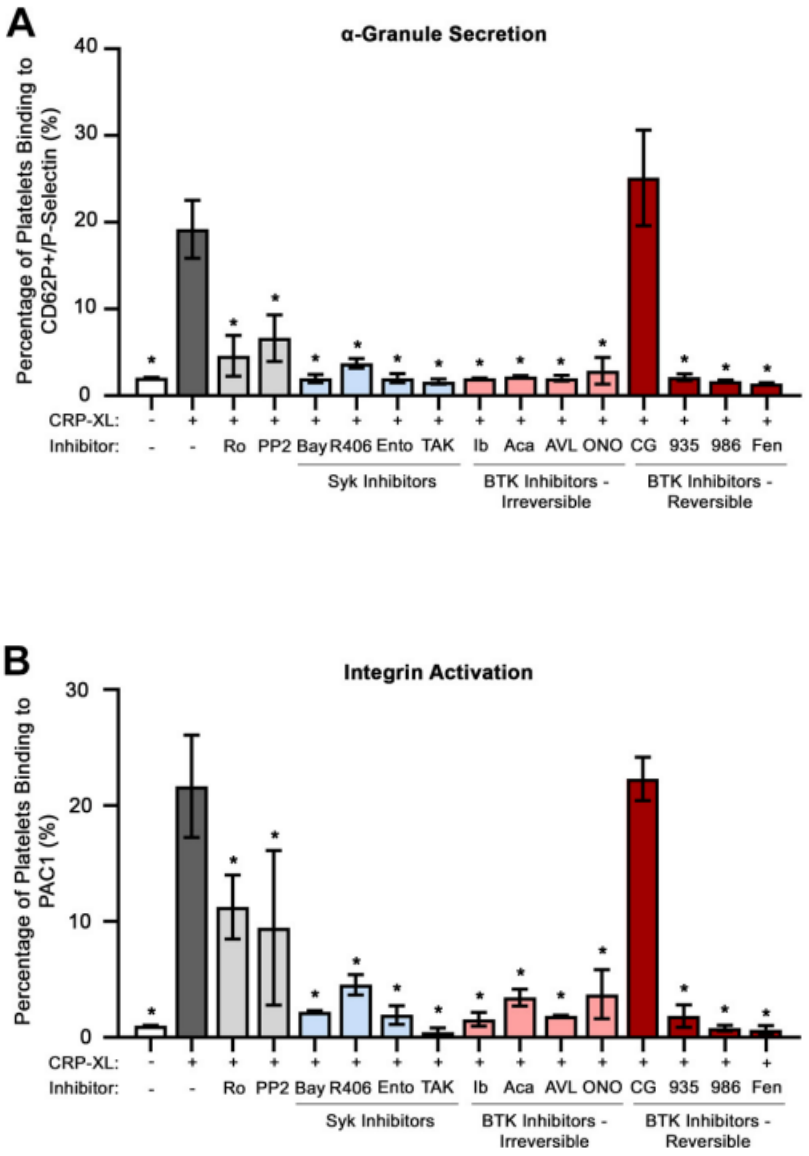

Figure 3.3. Effects of Syk and BTK inhibitors on platelet α-granule secretion and integrin activation. (A) Replicate samples (n = 3) of washed human platelets (2×10^8/ml) were treated with the selected Syk and BTK inhibitors or with vehicle (0.1% DMSO), stimulated with CRP-XL (10 µg/ml), and stained with APC-CD62P and FITC-PAC1 to monitor for platelet surface expression of P-selectin and integrin activation, respectively, using flow cytometry. Thresholds for platelet surface integrin and P-selectin expression were set based on the negative control (-CRP-XL/-inhibitor), such that percentage of expression is 0.5%. Representative FACS traces are depicted in Supplementary Figure S2. Statistical analysis was performed using one-way ANOVA test on GraphPad PRISM, where a P value < 0.05 was considered significant, indicated by *.

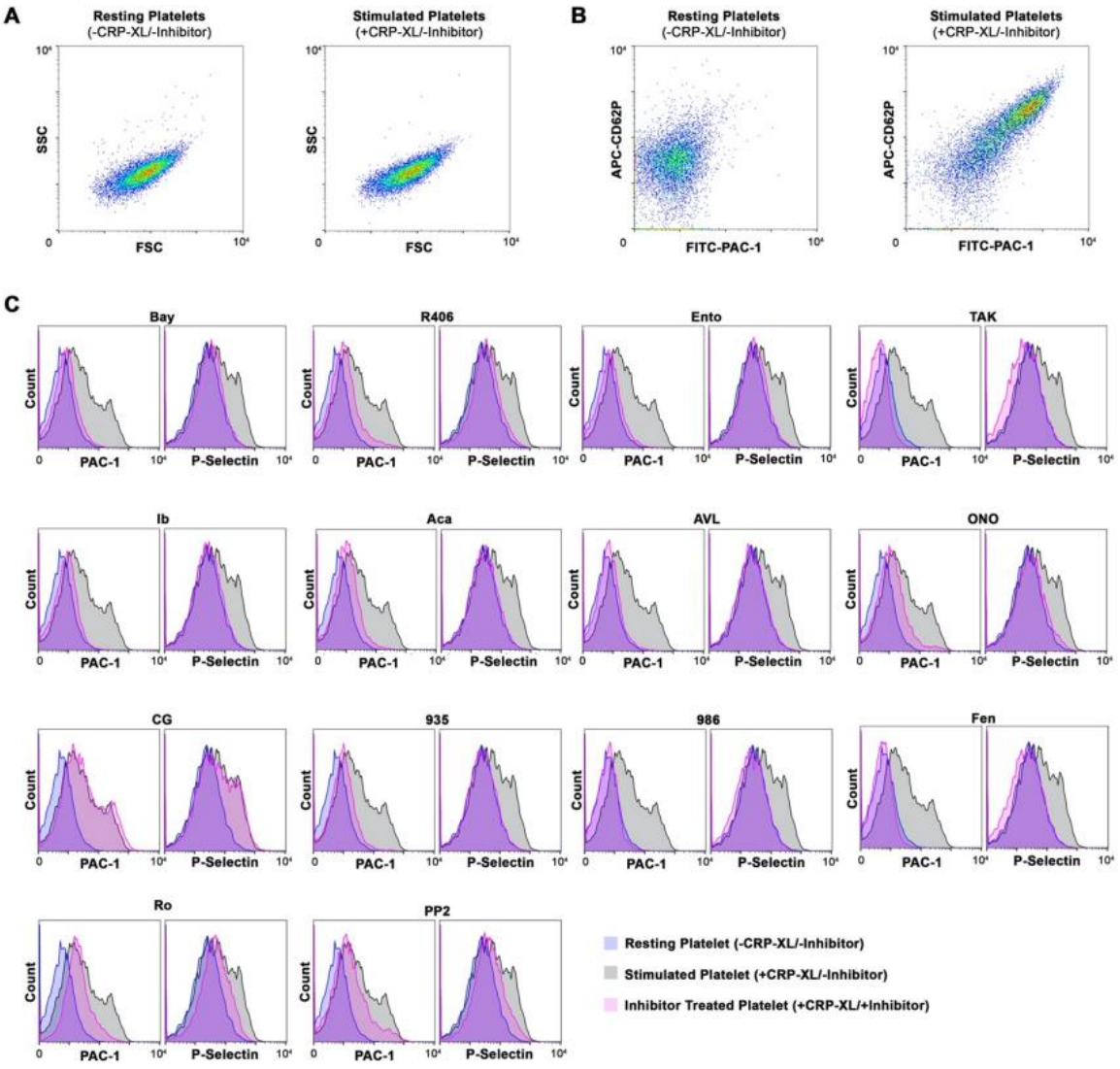

Figure 3.4. Flow cytometry analysis of Syk/BTK inhibitor treated platelet a-granule secretion and integrin activation. (A) Replicate samples (n = 3) of washed human platelets (2 ´ 108/ml) were treated with the selected Syk and BTK inhibitors or with vehicle (0.1% DMSO), stimulated with CRP-XL (10 µg/ml), and stained with APC-CD62P and FITC-PAC1 to monitor for platelet surface expression of P-selectin and integrin activation, respectively, using flow cytometry. (A) Representative fluorescence-activated cell sorting (FACS) traces of forward scatter (FSC) vs. side scatter (SSC) detection in resting platelets (-CRP-XL/-inhibitor) and stimulated platelets (+CRP-XL/-inhibitor) are shown. (B) Representative FACS traces of FITC-PAC1 vs. APC-CD62P detection in resting platelets (-CRP-XL/-inhibitors) and stimulated platelets (+CRP-XL/-inhibitors) are shown. (C) Representative FACS traces of platelets stained with APC-CD62P and FITC-PAC1 to monitor for platelet surface expression of P-selectin and integrin activation, respectively, are shown for each inhibitor treatment.

conformation of human integrin $\alpha_{IIb}\beta_3$ to monitor platelet surface integrin $\alpha_{IIb}\beta_3$ activation using flow cytometry. As seen in **Figure 3.3B**, the percentage of platelets binding PAC-1 increased in response to CRP-XL stimulation from 2.03 ± 0.03% to 43.3 ± 8.8%. Pre-incubation of platelets with the majority of Syk and BTK inhibitors prior to stimulation with CRP-XL significantly decreased platelet PAC-1 binding in response to CRP-XL. However, like P-selectin surface exposure, the BTK inhibitor CG-806 (33.5% ± 11.0%) did not significantly decrease platelet PAC-1 binding in response to CRP-XL (**Figure 3.3B**).

3.4.3 Effects of Syk and BTK Inhibitors on PKC and PI3K/Akt Proximal Signaling Events

Following activation of GPVI, a Syk-dependent signaling cascade leads to formation of the LAT signalosome and activation of PLCγ2, BTK, PKC, PI3K/Akt and other effectors to mediate platelet adhesion, secretion, and other responses. To determine the effects of the Syk and BTK inhibitors on the Syk-BTK-PI3K signaling axis, we next examined the effects on intracellular phosphorylation events downstream of GPVI activation. Under vehicle-treated conditions, CRP-XL stimulation upregulated the phosphorylation of several markers of GPVI activation, including Syk Y_{525}, BTK Y_{551}, DAPP1 Y_{139}, PLCγ2 Y_{1217}, Akt T_{308} and Akt S_{473}, as well as generalized PKC and Akt substrates (**Figure 3.5**). Pre-incubation of platelets with PP2 (a well-established inhibitor of signaling events downstream of GPVI activation) inhibited the CRP-XL evoked phosphorylation of all substrates examined. Pre-treatment of platelets with the PKC inhibitor Ro 31-8220 prevented the phosphorylation of PKC substrates in response to CRP-XL, with minimal

effects on the upstream phosphorylation of Syk, BTK, and PLCγ2 as well as divergent Akt signaling pathways.

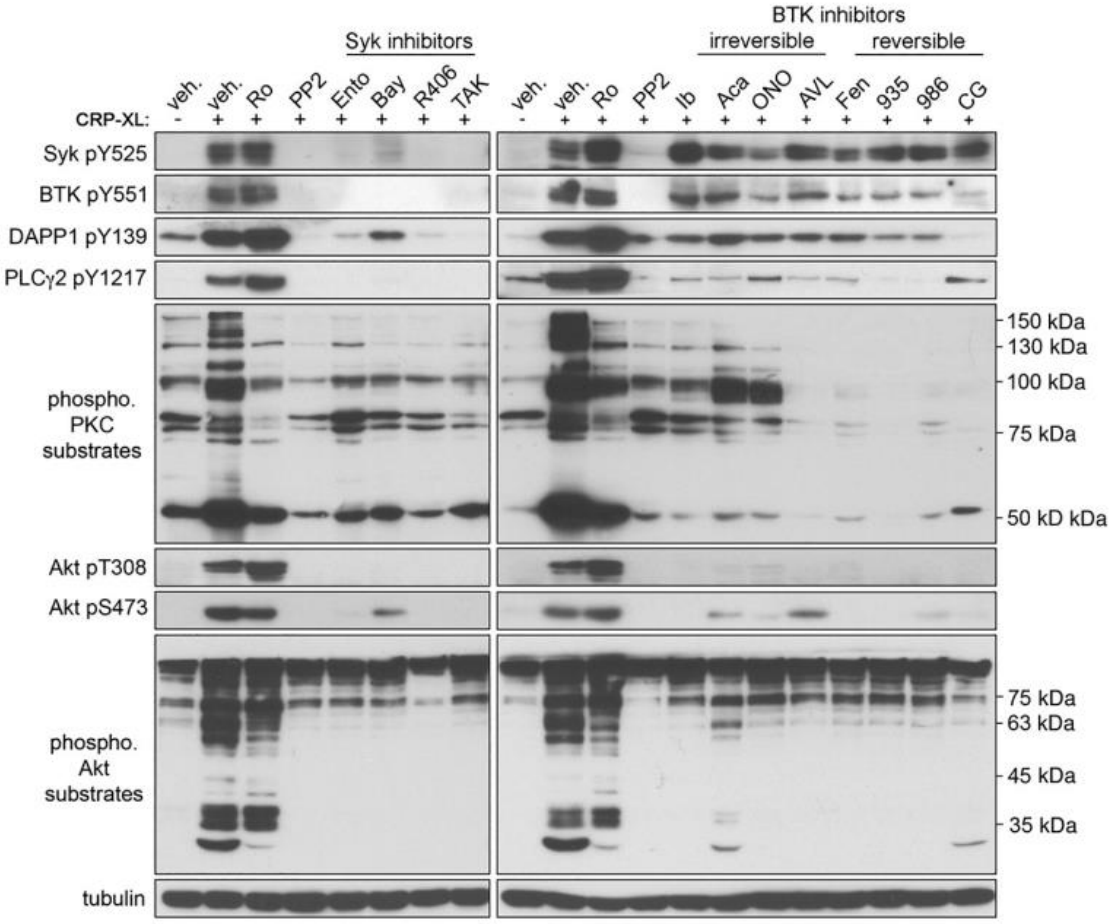

Figure 3.5. Effects of Syk and BTK inhibitors on platelet activation signaling proteins. Replicate samples (n = 3) of purified, washed human platelets (1×10^9/ml) were incubated with the selected Syk and BTK inhibitors or with (0.1% DMSO) in solution and stimulated with CRP-XL. After collection into Laemmli sample buffer, platelet lysates were separated by SDS-PAGE and transferred to nitrocellulose. Western blots were conducted using antibodies for phosphorylated Syk Y_{525}, BTK Y_{551}, DAPP1 Y_{139}, PLCγ2 Y_{1217}, Akt T_{308}, Akt S_{473}, Akt substrates and PKC substrates; α-tubulin serves as a loading control. Positions of molecular weight (kD) markers relative to phosphorylated PKC and Akt substrates are indicated. Results representative of n = 4 experiments are shown.

Previous studies have examined the effects of several Syk and BTK inhibitors including R406 and ibrutinib on platelet GPVI signaling (84, 201, 202); however, comparative analyses of these and other related agents have not yet been carried out. Additionally, a number of "next generation" Syk and BTK inhibitors (i.e. TAK-659, BMS-986195) have not yet been studied for effects on platelet signaling. As seen in **Figure 3.5**, pre-incubation of platelets with Syk inhibitors (entospletinib, Bay 61-3606, R406, TAK-659) eliminated CRP-XL evoked auto-phosphorylation of Syk Y_{525} as well as the downstream phosphorylation of BTK Y_{551} and PLCγ2 Y_{1217}. Pre-treatment of platelets with all the Syk inhibitors also prevented the phosphorylation Akt and associated Akt substrates in platelets in response to GPVI activation (**Figure 3.5**). All Syk inhibitors tested likewise prevented the phosphorylation of DAPP1 Y_{139} as well as PKC substrates following GPVI activation. However, the extent of inhibition suggested some inhibitor-specific variation; for example, the degree of inhibition of DAPP1 Y_{139} phosphorylation was reduced for entospletinib and Bay 61-3606 relative to TAK-659 and R406, despite complete inhibition of upstream activating phosphorylation of Syk Y_{525} and BTK Y_{551} by these Syk inhibitors (**Figure 3.5**).

As seen in **Figure 3.5**, pre-treatment of platelets with eight different BTK inhibitors also prevented BTK-mediated phosphorylation of PLCγ2 Y_{1217} without altering upstream Syk autophosphorylation of Syk Y_{525} in response to CRP-XL stimulation. However, BTK inhibitors had varying effects on the phosphorylation of PKC substrates in response to CRP-XL stimulation, where AVL-292, fenebrutinib, BMS-935177, BMS-986142, and CG-806 had more potent inhibitory effects compared to ibrutinib, acalabrutinib, and

ONO-4059. Overall, the effects of all BTK inhibitors on DAPP1 Y_{139} phosphorylation were less than those of Syk inhibitors; however, CG-806, which completely inhibited CRP-evoked DAPP1 phosphorylation, did not without fully inhibit PLCγ2 and Akt substrate phosphorylation. Together, these results demonstrate that all 12 Syk and BTK inhibitors examined in this chapter have inhibitory effects on GPVI-mediated activation of Syk and BTK, as expected; however, some downstream phosphorylation events may be altered in an inhibitor specific manner.

3.4.4 Effects of Syk and BTK Inhibitors on Platelet Integrin Activation and Spreading on Fibrinogen

Complementary to signaling events downstream of GPVI activation, fibrinogen binding to the platelet integrin $\alpha_{IIb}\beta_3$ invokes a parallel "outside-in" ITAM-mediated signaling cascade also involving Syk and BTK as well as PKC, PI3K/Akt and other related pathways to mediate cytoskeletal assembly and platelet aggregation (203). We assessed these platelet integrin activation responses *in vitro* by determining the ability of purified platelets to spread on surfaces of immobilized fibrinogen in the presence of Syk and BTK inhibitors. Washed, purified platelets (2×10^7/ml) were treated with selected Syk and BTK inhibitors or vehicle (0.1% DMSO) in solution, prior to incubation on fibrinogen-coated coverslips (37°C, 45 min). Platelets were then visualized by DIC microscopy to assess the extent of spreading on fibrinogen, determined by the average surface area per adherent platelet. As seen in **Figure 3.6A**, platelets readily adhered to fibrinogen-coated coverslips and spread to a mean surface area of 33.3 ± 0.6 μm^2 per platelet (**Figure 3.6B**). Pre-incubation of platelets with PP2, Ro 31-8220, or TKIs targeting Syk and BTK

significantly decreased the mean surface area of platelets adherent to fibrinogen (**Figure 3.6B**). However, inhibitor-specific variations were observed for the distribution frequency of platelet surface areas for each inhibitor (gray curves in **Figure 3.6C**, relative to control, white curve). For instance, while the Syk inhibitors Bay 61-3606 (22.9 ± 0.5 μm^2 in surface area) and R406 (24.1 ± 0.4 μm^2) inhibited platelet spreading to a similar extent, Syk inhibitor TAK-659 (20 ± 1 μm^2) and entospletinib (20.3 ± 0.5 μm^2) further reduced platelet spreading (**Figure 3.6B**), shifting the distribution of platelet surface areas towards lower values relative to controls (**Figure 3.6C**). Similarly, while BTK inhibitor ONO-4059 (25.8 ± 0.6 μm^2), BMS-935177 (24.0 ± 1.8 μm^2), and fenebrutinib (24.2 ± 1.0 μm^2) inhibited platelet spreading to a similar extent, BTK inhibitor ibrutinib (21.1 ± 0.5 μm^2), AVL-292 (20.3 ± 0.4 μm^2), and BMS-986195 (20.4 ± 0.8 μm^2) reduced platelet spreading to an even greater extent. Despite limiting the spreading of some platelets, the BTK inhibitors CG-806 and fenebrutinib had less pronounced effects on mean platelet surface areas (31.0 ± 0.4 μm^2) (**Figure 3.6B**), while broadening the distribution of measured platelet surface areas (**Figure 3.6C**). Together, these results demonstrate that all Syk and BTK inhibitors examined in this chapter have inhibitory effects on platelet spreading on fibrinogen.

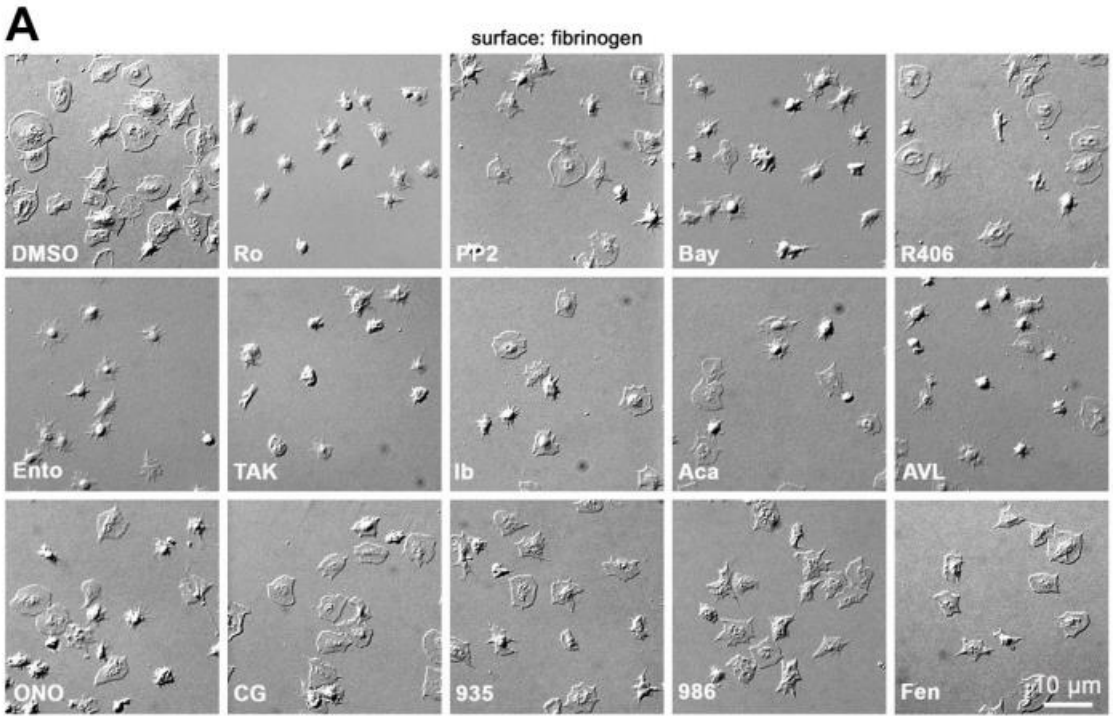
A
surface: fibrinogen
DMSO
Ro
PP2
Bay
R406
Ento
TAK
Ib
Aca
AVL
ONO
CG
935
986
Fen
10 µm

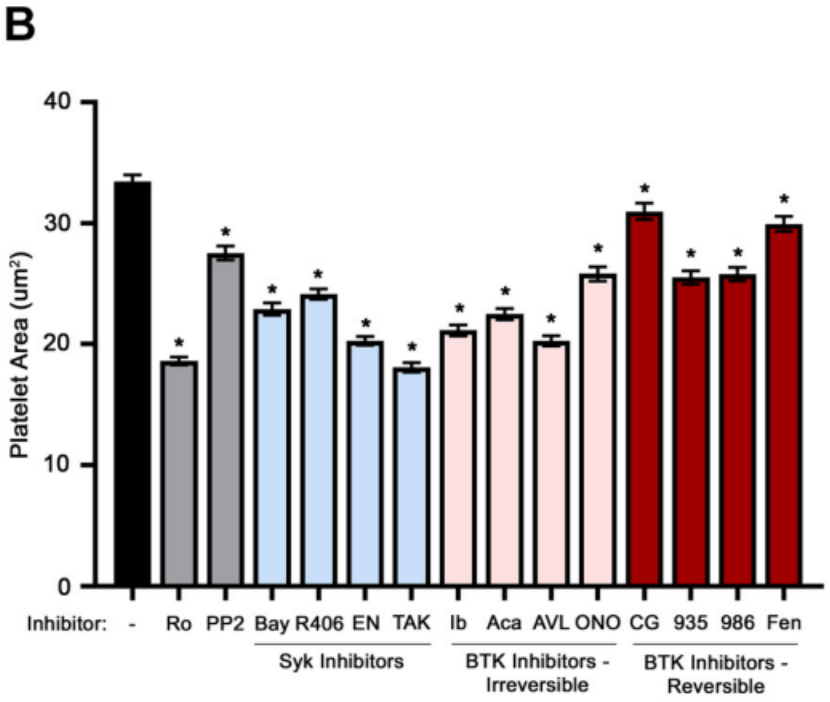
B
Platelet Area (um²)
40
30
20
10
0
Inhibitor: - Ro PP2 Bay R406 EN TAK Ib Aca AVL ONO CG 935 986 Fen
Syk Inhibitors
BTK Inhibitors - Irreversible
BTK Inhibitors - Reversible

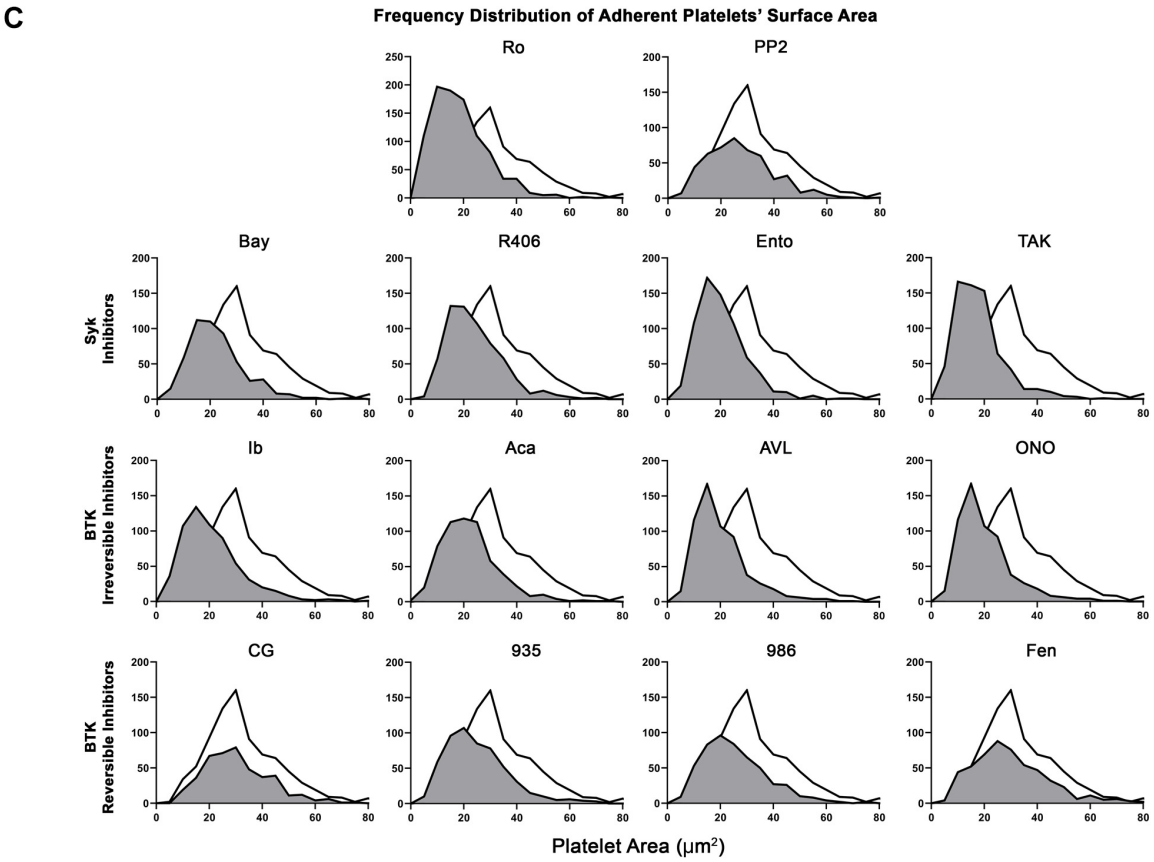

Figure 3.6. Effects of Syk and BTK inhibitors on platelet spreading on fibrinogen. **(A)** Replicate samples (n = 3) of washed human platelets (2×10^7/ml) were incubated with the selected Syk and BTK inhibitors or vehicle (0.1% DMSO) for 10 min and incubated on a fibrinogen coated glass cover glass at 37 °C for 45 min. After fixation, adherent platelets were visualized using differential interference contrast (DIC) microscopy. Images representative of each replicate sample is shown. Scale bar = 10 μm. **(B)** Images were analyzed with Image J software to determine the per platelet surface areas (μm^2) of adherent platelets per inhibitor condition. Data is shown as mean ± SEM; statistical analysis were conducted using a one-way ANOVA test on GraphPad PRISM, where a P value < 0.05 was considered significant, indicated by *. **(C)** Frequency distribution plots numbers of platelets (y-axis) vs. measured individual platelet surface area (μm^2 – x axis) for each inhibitor condition tested.

3.4.5 Effects of Syk and BTK Inhibitors on PI3K Spatial Localization in Platelets

Together, experiments above suggest that TKIs targeting Syk and BTK inhibit essential platelet adhesion and secretion responses, with potential differential effects on downstream PI3K and PKC signaling events important to the kinetics of platelet activation and spreading on fibrinogen. Previous studies from our group and others have shown that SFK-driven Syk and BTK signaling regulates a (de)polymerization of platelet microtubules in manner orchestrating platelet activation (204-208). More recently, we also showed that PKC signaling events take place in physical proximity to platelet microtubules in a manner related to platelet Rho GTPase regulation and spreading on fibrinogen (188, 190, 209). Interestingly, classical studies of PI3K signaling also noted a localization of the PI3K p85 regulatory subunit at microtubules (210, 211) in a manner supporting signaling events important to cell adhesion (212). Previous studies have likewise noted a dramatic increase in PI3K p85 subunit in cytoskeletal fractions of activating platelets (213), but relationships between PI3K localization and signaling mechanisms in activating platelets have not yet been established.

To further determine the effects of Syk and BTK inhibitors on intracellular signaling events and platelet cell physiology *in vitro*, we examined the organization of key signaling molecules in activated platelets with fluorescence microscopy. Previous studies from our group and others have noted an association between PI3K and PKC signaling systems and microtubules in platelets and other cell types (190, 210, 211). As seen in **Figure 3.7**, PI3K p85α regulatory subunit colocalized with microtubules (α-tubulin) in platelets adherent to fibrinogen. To quantify the localization, a Pearson's coefficient

(PCC) is determined as the degree of fluorescence intensity correlation between the tubulin signal in channel 1 with PI3K or PKC signal in channel 2 and Mander's overlap coefficient (MOC) is determined as the percentage of overlap between the two channels. The PCC was found to be 0.834 ± 0.0216 and MOC of 0.76 ± 0.02. The colocalization of PI3K and α-tubulin was related to microtubule structure, as treatment of platelets with nocodazole (microtubule destabilizer) significantly decreased the association between PI3K and α-tubulin (PCC = 0.67 ± 0.02; MOC = 0.66 ± 0.04), while taxol (microtubule stabilizer) significantly increased their association (PCC = 0.9 ± 0.01; MOC =0.93 ± 0.01). As seen in **Figure 3.7B** and **Figure 3.7C**, pretreatment of platelets with Syk and BTK inhibitors significantly affected the colocalization of PI3K and α-tubulin, where reversible BTK inhibitors had the strongest effects. Specifically, the PCC was decreased (in which Bay, BMS935, and BMS986 were significant), suggesting that the correlation between tubulin and PI3K fluorescence intensity was decreased. In addition, all the Syk and BTK inhibitors tested significantly increased the MOC. This indicates a higher degree of overlap between tubulin and PI3K in platelets treated with the select inhibitors, suggesting that PI3K becomes more dispersed in relation to tubulin when treated with the select Syk and BTK inhibitors. Similarly, Syk and BTK inhibitors also had significant effects on the organization and colocalization of PKC with microtubules in platelets adherent to fibrinogen (**Figure 3.8**). Together, these results suggest a relationship between microtubule organization and PI3K and other signaling systems in platelets, where small molecules targeting Syk and BTK may alter the localization of platelet signaling proteins in a manner specific to the inhibitor's pharmacology (**Figure 3.7** and **Figure 3.8**) (214).

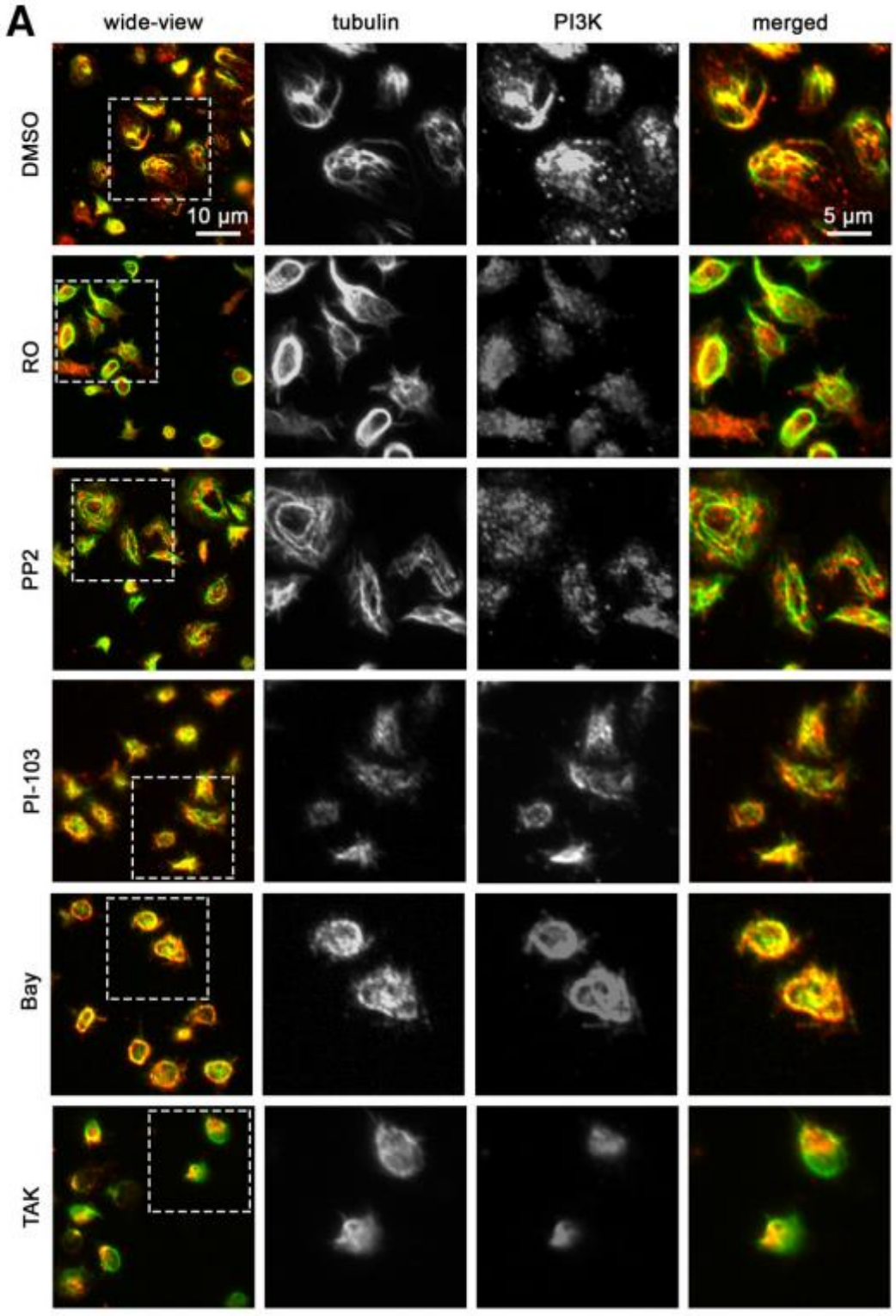
A
wide-view
tubulin
PI3K
merged
DMSO
RO
PP2
PI-103
Bay
TAK
10 µm
5 µm

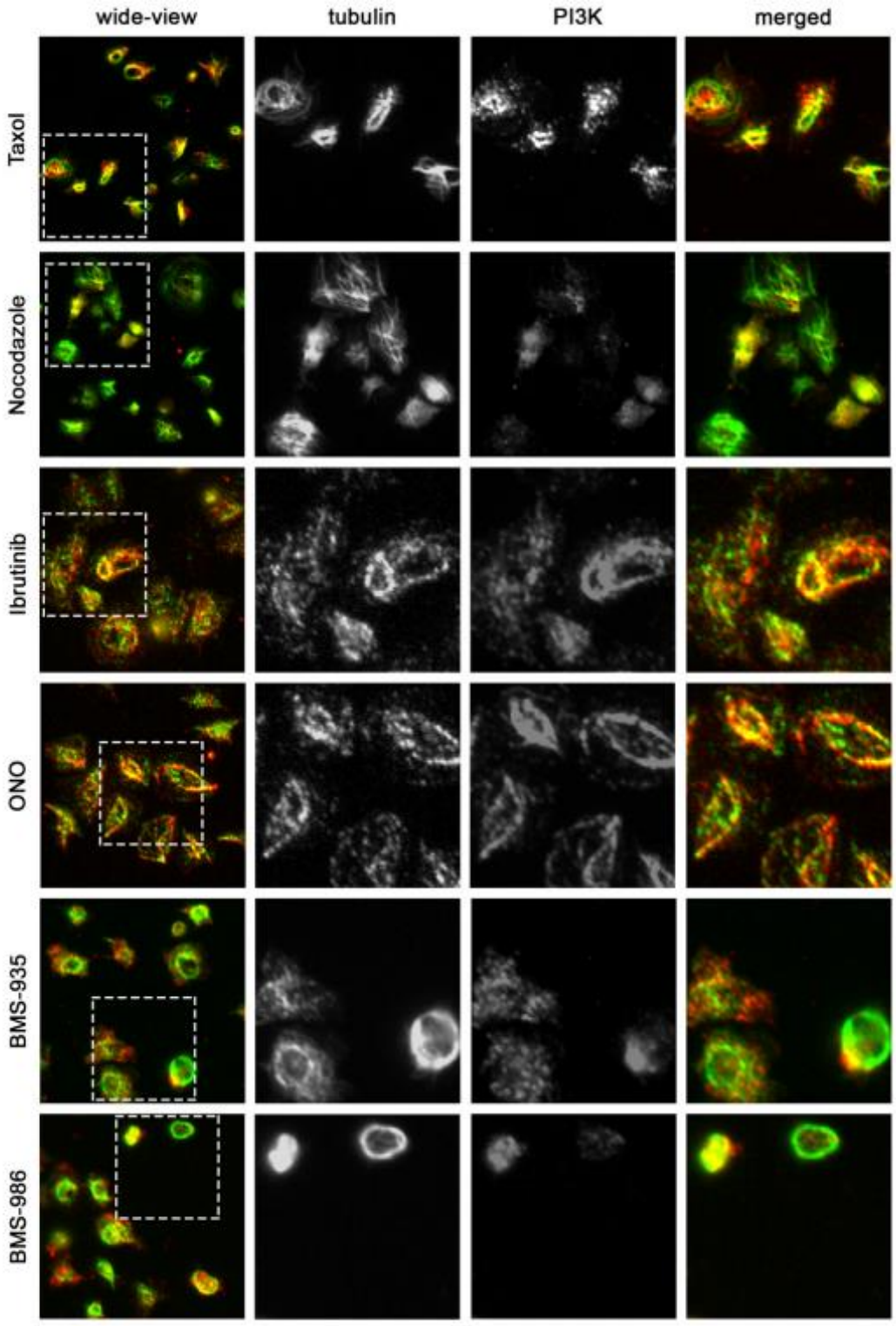
wide-view
tubulin
PI3K
merged
Taxol
Nocodazole
Ibrutinib
ONO
BMS-935
BMS-986

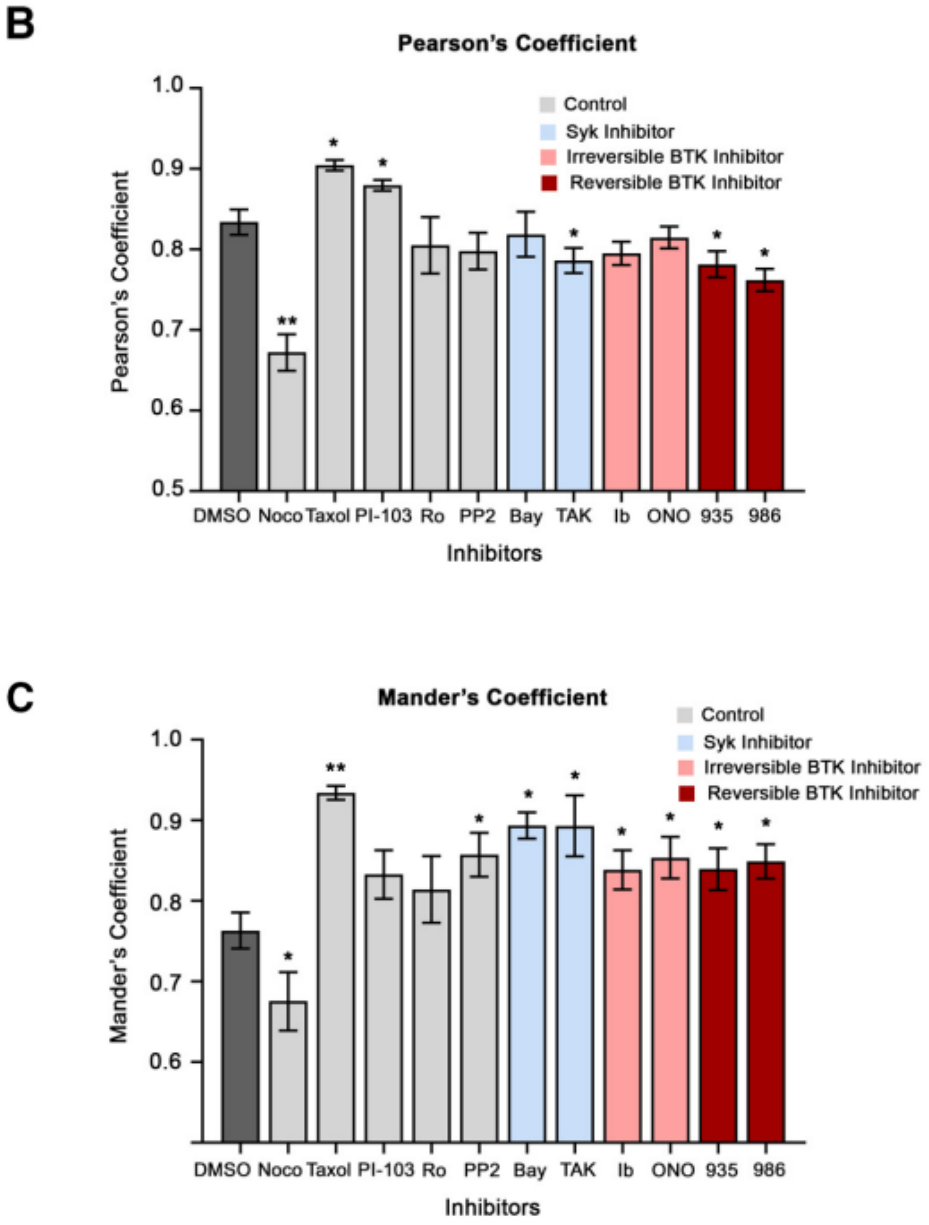

Figure 3.7. Effects of Syk and BTK inhibitors on platelet microtubules and PI3K organization. Replicate samples (n = 3) of washed human platelets (2×10^7/ml) were treated with the selected Syk or BTK inhibitors or vehicle (0.1% DMSO) for 10 min and incubated on fibrinogen coated cover glass at 37°C for 45 min. Platelets are fixed and stained for p85 PI3K (green) and microtubules (red) with anti-p85 PI3K (Santa Cruz) and anti-α-tubulin (Sigma T6199) primary antibodies. **(A)** Adherent platelets were visualized using fluorescence microscopy. Images were quantified using a custom MATLAB script to determine **(B)** the Pearson's correlation coefficient and **(C)** the Mander's overlap coefficient. Data is shown as mean ± SEM; statistical analysis were conducted using a one-way ANOVA test on GraphPad PRISM, where a P value < 0.05 was considered significant, indicated by *. Images representative of replicate (n = 3) samples are shown. Scale bar = 10 µm.

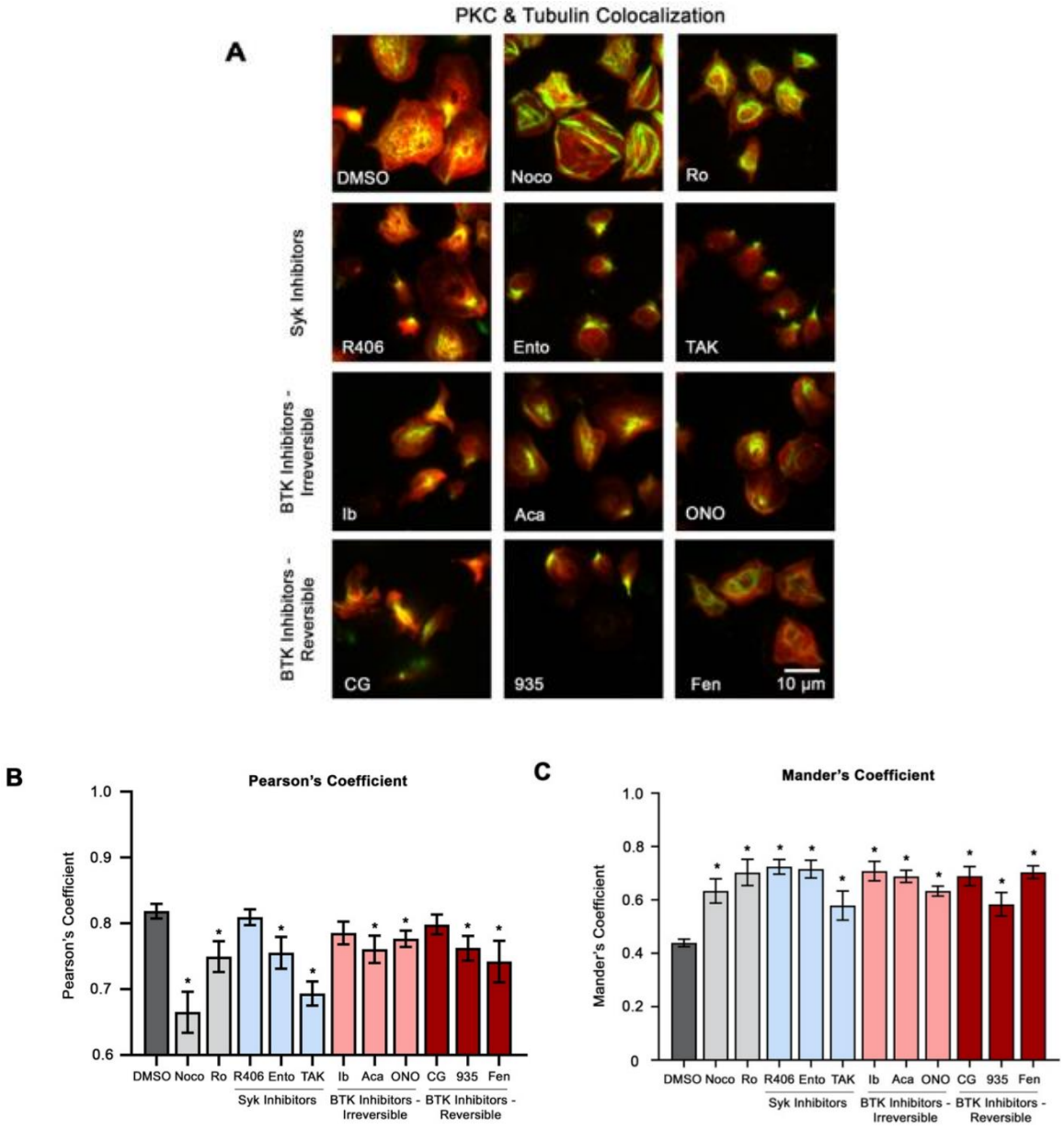

Figure 3.8. Effects of Syk and BTK inhibitors on platelet microtubules and PKC organization. Replicate samples (n = 3) of washed human platelets (2 ´ 107/ml) were treated with the selected Syk or BTK inhibitors or vehicle (0.1% DMSO) for 10 min and incubated on fibrinogen coated cover glass at 37°C for 45 min. Platelets are fixed and stained for PKC (red) and microtubules (green) with anti-PKC (Santa Cruz) and anti-α-tubulin (Sigma T6199) primary antibodies. (A) Adherent platelets were visualized using fluorescence microscopy. Images were quantified to determine (B) the Pearson's correlation coefficient and (C) the Mander's overlap coefficient. Statistical analysis was performed using one-way ANOVA test on GraphPad PRISM, where a P value < 0.05 was considered significant and indicated by *. Images representative of replicate (n = 3) samples are shown. Scale bar = 10 µm.

3.4.6 Effects of Syk and BTK Inhibitors on Platelet under Physiological Flow

To investigate the effects of Syk and BTK inhibitors on platelet function under additional physiological conditions, we assessed for platelet adhesion and platelet aggregation under continuous human venous blood flow conditions. To do this, whole blood was pre-treated with a subset of selected TKIs including entospletinib, ibrutinib, and fenebrutinib and perfused through a glass capillary tube coated with fibrillar collagen. Following blood perfusion, resulting platelet aggregates were imaged with DIC microscopy to acquire Z-stacks. As seen in **Figure 3.9A**, platelets from whole blood treated with vehicle alone readily adhered to collagen surfaces under physiological venous flow and formed robust platelet aggregates, with an average total surface area of 4270 ± 112 μm^2 (**Figure 3.9B**) and an average total volume of 13,600 ± 931 μm^3 (**Figure 3.9C**) per imaged field of view. Pre-treatment of whole blood with TKIs entospletinib (3640 ± 500 μm^2), ibrutinib (3310 ± 368 μm^2), and fenebrutinib (4390 ± 903 μm^2) did not significantly affect the adhesion or total surface area of platelets (**Figure 3.9B**). In contrast, when pre-treated with the selected TKIs, entospletinib (9290 ± 1150 μm^3, 31.9% reduction), ibrutinib (6630 ± 414 μm^3, 51.4% reduction), and fenebrutinib (8560 ± 899 μm^3, 37.3% reduction), all significantly reduced the platelet aggregates' total volume (**Figure 3.9C**). This suggests that in a more physiological setting, the subset of Syk and BTK inhibitors tested reduced platelet aggregation, but preserved platelet adhesion to collagen under human venous flow.

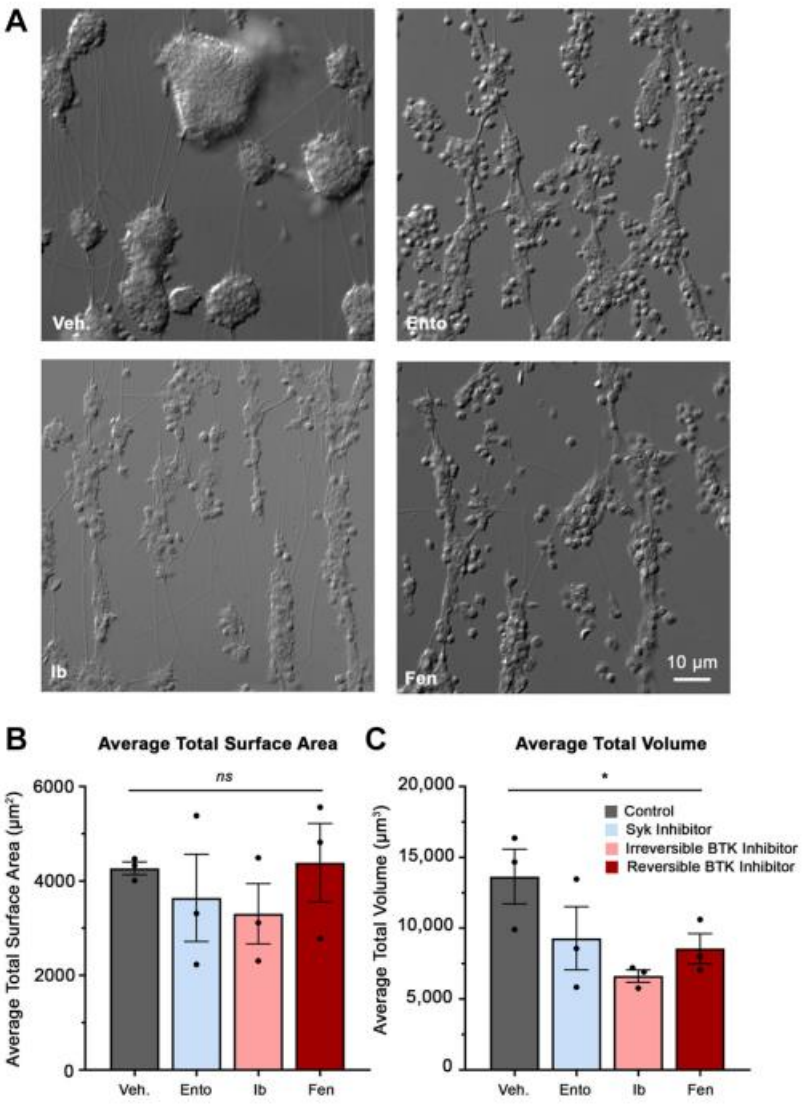

Figure 3.9. Effects of Syk and BTK inhibitors on platelet adhesion and platelet aggregation under physiological flow conditions. Replicate samples (n = 3) of human venous whole blood were pre-treated with a subset of Syk and BTK inhibitors, including entospletinib, ibrutinib, and fenebrutinib (10 µM) or vehicle (0.1% DMSO) for 10 min. Sample was then perfused through a glass capillary tube (0.2 × 2 × 200 mm) coated with fibrillar collagen (100 µg/ml) at a venous shear rate of 300 s^{-1} for 10 min. **(A)** Following blood perfusion, resulting platelet aggregates are imaged using Z-stack microscopy. Using a custom MATLAB script, the Z-stack images were processed to determine the platelet aggregates' **(B)** total surface area and **(C)** total volume per imaged field of view for each treatment condition. Data is shown as mean ± SEM; statistical analysis were conducted using a one-way ANOVA test on GraphPad PRISM, where a P value < 0.05 was considered significant, indicated by *.

3.5 Discussion

In this chapter, we examined the effects of 12 different tyrosine kinase inhibitors (TKIs) targeting Syk and BTK signaling on human platelet function. We find that *in vitro*, four different Syk inhibitors and eight different BTK inhibitors all reduced platelet adhesion to collagen and dense granule secretion while having a more varied range of effects on alpha granule secretion, integrin activation, and PI3K/Akt and PKC signaling downstream of Syk-BTK. Under physiological flow conditions, selected subset of TKIs inhibited platelet aggregation, but preserved platelet adhesion. Our results provide insight on the mechanisms of Syk and BTK inhibitors on platelets, while also illuminating aspects of platelet cell physiology around the Syk-BTK-PI3K signaling axis.

Over the past decade, small molecule TKIs targeting Syk (i.e., fostamatinib) and BTK (i.e., ibrutinib) have emerged as effective agents in the treatment of hematopoietic malignancies and autoimmune and inflammatory disorders (76, 180, 181, 215). The Syk inhibitor fostamatinib (R406) was originally identified as an inhibitor FcεRI mast cell degranulation (216). The BTK inhibitor ibrutinib (PCI-32765) was developed as an inhibitor of B cell receptor signaling to treat B cell lymphoma and autoimmune diseases. Ibrutinib further demonstrated a proof of concept that small molecules that covalently target Cys residues proximal to active sites in Tec family kinases (Cys 481) could serve as a means to covalently and irreversibly inhibit kinases with high potency and selectivity (217). BTK inhibitors such as ibrutinib (202) and acalabrutinib (218) are far more commonly associated with platelet inhibition and bleeding in comparison to fostamatinib and other Syk inhibitors (73, 215) for reasons that remain unexplored.

To this end, this chapter aimed to investigate the effects of 12 clinically relevant Syk and BTK inhibitors. For this study, four Syk inhibitors (Bay, R406, Ento, TAK), four irreversible BTK inhibitors (ibrutinib, acalabrutinib, AVL, tirabrutinib), and four reversible BTK inhibitors (CG, BMS935, BMS896, fenebrutinib) are evaluated and compared. Within each group, a range of first generation to third generation inhibitors are selected. For instance, ibrutinib is a first generation irreversible BTK inhibitor with a reported IC50 value of 0.5 nM, while remaining selective with an IC50 value for Syk > 10,000 nM. Similarly, acalabrutinib is a second generation irreversible BTK inhibitor with lesser potency, but greater specificity towards BTK. It inhibits BTK with a reported IC50 value of 3 nM, with no reported inhibition on Syk. The IC50 values for each Syk and BTK inhibitor used in this study are listed in Table S1 detailing its specificity and potency in addition to secondary kinases that each drug inhibits.

Syk and BTK are well known components of platelet GPVI signaling. Numerous studies have demonstrated that small molecule inhibitors targeting Syk and BTK have antiplatelet effects *in vivo* and inhibiting platelet aggregation *in vitro* (36, 177, 201, 219, 220). However, while several Syk and BTK inhibitors have been examined for inhibitory effects against platelet aggregation, specific mechanistic effects of inhibitors on platelet signaling, adhesion, secretion and other cell physiological factors have only been minimally examined for a number of compounds apart from more commonly studied agents such as ibrutinib and fostamatinib (R406). Given the key role of BTK in platelet GPVI-mediated signaling, it is unsurprising that ibrutinib use may inhibit platelet

function *in vivo*. However, ibrutinib was early on found to be associated with bleeding in a manner perhaps beyond expected from platelet GPVI signaling alone (182), especially given the lack of bleeding in patients with BTK mutations X-linked agammaglobulinemia (XLA) as well as BTK knockout mouse models (36). Moreover, pharmacological inhibitors of Syk are not typically associated with bleeding (221), despite inhibiting BTK activation and PLCγ2 phosphorylation, including fostamatinib which has a relatively promiscuous off-target profile. Similar unexpected off target effects such as atrial fibrillation was also noted for BTK inhibitors, but not Syk inhibitors (222). Moreover, few studies have examined the effects of inhibitors relative to one another simultaneously in parallel.

Historically, studies of Syk and BTK inhibition have helped to illuminate physiologically relevant signaling mechanisms in platelets and other blood cells through *in vivo* as well as *in vitro* studies (36, 223). In this chapter, we find that 12 different Syk and BTK inhibitors all effectively inhibit *in vitro* platelet adhesion to collagen (**Figure 3.1**), GPVI-evoked dense granule secretion (**Figure 3.2**), and GPVI-mediated signaling (**Figure 3.5**). All Syk and BTK inhibitors examined also similarly significantly inhibited platelet α-granule secretion and integrin activation following CRP-XL stimulation, with the exception of CG-806 (224), a next generation reversible BTK inhibitor that does not target Tec, but does inhibit a number of therapeutically relevant kinases (FLT3, TRKA, etc.) (224). These results suggest that a range of different Syk and BTK inhibitors all similarly inhibit essential aspects of platelet function following GPVI activation. Current models of platelet signaling place Syk and BTK in key positions in signaling downstream

of GPVI as well as integrins and other receptors (i.e., CLEC2, FcγRIIA) (36, 225). We found that Syk and BTK inhibitors all inhibit the initial steps of Syk and BTK signaling (**Figure 3.5**). While all 12 inhibitors inhibited platelet ITAM signaling downstream of GPVI and Syk→BTK activation, some inhibitor specific variations in downstream signaling were apparent. For instance, Syk inhibitors more potently inhibited GPVI-evoked phosphorylation of PLCγ2 and DAPP1, while next generation reversible BTK inhibitors had more pronounced effects on PKC substrate phosphorylation. While CG-806 had the most variable effects on platelet functions, CG-806 potently inhibited signaling events downstream of BTK.

In addition to assays of GPVI-mediated platelet function in response to agonists such as CRP-XL, effects of inhibitors on platelet function are also commonly assayed by following effects of inhibitors on platelet spreading on fibrinogen. In line with other results, we found that all 12 Syk and BTK inhibitors diminished the ability of platelets to spread on fibrinogen to a similar extent. Interestingly, some differences were apparent in the numbers of platelets that were inhibited and the extent of inhibition by reversible BTK inhibitors, relative to irreversible BTK inhibitors and Syk inhibitors, suggesting different cell physiological effects of reversible BTK inhibitors on platelet responses in this context. Similar to our recent analyses of PKC signaling in platelet adherent to fibrinogen (190), we find that the regulatory p85α subunit of PI3K localizes to microtubules in activating platelets in a manner that may support orchestration of platelet activation. Interestingly, while all Syk and BTK inhibitors examined in this chapter perturb the colocalization of p85α PI3K and tubulin, reversible BTK have more dramatic

effects. Indeed, somewhat unexpectedly, reversible inhibitors of BTK are found to be more potent inhibitors of platelet signaling and activation than ibrutinib and other inhibitors that target BTK through covalent mechanisms. These findings are in line with a recent study of the reversible BTK inhibitor fenebrutinib as more potent inhibitor of FcγRIIa mediated platelet activation compared to ibrutinib and other inhibitors (226).

As BTK associates with several components within the LAT signalosome (i.e., PLCγ2, SLP-76) critical for platelet function (225, 227), we suspected that permanent, irreversible, covalent chemical modification of BTK with irreversible inhibitors such as ibrutinib may disrupt organization and alter platelet function in a manner apart from BTK kinase activities, where BTK may have roles as an adaptor protein or molecular scaffold (219). While such mechanisms have not yet been reported for ibrutinib and BTK, mechanisms are emerging as the field of covalent inhibitors develops. For instance, the Cravatt group has recently shown that dimethyl fumarate (DMF) inhibits inflammatory signaling by covalently modifying IRAK4 to disrupt intermolecular interactions with MyD88 to inhibit cytokine production and systemic inflammation (228). In addition to interactions with the LAT signalosome (220), other potential scaffolds around BTK signaling include microtubules, which are known to serve as platforms or adaptors for related signaling processes in a number of cell types, including PI3K signaling in cell lines (210, 211) and Ca^{2+} mediated PKC signaling in platelets (190, 229); however, scaffolding of PI3K/Akt signaling at microtubules in platelets remains largely unexplored. Interestingly, we found that PI3K p85 localizes to microtubules in activating platelets in a manner related to PI3K/Akt signaling. Recent efforts by other groups aim to

target platelet inflammatory signaling with colchicine (230, 231) as well as a cooperativity of microtubule polymerization inhibitors in treating TKI-resistant cancers (and vice versa) (232). Accordingly, a cooperativity between BTK signaling and microtubule regulation may be impacted by specific TKIs in a manner relevant to platelet function. Future studies that target BTK for degradation with protac molecules will further help to resolve structural vs. enzymatic roles for BTK in GPVI-mediated platelet function (233, 234).

Given the key roles of Syk and BTK in platelet signaling events, a number of physiological studies have aimed to better understand how these kinases and drugs against them (i.e., ibrutinib) cause platelet inhibition associated with bleeding. Recent efforts suggest that these effects may be therapeutically exploited, as BTK inhibitors may serve as specific antiplatelet agents for cardiovascular disease (235) and platelet-related inflammatory conditions (226, 236). Roles for Syk inhibitors remain unexplored but may emerge as trials of other inhibitors (many explored in this chapter) are evaluated for safety and efficacy in inflammatory and other conditions. Interestingly, a recent study of BTK inhibitors as potential agents against heparin-induced thrombocytopenia (HIT) similarly found that fenebrutinib – a reversible BTK not associated with bleeding complications in clinical studies – is a more potent inhibitor of BTK signaling than ibrutinib (226). We similarly find that fenebrutinib is a potent inhibitor of GPVI-mediated platelet function. Previous studies have also demonstrated that a highly selective reversible BTK inhibitor RN486 more potently inhibits platelet GPVI responses *in vitro,* but without off target effects of ibrutinib.

In conclusion, this chapter demonstrates that a range of pharmacologically distinct Syk and BTK inhibitors similarly disrupt Syk-BTK signaling events in platelets and essential ITAM-mediated platelet responses. In addition to expanding knowledge of roles for Syk and BTK in platelet cellular physiology, the results from this chapter may help to understand how "off target" or undesired effects of TKIs on platelets and physiologically relevant cells come about. Models following from our results may also inform efforts to target platelet GPVI signaling in immunothrombosis, where Syk and BTK signaling likely have roles in pathologies ranging from atherothrombosis (235) to COVID-19 (237). As TKIs targeting Syk, BTK and other kinases are further developed and implemented for an increasing number of inflammatory, oncogenic and other conditions, studies such as our work herein will help to address a growing need to better understand the effects of such compounds on essential molecular machinery around Syk-BTK signaling in platelets and other physiologically relevant cell types.

Chapter 4: Effects of antiplatelet agents and tyrosine kinase inhibitors on oxLDL-mediated platelet procoagulant activity

Tony J. Zheng, Tia C.L. Kohs, Jiaqing Pang, Stéphanie E. Reitsma, Iván Parra-Izquierdo, Alexander R. Melrose, Mark K. Larson, Craig D. Williams, Monica T. Hinds, Owen J. T. McCarty, and Joseph E. Aslan

This work is currently in submission and under review by the journal *Blood Advances* 2022.

4.1 Abstract

Oxidized low density lipoprotein (oxLDL) contributes to atherogenesis and cardiovascular disease through interactions with peripheral blood cells, especially platelets. However, mechanisms by which oxLDL affects platelet activation and atherothrombosis, and how to best therapeutically target and safely prevent such responses remains unclear. Here, we investigate how oxLDL upregulates glycoprotein VI (GPVI) mediated platelet hemostatic and procoagulant responses, and how traditional and emerging antiplatelet therapies affect oxLDL-enhanced platelet activity *ex vivo*. Human platelets were treated with oxLDL and GPVI specific agonist, crosslinked collagen-related peptide (CRP-XL) and assayed for hemostatic and procoagulant responses in the presence of inhibitors of purinergic receptors (P2Y), cyclooxygenase (COX), and tyrosine kinases. *Ex vivo*, oxLDL enhanced GPVI-mediated platelet dense granule secretion, alpha granule secretion, integrin activation, and aggregation, as well as

procoagulant phosphatidylserine exposure and fibrin generation. P2Y antagonists (e.g., ticagrelor) and BTK inhibitors (e.g., ibrutinib) reduced oxLDL-mediated platelet responses and procoagulant activity, whereas COX inhibitors (e.g., aspirin) had no significant effect. Together, our results demonstrate that oxLDL enhances *ex vivo* platelet responses and procoagulant activity downstream of GPVI signaling in a manner that may be reduced by P2Y antagonists and tyrosine kinase inhibitors, but not significantly affected by COX inhibitors.

4.1.1 Graphical Abstract

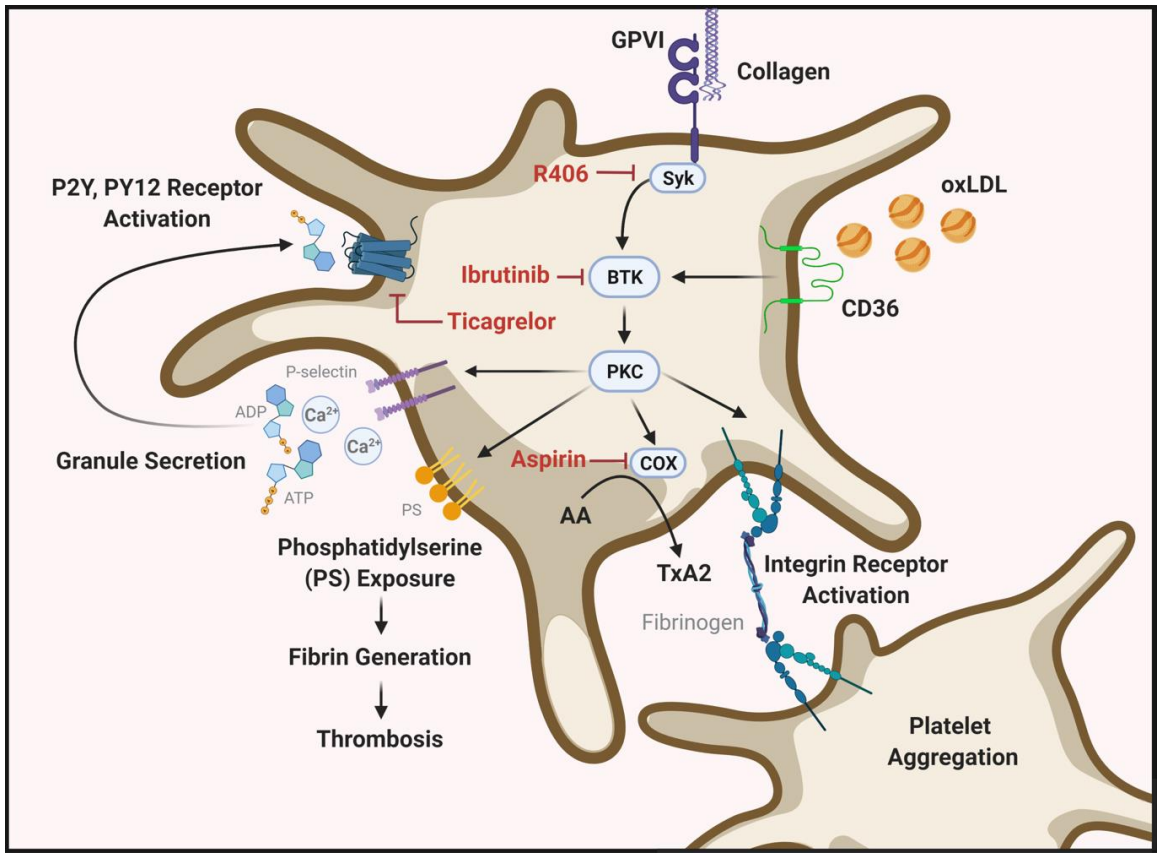

4.2 Introduction

Dyslipidemia and lipoprotein accumulation in the vasculature drive atherogenesis and cardiovascular disease – a leading preventable cause of mortality worldwide.(238-240) Lipoprotein levels are well established risk factors for atherosclerosis and clinically significant atherothrombotic events, such as myocardial infarction, stroke, and sudden death. In these contexts, atherosclerotic plaques and features of a diseased vessel wall initiate and promote thrombosis through interactions with platelets.(241) In particular, oxidized low density lipoprotein (oxLDL) at the site of inflammation and plaque rupture directly and indirectly contribute to platelet activation. OxLDL is recognized to lower platelet activation threshold *ex vivo*; (242-244) however, the mechanisms by which oxLDL interacts with platelets and potentiates platelet activation, and how to best therapeutically target such interactions to safely prevent cardiovascular disease, atherothrombosis, and death still remains to be elucidated.

In addition to progressing atherogenesis, oxLDL enhances platelet activity in thrombosis. Circulating LDL becomes oxidized at sites of inflammation and specific oxidized lipid motifs bind to platelets on CD36, a highly expressed scavenger glycoprotein receptor on the platelet surface.(245) Following interactions with oxLDL, platelet CD36 associates with spleen tyrosine kinase (Syk) and Src family kinases (SFKs), Lyn and Fyn, in a manner posited to lower the activation threshold by other agonists.(243, 246-248) In ana analogous manner, as we seen in Chapter 3, collagen activated glycoprotein VI (GPVI) receptor associates with Fc receptor γ-chain (FcRγ) and becomes activated by SFKs on intracellular immunoreceptor tyrosine-based activation motifs (ITAMs) to phosphorylate

downstream substrates, such as Bruton's tyrosine kinase (BTK), that drive thrombo-inflammatory and procoagulant platelet responses (36, 38). Once activated, platelets upregulate externalization of phosphatidylserine on their extracellular surface, supporting thrombin generation, fibrin formation, and coagulation.(249, 250) However, the biochemical and functional connections between CD36 and GPVI and their combined roles in platelet physiological responses and procoagulant activity still remain largely unknown. For instance, the role of secondary mediators in oxLDL-enhanced platelet responses, including purinergic receptors, cyclooxygenases, and other targets of antiplatelet therapies, remain unspecified.

Current antiplatelet therapies are effective at reducing specific platelet activation responses, especially in secondary prevention. For instance, dual anti-platelet therapy (DAPT), a combination of cyclooxygenase (COX) inhibitor aspirin and a purinergic receptor ($P2Y_{12}$) antagonist, typically ticagrelor, clopidogrel, or prasugrel, is commonly used after coronary intervention procedures.(251) However, these antiplatelet agents also carry risks of bleeding and are further ineffective at preventing reoccurring thrombotic events.(251) Furthermore, the efficacy of aspirin versus $P2Y_{12}$ inhibitors is not well established and more novel antiplatelet agents targeting platelet signaling to limit platelet activation has yet to be actualized.(252-254) In addition, it still remains largely uncharacterized how these antiplatelet agents affect oxLDL interactions with classic platelet activation pathways, such as GPVI-mediated signaling, and how they affect platelet functional responses and coagulation that drives thrombosis.

In this chapter, we investigate how oxLDL affects platelet hemostatic and procoagulant activity, and how traditional and more novel antiplatelet therapies affect these platelet responses *ex vivo*. Our findings provide insight into how oxLDL enhances platelet GPVI responses and inform how clinically relevant $P2Y_{12}$ inhibitors (e.g., ticagrelor) and COX inhibitors (e.g., aspirin), as well as therapeutic kinase inhibitors targeting BTK (ibrutinib) and Syk (fostamatinib), may effectively limit platelet activity in dyslipidemia. Altogether, we elucidate essential mechanisms by which oxLDL potentiates platelet activation downstream of GPVI and assess the potential of pharmacologic agents to reduce platelet activation and the procoagulant and thrombotic characteristics induced by oxLDL in the setting of hyperlipidemia, atherosclerosis, and thrombosis.

4.3 Materials and Methods

4.3.1 Reagents

Prostaglandin I_2 (PGI_2) was obtained from Cayman Chemical (Ann Arbor, Michigan, USA). GPVI specific agonist, crosslinked collagen-related peptide (CRP-XL), was obtained from R. Farndale (CambCol Laboratories, Cambridge University, UK). CHRONO-LUME® detection reagent was obtained from Chrono-Log Corporation (Havertown, Pennsylvania, USA). Non-oxidized and oxidized LDL was obtained from Kalen Biomedical (Germantown, Maryland, USA). Ibrutinib (#S2680) and R406 (#S2194) were obtained from Selleck (Houston, Texas, USA). Ticagrelor was obtained from Oxchem Corporation (Wood Dale, Illinois, USA). $P2Y_{12}$ receptor antagonist AR-C 66096 (ARC), $P2Y_1$ receptor antagonist MRS2179 (MRS), and aspirin (acetylsalicylic acid, ASA) were obtained from Sigma-Aldrich (St. Louis, Missouri, USA), or as

previously described.(59) Primary antisera against phosphorylated Akt substrates (#9614S), PLCγ2 Y_{1217} (##3871S), DAPP1 Y_{139} (#13703S), phosphorylated MAPK substrates (#2325), and phosphorylated PKC substrates (#2261) were obtained from Cell Signaling Technology (Danvers, MA). Anti-α tubulin antibody (#T6199) was obtained from Sigma-Aldrich (St. Louis, Missouri, USA) and PI 3-kinase p85α antibody (#sc-376112) was obtained from Santa Cruz Biotechnology (Dallas, Texas, USA). Flow cytometry antibodies APC anti-human CD62P (#304910) was obtained from BioLegend (San Diego, California, USA), FITC mouse anti-human PAC-1 (#340507) was obtained from BD Biosciences (Franklin Lakes, New Jersey, USA), and FITC bovine lactadherin was obtained from Haematologic Technologies (Essex Junction, Vermont, USA). 4G10 (#05-321) was obtained from Sigma Millipore (St. Louis, Missouri, USA). All other reagents were obtained from Sigma-Aldrich (St. Louis, Missouri, USA).

4.3.2 Platelet Preparation

Human venous blood was drawn from healthy adult donors into 1:10 sodium citrate (3.8% w/v) and warmed 1:10 acid citrate dextrose at 30 ^{o}C following an Institutional Review Board approved by Oregon Health & Science University, as previously described.(39) All donors provided written, informed consent in accordance with the Declaration of Helsinki. The collected blood was centrifuged for 20 min at 200 *g* at room temperature to isolate and collect the platelet rich plasma (PRP). PGI_2 (0.1 µg/ml) was added to the PRP and the mixture was centrifuged for 10 mins at 1,000 *g* to isolate and obtain platelets. The collected platelets were re-suspended in modified HEPES/Tyrode buffer (129 mM NaCl, 0.34 mM Na_2HPO_4, 2.9 mM KCl, 12 mM $NaHCO_3$, 20 mM

HEPES, 5 mM glucose, 1 mM $MgCl_2$, pH 7.3) to the desired concentration for experimental use.

4.3.3 Dense Granule Secretion Assay

Washed human platelets (2×10^8/ml) were incubated with the selected inhibitors for 10 mins in a clear, flat bottom 96-well plate (Corning Costar, Tewksbury, Massachusetts, USA) and then stimulated with GPVI specific agonist, CRP-XL and/or oxLDL at indicated concentrations. A stock solution of aspirin was prepared daily at 2.5 M in DMSO, as previously described.(255) The detection reagent CHRONO-LUME® was added to each well and the 96-well plate was placed in an Infinite M200 spectrophotometer (TECAN, Mannderdorf, Switzerland). An automated protocol is carried out where sample was shaken for 10 s and the luminescence was measured and record at 30 s intervals for 5 mins. Four kinetic luminescence profiles were recorded for each condition and the average luminescence measured at 4 min was calculated and normalized by the luminescence of unstimulated and untreated platelets.

4.3.4 Flow Cytometry and Analysis

Washed, purified platelets (2×10^7/ml) were incubated with the selected inhibitors ticagrelor (0.25, 0.50, 0.75, 1, 5, 10 µM), ARC/MRS (10 µM), aspirin (0.01, 0.02, 1, 2 mM), indomethacin (10 µM), ibrutinib (10 µM), R406 (10 µM), or vehicle (0.1% DMSO) for 10 mins at room temperature. APC CD62P (1:50), FITC PAC-1 (1:50), or FITC bovine lactadherin (1:20) were added to stain for P-selectin expression, activated integrin $\alpha_{IIb}\beta_3$, and phosphatidylserine exposure, respectively. Each platelet mixture was

stimulated with CRP-XL (0.1, 0.5, 1, 5 µg/ml) and/or non-oxidized or oxLDL (1, 5, 10, 20, 50 µg/ml) and incubated at 37 ^{o}C for 30 mins. Each sample was fixed in 2% paraformaldehyde, diluted with modified HEPES/Tyrode buffer, and analyzed using flow cytometry on a FACSCantoII flow cytometer (Becton Dickinson, Franklin Lakes, New Jersey, USA). Platelet populations were identified and gated based forward scatter and side scatter characteristics. Data was analyzed using FlowJo software, in which the thresholds for percentage of platelets binding to CD62P, PAC-1, and lactadherin were set based on the negative control (unstimulated and untreated platelets), such that percentage of platelets bound is ~1.0%.

4.3.5 Fibrin Generation Assay and Analysis

Washed, purified platelets (1.5×10^8/ml) were incubated with the selected inhibitors ticagrelor (750 nM), aspirin (1 mM), indomethacin (10 µM), ibrutinib (10 µM), R406 (10 µM), or vehicle (0.1% DMSO) for 10 mins at room temperature in a 96-well plate pre-blocked by 2% polyethylene glycol (PEG) 2000 for 1 h and washed with HEPES buffer saline (HBS, pH 7.4). Each platelet mixture (50 µl) was stimulated with GPVI specific agonist CRP-XL (0.5 µg/ml) and/or oxLDL (20 µg/ml) and incubated for 10 mins at room temperature. Citrated platelet poor plasma (PPP, 50 µl) followed by $CaCl_2$ (25 mM, 50 µl) were added to each platelet mixture. Fibrin formation was measured as a change in turbidity at an absorbance of 405 nm at 1 min intervals over the course of 2 h using an Infinite M200 spectrophotometer (TECAN, Mannderdorf, Switzerland). The lag time and time to reach half of maximum turbidity were calculated.

4.3.6 Platelet Aggregation and Thromboxane Generation Assay

Washed, purified platelets (3×10^8/ml, 300 µl) were incubated with the selected inhibitors ticagrelor (750 nM), aspirin (1 mM), indomethacin (10 µM), ibrutinib (10 µM), R406 (10 µM), or vehicle (0.1% DMSO) for 10 mins at room temperature in glass cuvettes. Each platelet mixture was stimulated with GPVI specific agonist CRP-XL (0.1, 0.5, 1.0 µg/ml) and/or oxLDL (20 µg/ml) and monitored under continuous stirring at 1200 rpm. The change in light transmission was measured using a 490 + 4 + 4 aggregometer for 4 mins (Chrono Log Corporation), as previously described.(141) A representative trace of 3 different experiments are presented. After aggregation, the solutions were removed from the glass cuvettes and centrifuged. The supernatant was extracted and analyzed for the amount of thromboxane generated using an ELISA assay (Enzo Life Sciences, #ADI-901-002, Farmingdale, New York, USA), as previously described.(39)

4.3.7 Western Blotting

Washed, purified platelets (1×10^9/ml) were incubated with the selected inhibitors ticagrelor (750 nM), aspirin (1 mM), ibrutinib (10 µM), R406 (10 µM), or vehicle (0.1% DMSO) for 10 mins at room temperature and then stimulated with GPVI specific agonist CRP-XL (0.5 µg/ml) and/or oxLDL (20 µg/ml) at 37^{o}C under 200 rpm. Platelet lysates were prepared in Laemmli sample buffer with dithiothreitol (DTT, 200 mM), separated by SDS-PAGE, and then transferred to nitrocellulose membranes. Each platelet mixture was blotted and stained using the antibodies for phospho-DAPP1 (Tyr139), phospho-PLCγ2 (Tyr1217), phospho-Akt (Thr308), phospho-Akt substrate, phospho-(Ser) PKC

substrate, phosphorylated MAPK substrates, 4G10, and α-tubulin, as previously described.(256)

4.3.8 Statistical Analysis

Data was analyzed using GraphPad Prism 9 software (San Diego, California, USA) and represented as the mean ± standard error of the mean. Samples were analyzed using a one- or two-way ANOVA with Dunnett's multiple comparison's test, where a *P*-value of < 0.05 was used to test for significance. The *P*-values are denoted. For all the experiments, *n* indicates the number of independent experiments conducted from platelets isolated from different donors.

4.4 Results

4.4.1 Oxidized LDL enhances platelet aggregation and procoagulant activity

We first sought to specify the effects of oxLDL on platelet aggregation and platelet procoagulant activity. Washed platelets were prepared from healthy human donors and pre-treated with oxLDL (20 µg/ml) alone and in combination with the glycoprotein VI (GPVI) specific agonist, crosslinked collagen-related peptide (CRP-XL; 0.1, 0.5, 1.0 µg/ml) (**Figure 4.2A-C**). OxLDL alone (20 µg/ml) and CRP-XL alone (0.5 µg/ml) did not induce significant platelet aggregation, (2.6% ± 0.4% and 5% ± 3%, respectively). However, pretreatment of platelets with oxLDL prior to CRP-XL stimulation potentiated platelet aggregation to 81.8% (± 3.9%) (**Figure 4.2B**). No effects of oxLDL were noted following stimulation of platelets with 1 µg/ml CRP-XL, which maximally aggregated platelets in the absence of oxLDL (**Figure 4.2C**).

Next, we evaluated platelet procoagulant responses to oxLDL with flow cytometry to measure FITC-lactadherin binding of platelets as a marker of platelet phosphatidylserine (PS) exposure. Neither oxLDL nor CRP-XL treatment alone significantly increased platelet PS exposure, except at higher concentration of CRP-XL (5 µg/ml) (**Figure 4.3A-B**). Treatment of platelets with oxLDL in combination CRP-XL significantly increased platelet PS exposure (**Figure 4.2D**). For instance, 3.3% (± 0.8%) of platelets were positive for FITC-lactadherin binding when stimulated with CRP-XL alone (0.5 µg/ml); however, when platelets were pre-treated with oxLDL in combination with CRP-XL, the percentage of lactadherin-positive platelets increased ~10-fold to 37.2% (± 0.8%) (**Figure 4.2D**).

Given the effects of oxLDL on platelet PS exposure, we next evaluated fibrin generation with light absorbance turbidity assays over the course of 2 h (**Figure 4.2E**). Washed platelets were pre-treated with oxLDL (20 µg/ml) alone and in combination with CRP-XL (0.5 µg/ml). Citrated platelet poor plasma (PPP) and $CaCl_2$ (25 mM) were sequentially added to each platelet mixture in equal proportions. Fibrin generation began at a lag time of 2000 s (± 140 s) when stimulated CRP-XL alone and at 2700 s (± 215 s) when stimulated with oxLDL alone. When platelets were pre-treated with oxLDL in combination with CRP-XL, fibrin generation started at 1450 s (± 175 s) following stimulation, as quantified by the lag time (**Figure 4.2F**). The time to half of maximum fibrin generation was reached at

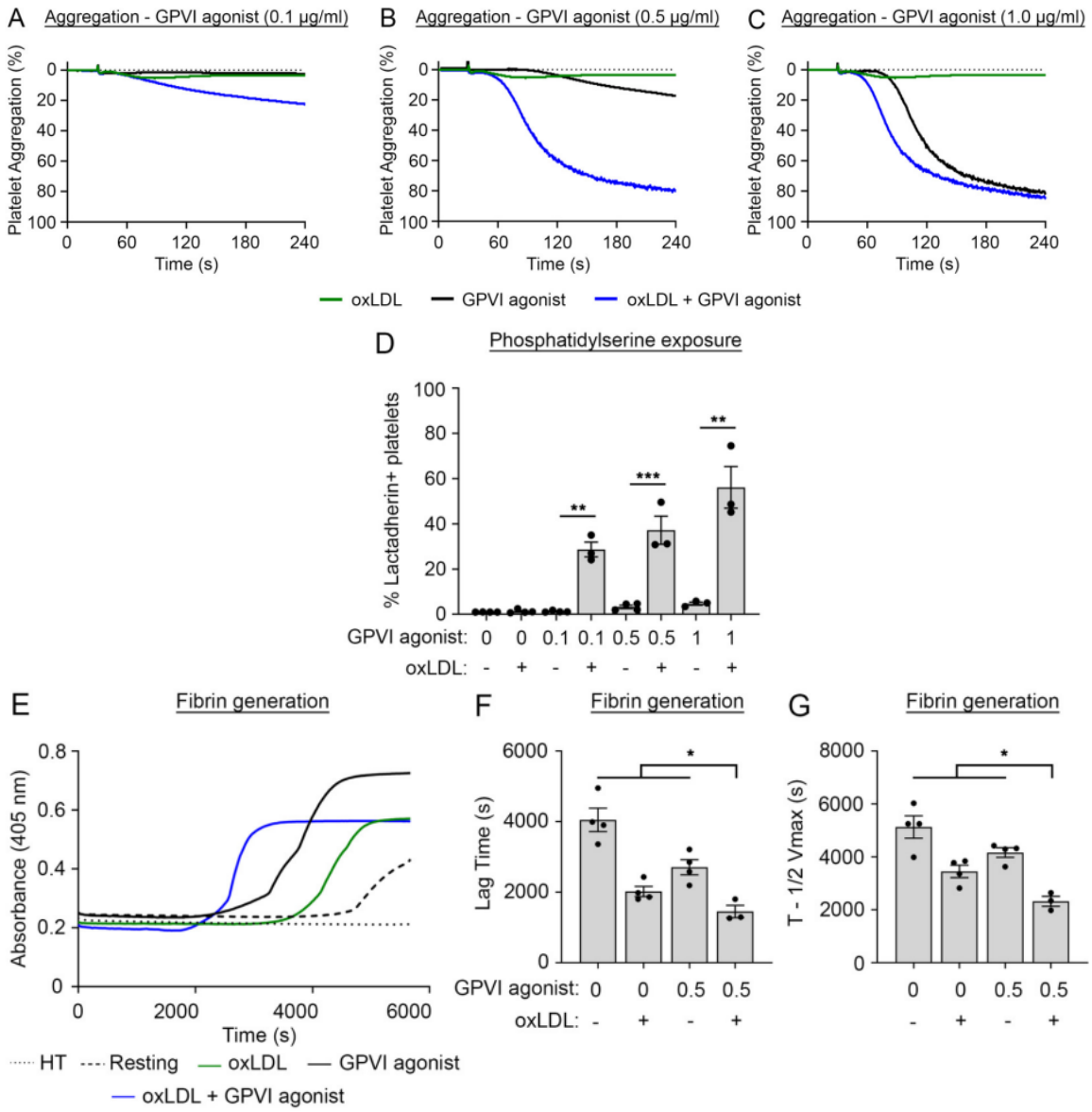

Figure 4.2. Oxidized LDL potentiates GPVI-mediated platelet aggregation, platelet phosphatidylserine exposure, and platelet driven fibrin formation. Replicate samples of washed and isolated human platelets (2×10^8/ml) were incubated with the GPVI specific agonist crosslinked collagen-related peptide (CRP-XL) alone (0.1, 0.5, 1 µg/ml), oxidized LDL (oxLDL) alone (20 µg/ml), and oxLDL in combination CRP-XL. Platelets samples were monitored at 37°C under continuous stirring at 1200 rpm and the changes in light transmission were measured **(A-C)**. Platelet samples were incubated with oxLDL (0, 20 µg/ml) in combination with GPVI specific agonist CRP-XL (0, 0.1, 0.5, 1 µg/ml) prior to fixation and staining with FITC-Lactadherin to monitor for platelet surface phosphatidylserine (PS) exposure **(D)**. Platelet samples were incubated with $CaCl_2$ (8.3 mM) and citrated platelet poor plasma (33% final). Fibrin formation was measured as a change in turbidity at an absorbance of 405 nm. Representative traces are shown **(E)** and the lag time and time to half the maximum absorbance were calculated **(F, G)**. Statistical analysis was performed using a one-way ANOVA test and the corresponding P-values of significance are as indicated: * P-value < 0.05, ** P-value < 0.01, and *** P-value < 0.001.

2320 s (± 190 s) following stimulation, versus at 4160 s (± 180 s) and 3450 s (± 235 s) when stimulated with oxLDL or CRP-XL alone, respectively (**Figure 4.2G**). The maximum fibrin generation is indicated by the plateau on the kinetic curves, whereas the time to half maximum indicates the rate of fibrin generation. Both these parameters are independent of the lag time. Together, these results demonstrate that oxLDL potentiates platelet aggregation as well as procoagulant activity in response to the GPVI specific agonist CRP-XL.

4.4.2 Oxidized LDL potentiates platelet signaling and platelet functional responses

OxLDL activation of CD36 has been detailed to prime platelet activation through NOX2-mediated reactive oxygen species (ROS) generation,(247) ERK5 signaling, and caspase-3 activation;(244) however, the roles for intracellular signaling (e.g., ITAM effectors) and secondary mediators (e.g., ADP secretion, thromboxane generation) remain to be incorporated into models of oxLDL-enhanced platelet activation. To elucidate whether and how oxLDL potentiates biochemical and cellular platelet activities underlying GPVI-mediated hemostatic and procoagulant responses, we next surveyed protein kinase activities in washed platelets stimulated with oxLDL and CRP-XL. Following SDS-PAGE and Western blot analysis, lysates of platelets stimulated with oxLDL alone (20 μg/ml) had minimal phosphorylation of generalized GPVI and downstream ITAM targets, including tyrosine kinase substrates, protein kinase C (PKC) substrates, Akt substrates, mitogen activated protein kinase (MAPK) substrates, and protein kinase A (PKA) substrates (**Figure 4.4A**). When platelets were simultaneously stimulated with both oxLDL and CRP-XL, the phosphorylation of all kinase substrates examined were

upregulated relative to effects of each agonist alone. These results support the hypothesis that CD36 and GPVI converge to activate signaling pathways that mediate platelet aggregation and procoagulant responses downstream of GPVI.

Following GPVI activation, platelets release ADP from dense granules, mobilize proteins through alpha granule secretion (e.g., P-selectin, CD62P), and promote activation of integrin $\alpha_{IIb}\beta_3$ on the platelet surface to drive platelet-platelet aggregation. We next sought to determine the effects of oxLDL on platelet dense granule secretion, P-selectin exposure, and "inside-out" integrin activation. Platelets were treated with oxLDL alone and in combination with CRP-XL prior to incubation with CHRONO-LUME® reagent to follow ADP secretion as a marker of dense granule secretion. In parallel, these platelet samples were also stained with APC-CD62P and FITC-PAC-1 to assess for alpha granule secretion and integrin activation, respectively, using flow cytometry. As detailed in **Figure 4.3**, CRP-XL alone increased platelet dense granule secretion, alpha granule secretion, and integrin activation (**Figure 4.3C, E, G**) in a concentration dependent manner, while oxLDL alone had no significant effect on these responses over a concentration range of 0 to 50 µg/ml (**Figure 4.3D, F, H**). Stimulation of platelets with oxLDL (20 µg/ml) in combination with a range of concentrations of CRP-XL (0.1, 0.5, 1.0 µg/ml) led to pronounced dense granule secretion (**Figure 4.4B**), alpha granule secretion (**Figure 4.4C**), and integrin activation (**Figure 4.4D**). For instance, ATP released by platelets stimulated with CRP-XL (0.5 µg/ml) alone was 1.9-fold greater than that of unstimulated platelets (normalized as 1.0 luminescence intensity). When platelets were pre-treated with oxLDL (20 µg/ml) in combination with CRP-XL (0.5 µg/ml), the

measured luminescence was 6.5-fold greater than that of unstimulated platelets (**Figure 4.4B**). Similarly, using flow cytometry to evaluate for platelet P-selectin exposure (CD62P)

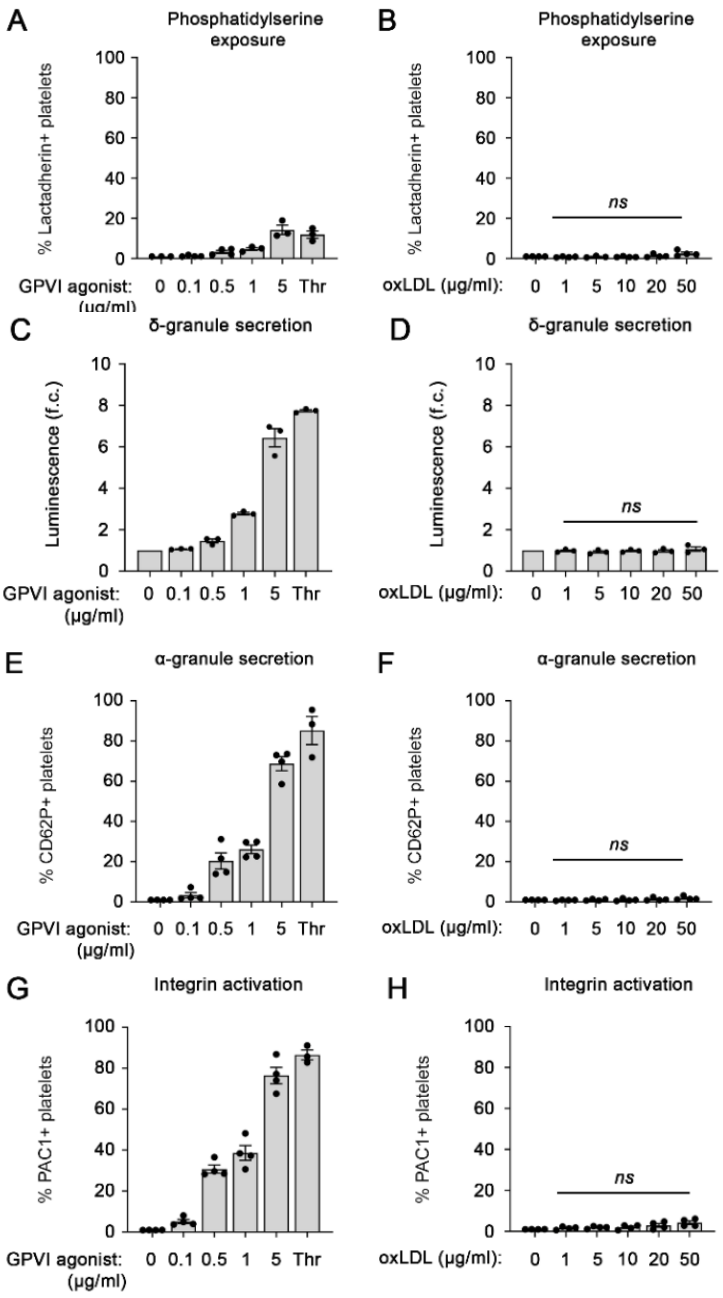

Figure 4.3 Dose response of oxidized LDL and GPVI specific agonist on platelet phosphatidylserine exposure, dense granule secretion, alpha granule secretion, and integrin activation. Replicate samples (n = 3) of washed and isolated human platelets (2 × 108 /ml) were incubated with oxLDL (0, 1, 5, 10, 20, 50 µg/ml) or GPVI specific agonist, crosslinked collagen related peptide (CRP-XL, 0, 0.1, 0.5, 1, 5 µg/ml). Platelet samples were stained with FITC-Lactadherin to monitor for platelet surface phosphatidylserine exposure (A, B). Platelet samples were monitored using the luciferase enzyme CHRONO-LUME® to detect the luminescence of ATP released as a measure of platelet dense granule secretion (C, D). Platelets were stained with APC-CD62P to monitor for platelet surface expression of P-selectin as a marker of alpha granule secretion (E, F) and stained with FITCPAC1 to monitor for platelet surface integrin activation (G, H). Statistical analysis was performed using a one-way ANOVA test on GraphPad Prism.

or PAC-1 binding as markers for alpha granule secretion and integrin activation, respectively, we found that 22.5% (± 4.8%) of platelets upregulated surface P-selectin and 31.5% (± 2.6%) of platelets bound to PAC-1 in response to CRP-XL treatment alone (0.5 µg/ml). However, when platelets were pre-treated with oxLDL (20 µg/ml) in combination with CRP-XL (0.5 µg/ml), the percentage of surface CD62P+ platelets increased to 55.7% (± 1.9%) (**Figure 4.4C**) and the percentage of PAC-1+ platelets increased to 71.0% (± 2.4%) (**Figure 4.4D**). These GPVI-mediated platelet activation parameters were enhanced in a manner correlated to LDL oxidation state, as non-, low- and medium-oxLDL preparations had less pronounced effects relative to highly oxLDL (**Figure 4.5**). In addition to luminescence and flow cytometry assays, we also collected platelet releasate following aggregometry for ELISA of thromboxane B2 (TxB2) as a marker of thromboxane A2 (TxA2) generation. Platelets stimulated with oxLDL alone (20 µg/ml) and CRP-XL alone (0.5 µg/ml) generated 46.7 pg/ml (± 6.3 pg/ml) and 132.2 pg/ml (± 15.3 pg/ml) TxB2, respectively. When platelets were stimulated with both agonists, thromboxane concentration was enhanced to 642.0 pg/ml (± 46.5 pg/ml) (**Figure 4.4E**). Altogether, these results demonstrate that in parallel to potentiating platelet aggregation and procoagulant responses, oxLDL enhances GPVI-driven platelet intracellular signaling, dense granule secretion, alpha granule secretion, integrin activation, and thromboxane generation.

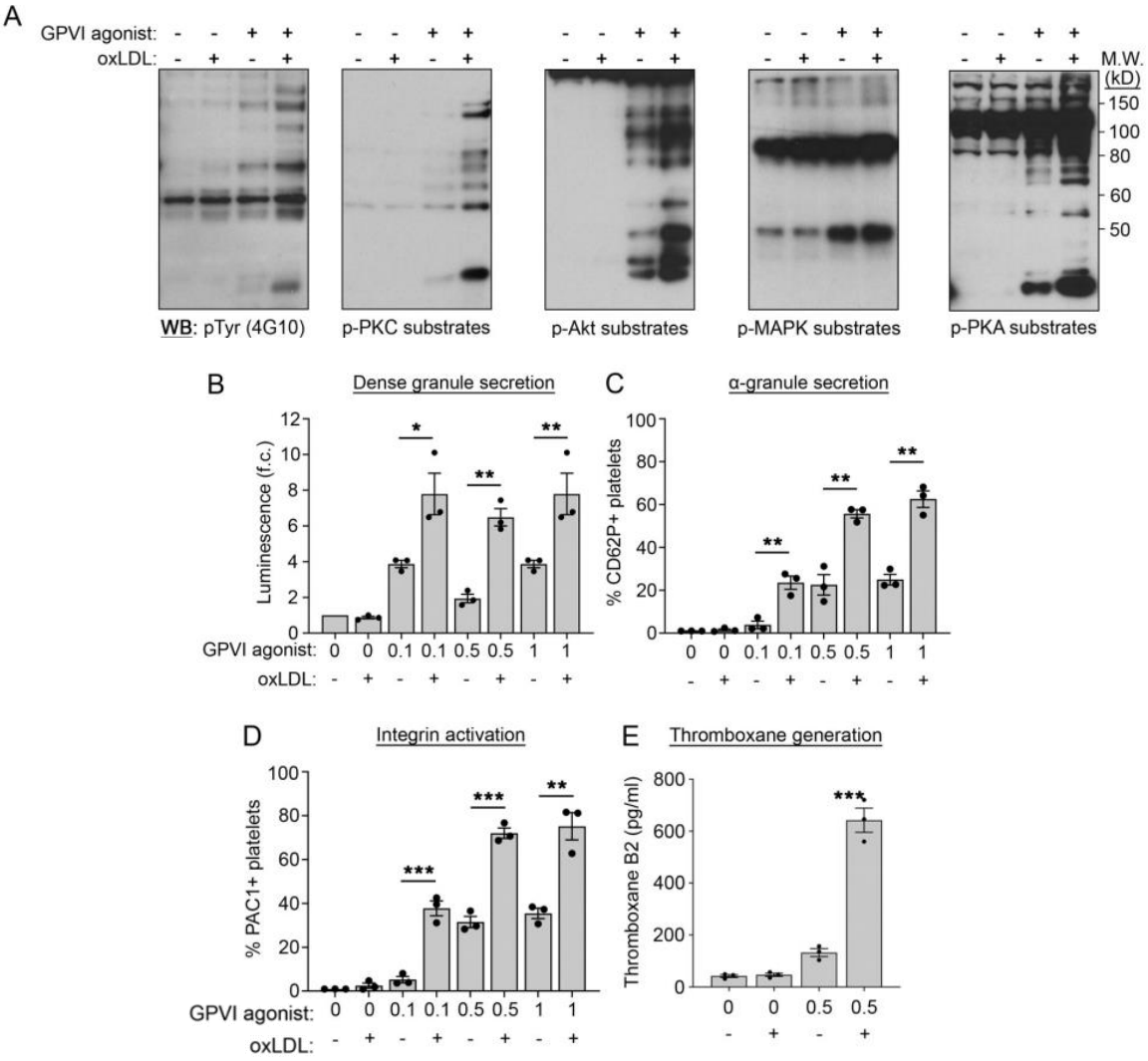

Figure 4.4. OxLDL potentiates GPVI-mediated platelet signaling, granule secretion, and integrin activation. Replicate samples (n = 3) of washed human platelets (1×10^9/ml) were incubated with oxLDL alone (20 μg/ml), GPVI specific agonist CRP-XL alone (0.5 μg/ml), oxLDL in combination with CRP-XL, or vehicle (0.1% DMSO) for 5 min at 37 ºC. After collection into Laemmli sample buffer, platelet lysates were separated by SDS-PAGE and transferred to nitrocellulose for Western blot analysis of phosphorylation of tyrosine kinase substrates, PKC substrates, Akt substrates, MAPK substrates, and PKA substrates; α-tubulin serves as a loading control for total protein levels. Positions of molecular weight (kD) markers are indicated. Washed platelets (2×10^8/ml) were incubated with oxLDL (0, 20 μg/ml) in combination with CRP-XL (0, 0.1, 0.5, 1 μg/ml) and monitored using luciferase enzyme activity (CHRONO-LUME) to detect ATP released as a measure of platelet dense granule secretion **(B)**. Platelets were stained with APC-CD62P to monitor for platelet surface expression of P-selectin as a marker of alpha granule secretion **(C)** and stained with FITC-PAC-1 to monitor for platelet surface integrin activation **(D)**. The supernatant of the platelet solution assessed for platelet aggregation previously was extracted and analyzed for the amount of thromboxane generated using an ELISA assay **(E)**. Statistical analysis was performed using a one-way ANOVA test and the corresponding P-values of significance are as indicated: * P-value < 0.05, ** P-value < 0.01, and *** P-value < 0.001.

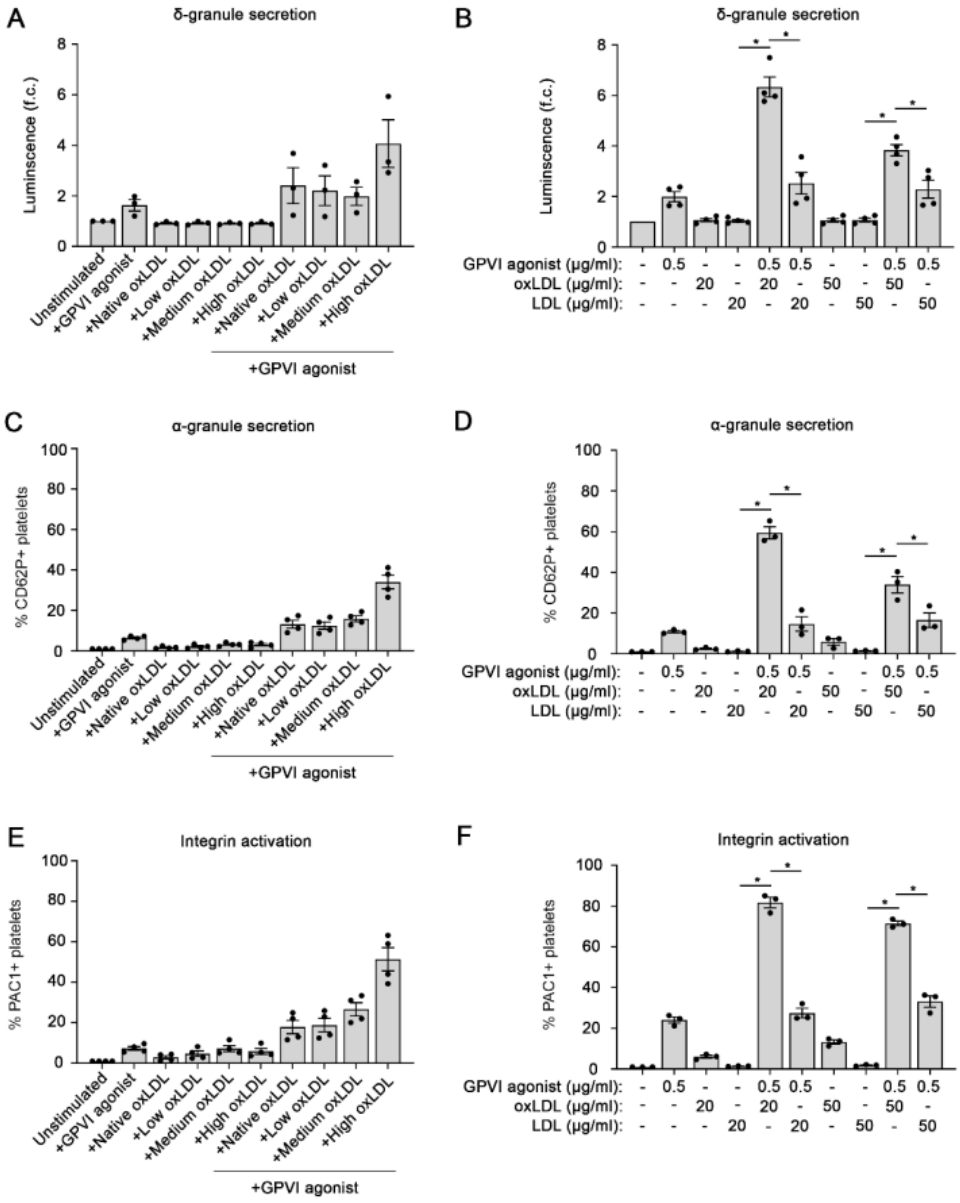

Supplementary Figure 4.5. Effects of various oxidation levels of LDL in inducing GPVI potentiation of platelet dense granule secretion, alpha granule secretion, and integrin activation. Replicate samples (n = 3) of washed and isolated human platelets (2 × 108 /ml) were incubated with oxLDL at various oxidation stages (native, low, medium, high oxidation) with and without GPVI specific agonist (0.5 μg/ml). Additional platelet samples were also prepared with various concentrations of high oxidized LDL (0, 20, 50 μg/ml) or native LDL (0, 20, 50 μg/ml) in combination with GPVI specific agonist (0.5 μg/ml). Platelet samples were monitored using the luciferase enzyme CHRONO-LUME® to detect the luminescence of ATP released as a measure of platelet dense granule secretion (A, B). Platelets were stained with APC-CD62P to monitor for platelet surface expression of P-selectin (C, D) and stained with FITC-PAC1 to monitor for platelet surface integrin activation (E, F). Statistical analysis was performed using a one-way ANOVA test on GraphPad Prism. A P-value > 0.05 was considered not significant, denoted by ns, otherwise the corresponding P-values of significance are as indicated: * P-value < 0.05.

4.4.3 Effects of purinergic receptor and cyclooxygenase inhibitors on oxLDL-mediated platelet responses

We next sought to assess the effects purinergic (P2Y) receptor and cyclooxygenase (COX) inhibitors on platelet responses sensitized by oxLDL. To investigate the effects of P2Y receptors and their inhibition on oxLDL-mediated platelet activation, washed human platelets were pre-treated with $P2Y_{12}$ receptor inhibitor ticagrelor (0.25, 0.50, 0.75, 1, 5, 10 μM), as well as a combination of $P2Y_{12}$ antagonist AR-C 66096 (ARC; 10 μM) and $P2Y_1$ antagonist MRS2179 (MRS; 10 μM). To investigate the effects of COX inhibition, we also treated platelets with low-dose aspirin (ASA; 0.01, 0.02 mM) and high-dose aspirin (ASA; 1.0, 2.0 mM) as well as indomethacin (10 μM). Platelets were then stimulated with oxLDL (20 μg/ml) and CRP-XL (0.5 μg/ml). Ticagrelor reduced platelet dense granule secretion (**Figure 4.6A**), alpha granule secretion (**Figure 4.6B**), and integrin activation (**Figure 4.6C**) in a dose dependent manner (**Figure 4.7A, C, D**). In contrast, aspirin had no significant effect on platelet dense granule secretion (**Figure 4.6A**), alpha granule secretion (**Figure 4.6B**), and integrin activation (**Figure 4.6C**) (**Figure 4.7B-D**). Similarly, small molecule inhibitors of P2Y (AR-C 66096 and MRS2179; 10 μM) but not COX (indomethacin, 10 μM) reduced the effect of oxLDL on GPVI-mediated platelet dense granule secretion (**Figure 4.6A**), alpha granule secretion (**Figure 4.6B**), and integrin activation (**Figure 4.6C**) to a similar extent as ticagrelor (750 nM). Together, these results demonstrate that P2Y inhibitors reduce the effects of oxLDL on platelet GPVI responses *ex vivo*.

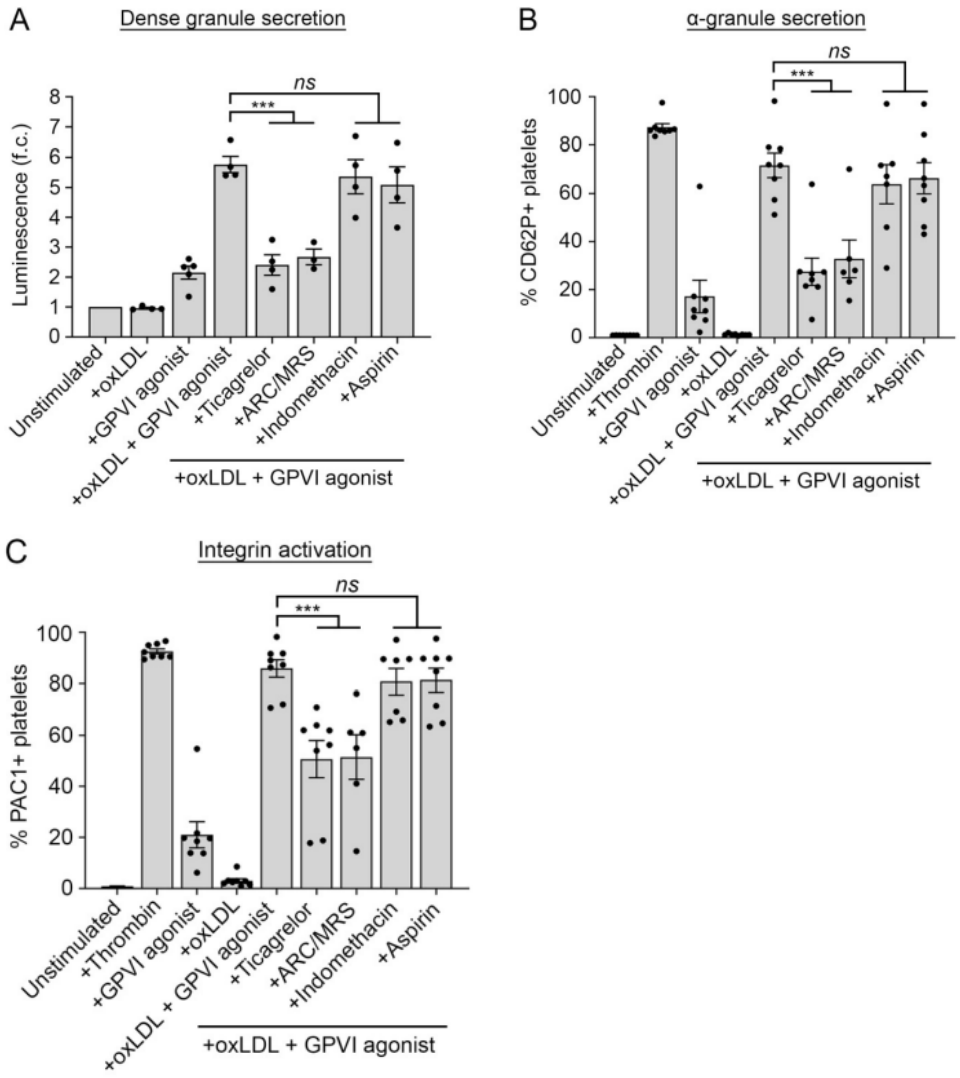

Figure 4.6. Purinergic receptor antagonists but not COX inhibitors reduce oxLDL potentiation of platelet GPVI responses. Replicate samples ($n \geq 3$) of washed human platelets (2×10^8/ml) were treated with P2Y inhibitors ticagrelor (750 nM), ARC/MRS (10 µM), COX inhibitors aspirin (1 mM), indomethacin (10 µM) for 10 mins and stimulated with oxLDL (20 µM) in combination with GPVI specific agonist CRP-XL (0.5 µg/ml). Platelet samples were monitored using the luciferase enzyme CHRONO-LUME® to detect the luminescence of ATP released as a measure of platelet dense granule secretion **(A)**. Platelets were stained with APC-CD62P to monitor for platelet surface expression of P-selectin **(B)** and stained with FITC-PAC-1 to monitor for platelet surface integrin activation **(C)**. Statistical analysis was performed using a one-way ANOVA test and the corresponding P-values of significance are as indicated: *** P-value < 0.001 and *ns* not significant.

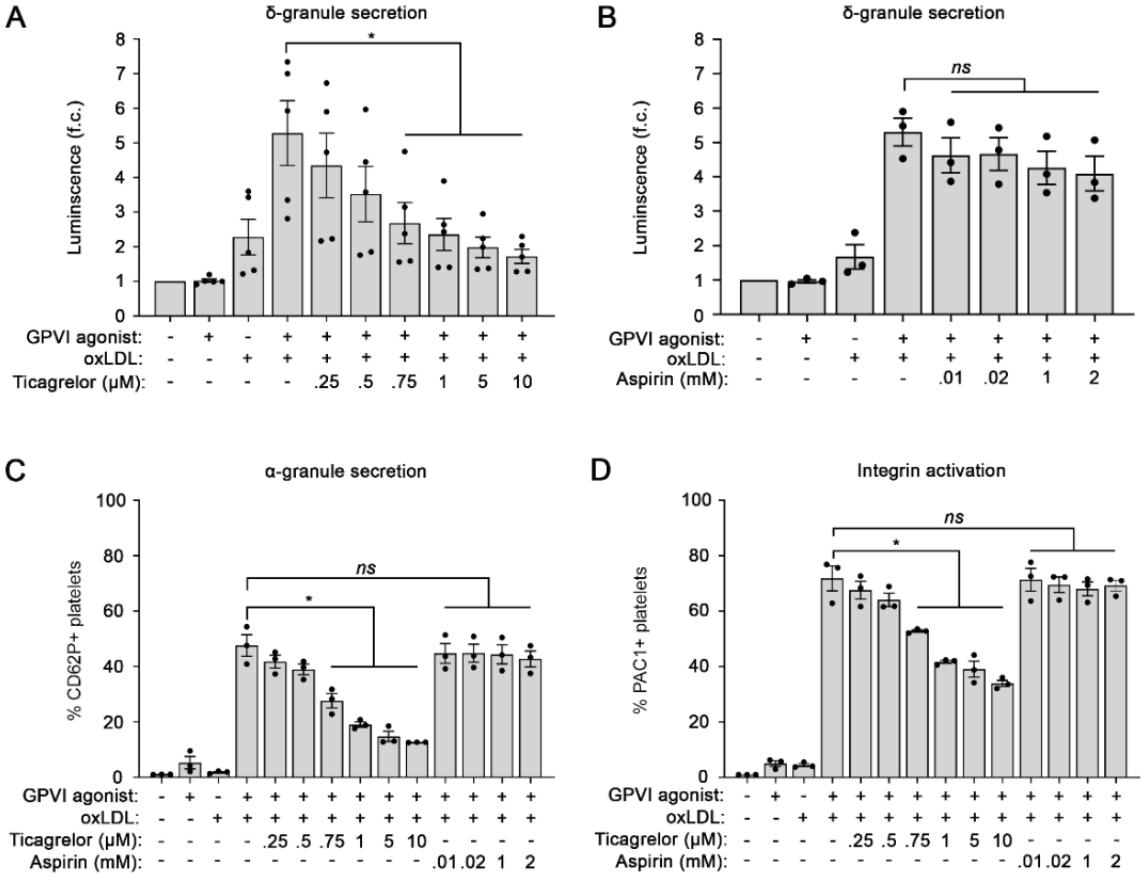

Figure 4.7. Dose response of P2Y inhibitor ticagrelor and COX inhibitor aspirin on potentiation of oxidized LDL induced GPVI activation of platelet dense granule secretion, alpha granule secretion, and integrin activation. Replicate samples (n = 3) of washed and isolated human platelets (2 × 108 /ml) were treated with P2Y inhibitors ticagrelor (0, 0.25, 0.50, 0.75, 1, 5, 10 μM) or COX inhibitors aspirin (0.01, 0.02, 1, 2 mM) for 10 mins and stimulated with GPVI specific agonist (0.5 μg/ml) in combination with oxLDL (20 μM). Platelet samples were monitored using the luciferase enzyme CHRONO-LUME® to detect the luminescence of ATP released as a measure of platelet dense granule secretion (A, B). Platelets were stained with APC-CD62P to monitor for platelet surface expression of P-selectin (C) and stained with FITC-PAC1 to monitor for platelet surface integrin activation (D). Statistical analysis was performed using a one-way ANOVA test on GraphPad Prism and the corresponding P-values of significance are as indicated: * P-value < 0.05 and ns not significant.

We next examined the effects of P2Y and COX inhibition on platelet aggregation and platelet procoagulant activity in the presence of oxLDL. Platelets were pre-treated P2Y inhibitors ticagrelor (750 nM) or ARC/MRS (10 μM) or COX inhibitors aspirin (1 mM) or indomethacin (10 μM), stimulated with oxLDL (20 μg/ml) in combination with CRP-XL (0.5 μg/ml), and continuously stirred at 1200 rpm for 5 mins while measuring changes in light transmission (**Figure 4.8A**). We found that the P2Y inhibitors, ticagrelor and ARC/MRS, significantly decreased platelet aggregation in response to oxLDL and CRP-XL, whereas COX inhibitors, aspirin and indomethacin, had only minor effects on platelet activation (**Figure 4.8A**). Next, we used flow cytometry to evaluate platelet:FITC-lactadherin binding as a marker of procoagulant platelet PS exposure. P2Y antagonists, ticagrelor and ARC/MRS, significantly reduced the percentage of lactadherin-positive platelets generated by combined oxLDL and CRP-XL stimulation, whereas COX inhibitors, aspirin and indomethacin had no significant effect (**Figure 4.8B**). For instance, when platelets were stimulated with CRP-XL (0.5 μg/ml) alone, 3.0% (± 0.7%) platelets were lactadherin-positive, whereas 68.7% (± 10.4%) of platelets were lactadherin-positive following when treated with oxLDL (20 μg/ml) in combination with CRP-XL (0.5 μg/ml). When platelets were pre-treated with P2Y inhibitors ticagrelor (750 nM) or ARC/MRS (10 μM), the percentage of lactadherin-positive platelets was reduced to 5.7% (± 1.1%) and 12.9% (± 8.0%), respectively, after stimulation with oxLDL and CRP-XL.

We similarly evaluated the effects of P2Y inhibition and COX inhibition on fibrin generation in the presence of platelets. Platelets were pre-treated with P2Y inhibitor

ticagrelor (750 nM) or COX inhibitors aspirin (1 mM) or indomethacin (10 µM), and then stimulated with oxLDL (20 µg/ml) in combination with CRP-XL (0.5 µg/ml). Citrated platelet poor plasma (PPP) and $CaCl_2$ (25 mM) were sequentially added to each platelet mixture in equal proportions, and fibrin formation was measured as a change in turbidity at an absorbance of 405 nm over the course of 2 h (**Figure 4.8C**). Evaluating for the lag time and time to half of maximum fibrin generation, we found that fibrin was first generated at 2050 s (± 50 s) and reached half to maximum at 2535 s (± 160 s), respectively, when stimulated with both oxLDL and CRP-XL. P2Y inhibitor ticagrelor increased the average lag time to 2760 s (± 80 s) and time to half maximum to 3400 s (± 180 s). In contrast, COX inhibitor aspirin did not significantly change the lag time or the time to half maximum, 1800 s (± 90 s) and 2670 s (± 180 s), respectively (**Figure 4.8D-E**). Altogether, these results demonstrate that P2Y inhibition reduced the potentiation of platelet aggregation and fibrin generation enhanced by oxLDL, whereas COX inhibition had no effect.

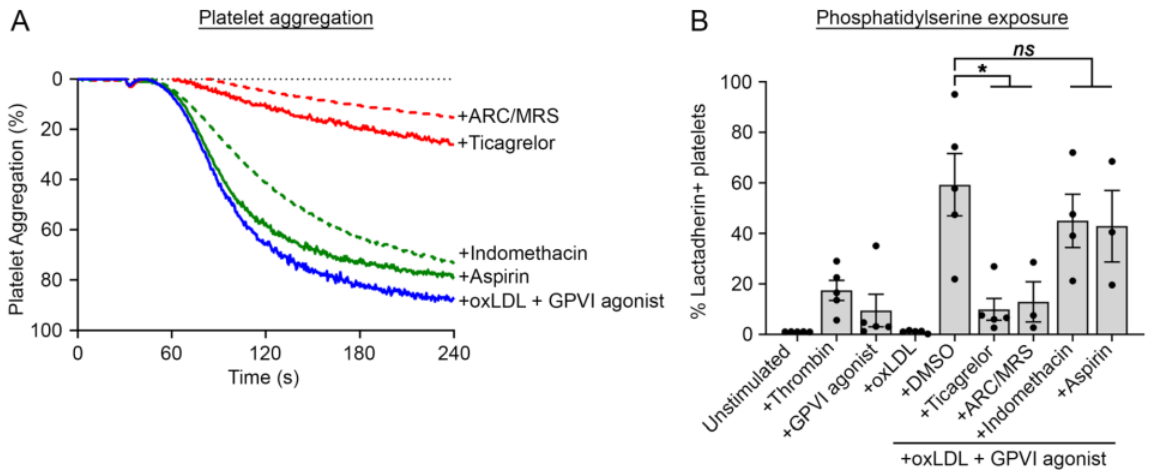

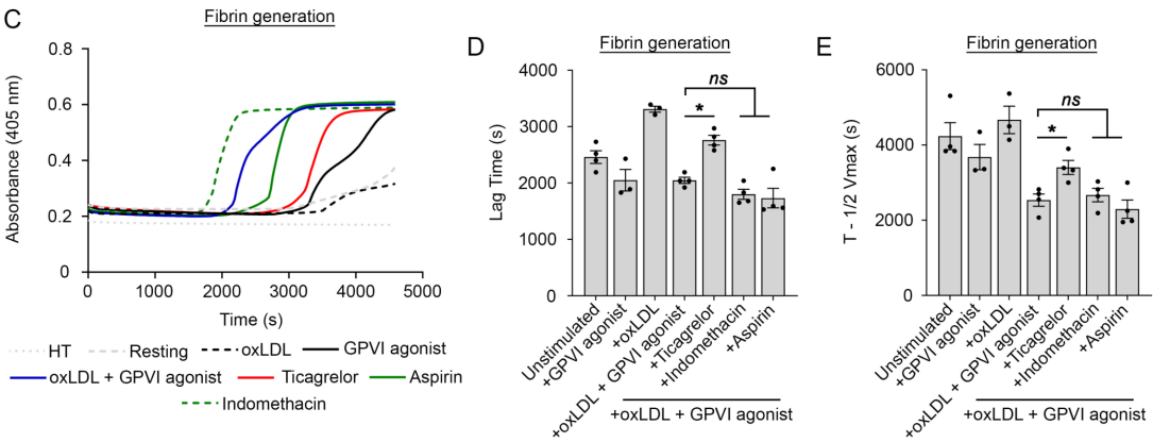

Figure 4.8. P2Y inhibitors reduce oxLDL potentiation of platelet aggregation and procoagulant responses. Replicate samples (n ≥ 3) of washed human platelets (2×10^8/ml) were treated with P2Y inhibitors ticagrelor (750 nM), ARC/MRS (10 µM), COX inhibitors aspirin (1 mM), indomethacin (10 µM) for 10 mins and stimulated with oxLDL (20 µM) in combination with GPVI specific agonist CRP-XL (0.5 µg/ml). Platelet samples were monitored at 37 ºC under continuous stirring at 1200 rpm and the changes in light transmission were measured. Representative traces of platelet samples treated with each select inhibitor are shown **(A)**. Platelets were stained with FITC-Lactadherin to monitor for platelet surface phosphatidylserine exposure **(B)**. Platelet samples were incubated with $CaCl_2$ (8.3 mM) and citrated platelet poor plasma (33% final). Fibrin formation was measured as a change in turbidity at an absorbance of 405 nm. Representative traces are shown **(C)** and the lag time and time to half the maximum absorbance were calculated **(D, E)**. Statistical analysis was performed using a one-way ANOVA test and the corresponding P-values of significance are as indicated: * P-value < 0.05 and *ns* not significant.

4.4.4 Assessment of GPVI/ITAM signaling and inhibition on oxLDL mediated platelet responses

As oxLDL enhanced GPVI-driven platelet signaling and other responses (**Figures 4.2-4.4**), we next sought to further specify how GPVI/ITAM signaling and inhibition affect oxLDL mediated platelet responses. Following GPVI activation, tyrosine kinases including spleen tyrosine kinase (Syk) and Bruton's tyrosine kinase (BTK) play critical

roles in transducing intracellular signals to progress platelet responses in hemostasis and thrombosis.(76, 175) Specifically, Syk mediates a signaling cascade through the formation of the linker for activation of T cells (LAT) signalosome, recruiting and activating a number of substrates, including: BTK, phospholipase C γ2 (PLCγ2), phosphoinositide 3-kinase (PI3K), MAPKs, Akt, PKC, and a number of other effectors that drive platelet responses. Washed human platelets were pre-treated with ticagrelor, aspirin, BTK inhibitor ibrutinib (10 μM) or Syk inhibitor fostamatinib (R406, 10 μM) before stimulating with oxLDL (20 μg/ml) in combination with CRP-XL (0.5 μg/ml). Following SDS-PAGE and Western blot analysis, oxLDL enhanced GPVI-mediated pTyr, PKC, Akt and MAPK substrate phosphorylation (**Figure 4.9**). In addition, oxLDL enhanced specific ITAM signaling (BTK, PLCγ2, PI3K) and MAPK activation (ERK, p38). Ibrutinib inhibited phosphorylation of all substrates and proteins examined. Ticagrelor effectively inhibited Akt responses and fostamatinib effectively reduced ITAM signaling (BTK, PLCγ2); however, aspirin had no effect on oxLDL-enhanced phosphorylation of these substrates. Together, these results demonstrate that ticagrelor, ibrutinib, and fostamatinib reduce the phosphorylation of proteins through an ITAM-BTK-PI3K/Akt signaling axis potentiated by oxLDL downstream of GPVI activation.

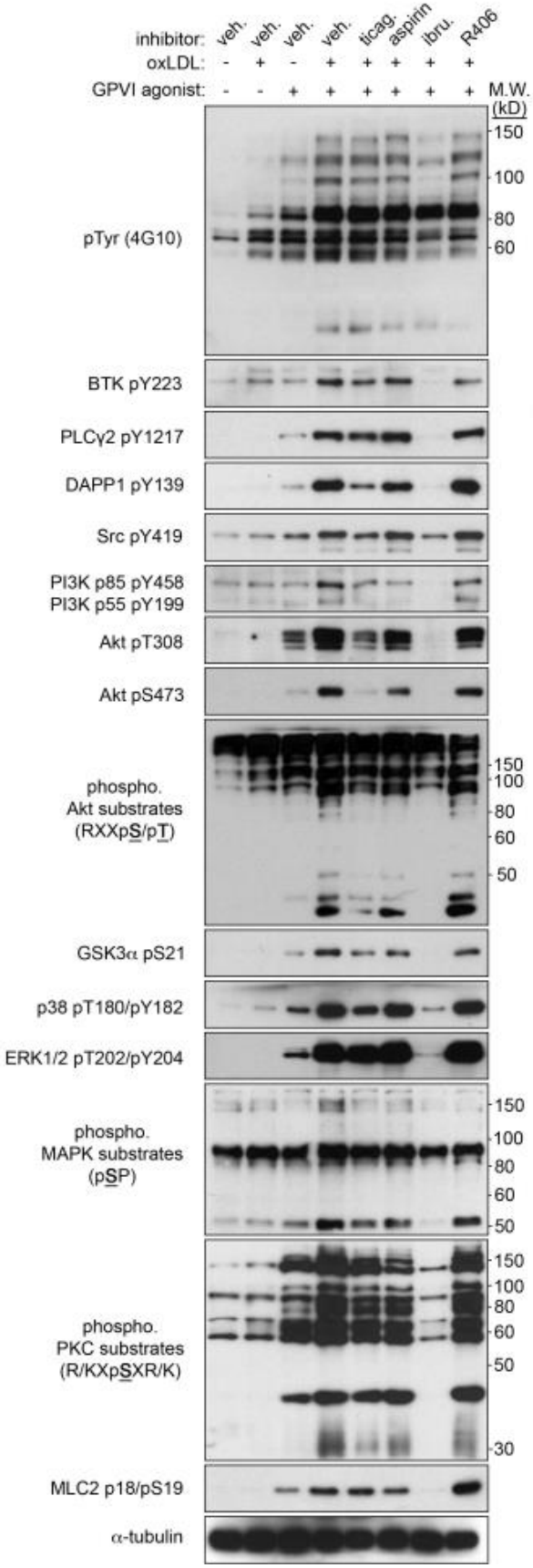

Figure 4.9. Antiplatelet agents and tyrosine kinase inhibitors differentially reduce oxLDL potentiation of platelet GPVI/ITAM signaling. Replicate samples (n = 3) of washed human platelets (1×10^9/ml) were treated with P2Y inhibitor ticagrelor, BTK inhibitor ibrutinib (10 μM), or Syk inhibitor R406 (10 μM) for 10 min and then stimulated with oxLDL (20 μM) in combination with GPVI specific agonist CRP-XL (0.5 μg/ml) for 5 min at 37 ºC. After collection into Laemmli sample buffer, platelet lysates were separated by SDS-PAGE and transferred to nitrocellulose for Western blots analysis with indicated antisera; α-tubulin serves as a loading control for total protein levels. Positions of molecular weight (kD) markers relative to phosphorylated proteins are indicated.

These results suggest that BTK signaling through PI3K/Akt plays a central role mediating the potentiated signal from both CD36 activation and GPVI activation from oxLDL and CRP-XL, respectively.

4.4.5 Ibrutinib and fostamatinib reduce oxLDL mediated platelet responses

Given the enhanced phosphorylation of ITAM signaling effectors in platelets stimulated with oxLDL and CRP-XL, we next sought to determine the effects of Syk and BTK inhibition on GPVI-mediated platelet responses mediated by oxLDL. Washed human platelets were pre-treated with BTK inhibitor ibrutinib (10 μM) or Syk inhibitor fostamatinib (R406, 10 μM) before stimulating with oxLDL (20 μg/ml) in combination with CRP-XL (0.5 μg/ml). Pretreatment of platelets with ibrutinib prior to oxLDL and CRP-XL stimulation reduced platelet dense granule secretion (**Figure 4.10A**), alpha granule secretion (**Figure 4.10B**), and integrin activation (**Figure 4.10C**) to levels similar to resting platelets. Syk inhibitor R406 similarly reduced platelet dense granule secretion (**Figure 4.10A**) and also significantly inhibited alpha granule secretion (**Figure 4.10B**) and integrin activation, but to a lesser extent (**Figure 4.10C**). Ibrutinib significantly inhibited thromboxane generation to levels similar to that of aspirin (**Figure 4.10D**). In light transmission aggregometry assays, pre-incubation of platelets with ibrutinib prior to combined oxLDL and CRP-XL stimulation eliminated platelet aggregation, whereas the Syk inhibitor R406 did not significantly change platelet aggregation in response to oxLDL and CRP-XL (**Figure 4.10E**). Flow cytometry assessment found that ibrutinib abrogated platelet PS exposure in response to oxLDL and CRP-XL, while R406 also significantly, although less completely, inhibited PS exposure (**Figure 4.10F**).

Lastly, to examine Syk and BTK inhibition on oxLDL-mediated platelet procoagulant activity, we evaluated the effects of R406 and ibrutinib on platelet stimulated fibrin generation. Platelets were pre-treated with R406 (10 µM) or ibrutinib (10 µM) and then stimulated with oxLDL (20 µg/ml) in combination with CRP-XL (0.5 µg/ml). Under control conditions, fibrin was first generated at 1730 s (± 180 s) and reached half to maximum at 2670 s (± 140 s), respectively. When pre-treated with ibrutinib, the lag time and time to half maximum increased to 4450 s (± 460 s) and 5700 s (± 740 s), respectively. In contrast, R406 did not significantly change the lag time or the time to half maximum, 2110 s (± 100 s) and 3240 s (± 580 s), respectively (**Figure 4.10G-H**). Together with findings above, these results suggest that R406 and ibrutinib both inhibit initial platelet responses to oxLDL and CRP-XL, while only ibrutinib effectively inhibits platelet aggregation and procoagulant activity.

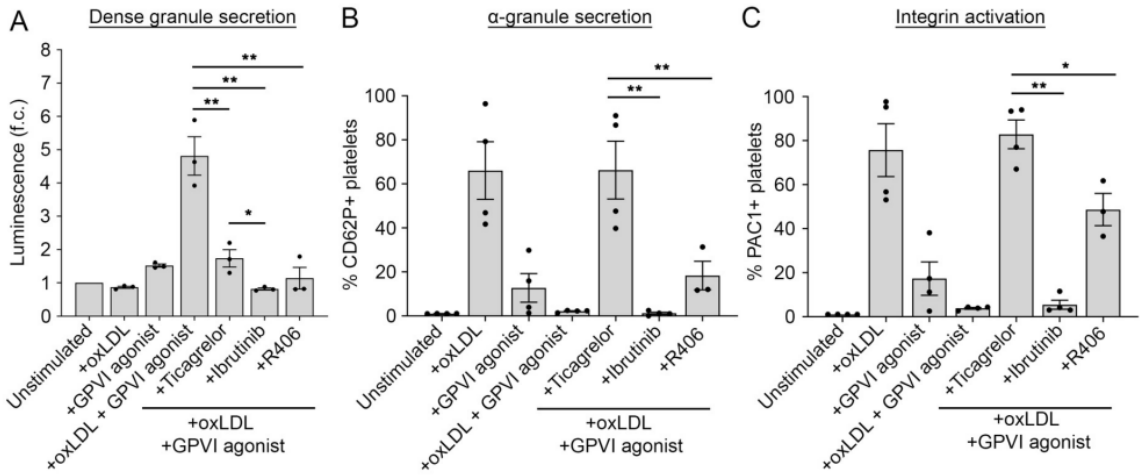

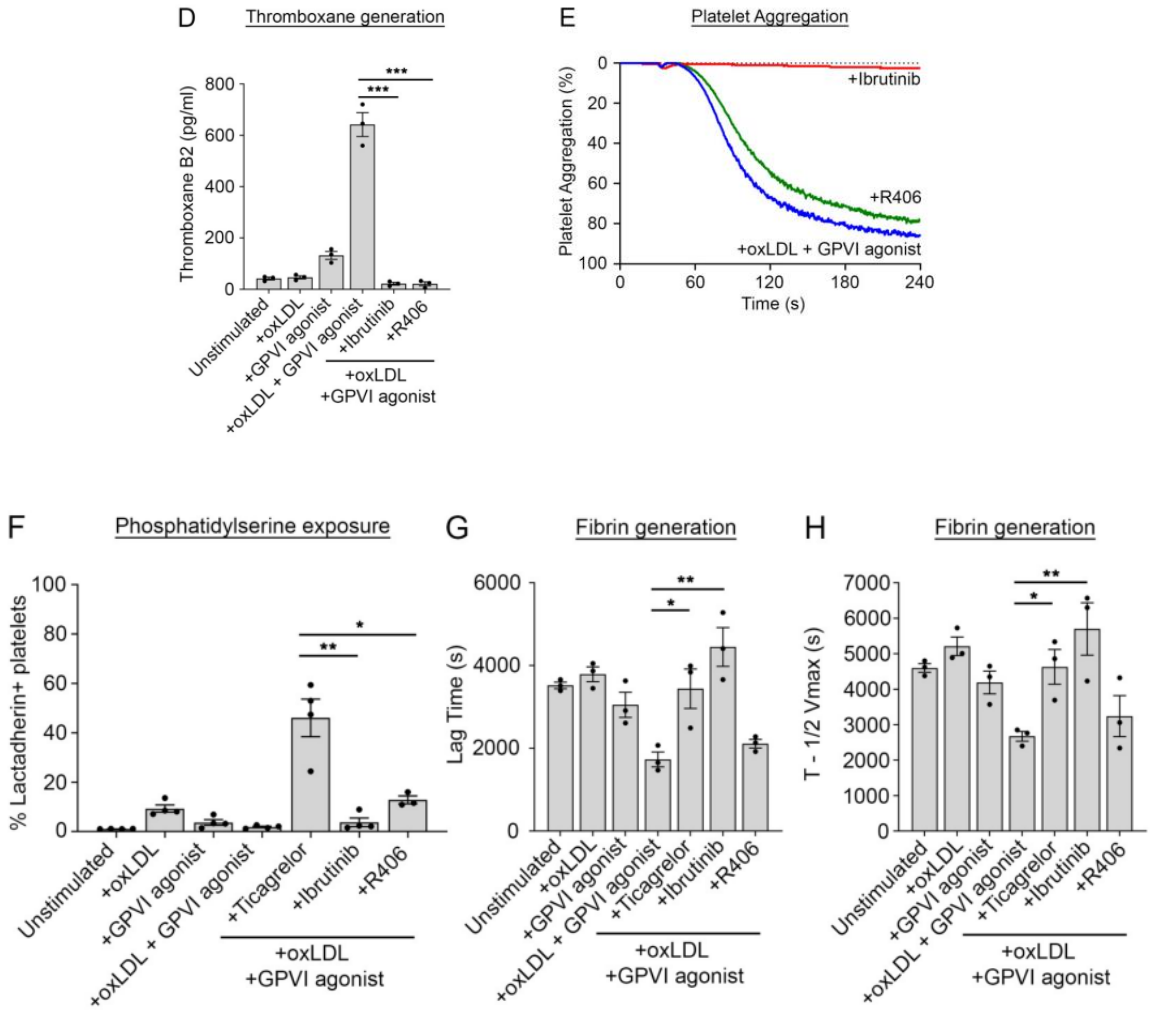

Figure 4.10. BTK (ibrutinib) and Syk (R406) inhibitors reduce oxLDL potentiation of platelet hemostatic and procoagulant activity. Replicate samples ($n \geq 3$) of washed human platelets (2×10^8/ml) were treated with BTK inhibitor ibrutinib (10 µM) or Syk inhibitor R406 (10 µM) for 10 mins and stimulated with GPVI specific agonist CRP-XL (0.5 µg/ml) in combination with oxLDL (20 µM). Platelets were monitored using the luciferase enzyme CHRONO-LUME® to detect the luminescence of ATP released as a measure of platelet dense granule secretion **(A)**, stained with APC-CD62P to monitor for platelet surface expression of P-selectin as a marker of alpha granule secretion **(B)**, and stained with FITC-PAC-1 to monitor for platelet surface integrin activation **(C)**. Platelets were monitored at 37 ºC under continuous stirring at 1200 rpm and the changes in light transmission were measured. The supernatant was extracted and analyzed for thromboxane content generated **(D)**. Representative platelet aggregation traces of platelet samples treated with each select inhibitor are shown **(E)**. Platelets were stained with FITC-Lactadherin to monitor for platelet surface phosphatidylserine (PS) exposure **(F)**. Platelet samples were incubated with $CaCl_2$ (8.3 mM) and citrated platelet poor plasma (33% final). Fibrin formation was measured as a change in turbidity at an absorbance of 405 nm. The lag time **(G)** and time to half the maximum absorbance **(H)** were quantified. Statistical analysis was performed using a one-way ANOVA test and the corresponding P-values of significance are as indicated: * P-value < 0.05, ** P-value < 0.01, and *** P-value < 0.001.

4.5 Discussion

In this chapter, we investigated how oxLDL augments platelet GPVI/ITAM signaling, secondary feedback activation mechanisms, and platelet procoagulant activity. We found that *ex vivo*, oxLDL enhances platelet activation in responses to GPVI agonists – including ITAM signaling, dense granule secretion, alpha granule secretion, integrin activation, platelet aggregation, and thromboxane generation. Likewise, oxLDL also upregulates platelet procoagulant activity, increasing phosphatidylserine (PS) exposure on the platelet surface and accelerating fibrin generation following GPVI stimulation. We also assessed the effects of antiplatelet agents, including P2Y inhibitor ticagrelor and COX inhibitor aspirin, as well as inhibitors targeting Syk (fostamatinib/R406) and BTK (ibrutinib) on these oxLDL mediated platelet responses. We find that *ex vivo*, P2Y blockade as well as Syk and BTK inhibition reduced oxLDL-mediated platelet responses and procoagulant activity, whereas COX inhibition with aspirin had no significant effects. Altogether, our results demonstrate that oxLDL primes platelets to be more susceptible to activation by GPVI stimulation and potentiates GPVI-mediated platelet responses and procoagulant activity in a manner limited by P2Y antagonists and Syk/BTK inhibitors.

Mechanistic studies have established that oxLDL activates the scavenger receptor CD36 on platelets to upregulate signaling pathways that enhance platelet responses, including reactive oxygen species (ROS) generation and caspase activation,(246, 257) and transduce intracellular signaling through associations amongst CD36, Syk, and SFKs.(245, 247, 248, 258) Studies have also shown that MAPK JNK2 is phosphorylated

in platelets exposed to oxLDL mediated by SFKs that is essential for downstream signaling events and upregulating ERK5 and MAPK signaling pathways.(246), (248, 259) However, it has remained generally unknown how oxLDL activation in combination with other platelet agonists affect protein activity along GPVI/ITAM signaling cascades. Our study further demonstrates that CD36 signaling overlaps with the GPVI signaling pathway, in such that the phosphorylation of proteins along the Syk-BTK-PI3K/Akt axis is increased at even sub-threshold levels of CD36 and GPVI stimulation. We found in combination with GPVI specific agonist CRP-XL, oxLDL enhanced the phosphorylation of generalize tyrosine kinase substrates, PKC substrates, Akt substrates, and MAPK substrates (**Figure 4.4A**), as well as DAPP1, PLCγ2, Akt, GSK3, ERK1/2, and other specific effectors of platelet activation (**Figure 4.9**). In addition, we also demonstrated that inhibition of central upstream kinases in particular Syk and BTK within this signaling cascade reduces the potentiation of protein phosphorylation induced by oxLDL (**Figure 4.9**). Notably, the BTK inhibitor ibrutinib inhibited platelet signaling as well as functional activity to a greater extent than fostamatinib, suggesting that BTK has a more of a central role in the convergent signaling cascade from CD36 and GPVI. Future systems biology as well as clinical studies will more precisely and comprehensively define these signaling events, with *ex vivo* as well as *in vivo* assays.(39, 40)

While tyrosine kinase inhibitors (TKIs) such as fostamatinib and ibrutinib may offer promise as antithrombotic agents in specific contexts,(235, 260) they are not yet a part of the arsenal of pharmacological therapies used to inhibit platelet activation in treating or preventing cardiovascular disease. At present, the efficacy of aspirin as an antiplatelet

agent for secondary prevention of CVD is well established, but the clinical benefit of aspirin as the primary prevention remains unclear, especially relative to complications from bleeding.(261) Moreover, the specific effects of aspirin on oxLDL-mediated platelet activation mechanisms have remained largely unaddressed. Likewise, roles for other widely used antiplatelet agents, including $P2Y_{12}$ antagonists, as inhibitors of oxLDL-enhanced platelet activity have not yet been explored.(252, 253, 262) In this chapter, we find that platelet $P2Y_{12}$ inhibition with ticagrelor significantly reduces the potentiation of platelet signaling, aggregation, and platelet procoagulant activity enhanced by oxLDL, whereas COX inhibition with aspirin had no significant effect. Ticagrelor treatment also significantly inhibited oxLDL-augmented dense granule secretion, alpha granule secretion, and integrin activation. These results suggest that oxLDL enhances platelet activities via the secondary feedback mechanisms of ADP secretion and purinergic receptor activation, where $P2Y_{12}$ inhibitors (ticagrelor) more potently inhibit activation relative to aspirin.

Aspirin and P2Y receptor antagonists are used together as dual anti-platelet therapy (DAPT), following procedures such as percutaneous coronary intervention to prevent thrombosis and cardiovascular events. However, bleeding complications still represent a limitation of DAPT. To this end, small molecule TKIs, that are now effective therapeutics in a range of hematologic malignancies as well as immunological and inflammatory disorders, also offer a means to inhibit specific aspects of platelet activation.(73, 182, 184) Our group and others have assessed roles for TKIs in GPVI-mediated platelet responses, including agents targeting Src, Syk, BTK, Jak and other tyrosine kinases (39,

140, 147, 187). In this chapter, we investigate how Syk/BTK may also reduce procoagulant platelet responses induced by oxLDL. We found that both BTK inhibitor ibrutinib and Syk inhibitor fostamatinib reduced platelet granule secretion, integrin activation, and procoagulant activity, decreasing phosphatidylserine exposure on the platelet surface and decreasing the rate of fibrin generation. Interestingly, ibrutinib was more potent than fostamatinib in reducing oxLDL mediated platelet responses, suggesting that BTK inhibitors may be more effective than Syk inhibitors in reducing the synergistic effects of CD36 and GPVI on platelet procoagulant activity. Altogether, our results suggest that tyrosine kinase signaling via BTK plays a central role in oxLDL-mediated platelet activation in a manner that may be therapeutically targeted to reduce platelet procoagulant activity in cardiovascular disease.

In conclusion, this chapter demonstrates that oxLDL potentiates platelet physiological responses and procoagulant activity in a manner involving upregulated dense granule secretion, purinergic receptor activation and ITAM signaling. In addition to expanding knowledge around mechanisms of oxLDL-mediated platelet sensitization, this chapter provides insight on differences between current antiplatelet agents such as ticagrelor and aspirin and evaluates their efficacy in reducing oxLDL mediated platelet responses. As such, future studies will more clearly specify roles for Syk, BTK, PI3K and other signaling proteins and as potential targets that mediate the effects oxLDL on platelets. Future studies following from our results may also inform how oxLDL synergizes with other platelet agonists and signaling pathways and extend it to *in vivo* models to further study lipid-platelet interactions as well as more novel antiplatelet agents and therapeutics.

Ultimately, this chapter offers novel mechanistic knowledge on the effects of oxLDL on platelet function and signaling downstream of GPVI and insight on antiplatelet agents that can reduce oxLDL mediated platelet responses and procoagulant phenotype in cardiovascular disease.

Chapter 5: Conclusions, Limitations, & Future Directions

5.1. Conclusions

The studies outlined in this dissertation explore the role of platelet tyrosine kinases in atherosclerosis. This was accomplished through the use of tyrosine kinase inhibitors (TKIs) not only as tools to investigate the mechanisms of tyrosine kinases in platelet signaling and platelet activation, but as well as to evaluate the potential of tyrosine kinases as druggable targets for antiplatelet agents. The ultimate goal of the research presented in this thesis is to improve our understanding of hemostasis and thrombosis such to gain new insight on how to effectively reduce thrombosis in disease without compromising hemostatic function and safety. Following, I will summarize the major findings and conclusions drawn from the studies in each chapter.

In Chapter 3, we explored the role of Bruton's tyrosine kinase (BTK) and spleen tyrosine kinase (Syk) in platelet physiology downstream of platelet glycoprotein VI (GPVI) and ITAM-mediated signaling pathways. To this end, we investigated the effects of 12 different Syk and BTK inhibitors on GPVI-mediated platelet signaling and function. We demonstrated that TKIs targeting Syk or BTK inhibit central platelet functional responses, reducing platelet spreading on fibrinogen and collagen, dense granule secretion, integrin activation, and alpha granule secretion, but differentially affected protein activities and organization in critical systems downstream of Syk and BTK in platelets. As these TKIs targeting Syk, BTK and other kinases are further developed and implemented for an increasing number of inflammatory, oncogenic and other conditions,

studies such as our work herein will help to address a growing need to better understand the effects of such compounds on essential molecular machinery around Syk-BTK signaling in platelets and other physiologically relevant cell types.

In Chapter 4, we investigated the effects of oxidized low-density lipoprotein (oxLDL) in enhancing platelet activation and atherothrombosis, and how to best therapeutically target and safely prevent such procoagulant responses by platelets. Here, demonstrate that oxLDL upregulates GPVI mediated platelet hemostatic and procoagulant responses, and how traditional antiplatelet therapies and tyrosine kinase inhibitors affect such oxLDL-enhanced platelet activity *ex vivo*. In this study, we demonstrate that oxLDL enhances platelet functional responses and procoagulant activity downstream of GPVI signaling. Therapeutically, we demonstrate that P2Y antagonists such as ticagrelor and tyrosine kinase inhibitors targeting BTK and Syk such as ibrutinib and fostamatinib, respectively, reduce such oxLDL-enhanced platelet responses, but COX inhibitors like aspirin do not.

Overall, the studies presented in this dissertation help characterize the role of tyrosine kinases in platelet activation, signaling pathways, and functional responses and provide insight on the potential use and development of tyrosine kinase inhibitors as safer antiplatelet agents in the setting of atherosclerosis.

5.2. Limitations

In Chapter 3, we explored the role of Bruton's tyrosine kinase (BTK) and spleen tyrosine kinase (Syk) in platelet physiology downstream of platelet glycoprotein VI (GPVI) and ITAM-mediated signaling pathways. Building upon this in Chapter 4, we investigated the effects of oxidized low-density lipoprotein (oxLDL) in enhancing GPVI-mediated platelet activation and atherothrombosis, and how to best therapeutically target and safely prevent such procoagulant responses by platelets utilizing previously studied tyrosine kinase inhibitors and traditional antiplatelet agents.

There are a number of limitations to these studies. First, all studies were conducted using an *ex vivo* model of washed and isolated human platelets. These studies would be greatly improved if studies were extended to *ex vivo* models using human whole blood and *in vivo* murine and non-human primate models. In particular, these *in vivo* models would allow us look at the effects tyrosine kinase inhibitors and antiplatelet agents such as ticagrelor and aspirin on oxLDL-mediated platelet and fibrin accumulation following injury of a vessel. For instance, such *in vivo* models can be done quickly by injecting mice with oxLDL intravenously to mimic a plaque rupture or extensively by placing mice on a high fat diet to represent a prothrombotic model of dyslipidemia. In both models, this will allow for a more physiological investigation of the effects of antiplatelet agents and tyrosine kinase inhibitors *in vivo*. Next, oxLDL is used throughout the studies described in Chapter 4. Because these studies rely heavily on oxLDL, it is important to characterize the oxLDL used and experimentally demonstrate the link between oxLDL and CD36 in platelets. This limitation should be addressed to establish how the extent of

LDL oxidation influences platelet activation through both CD36 dependent and CD36 independent mechanisms. In order to accomplish this, CD36 inhibitors or antibodies can be used to block CD36 receptors in similar phosphorylation and platelet functional studies.

To address these limitations, future directions (discussed in the following section) are aimed to extend these *ex vivo* studies to *in vivo* models. In the following section, future directions will detail preliminary murine models that investigate the *in vivo* effects of antiplatelet agents and tyrosine kinase inhibitors on oxLDL-mediated platelet procoagulant activity.

5.3. Future Directions

5.3.1 In vivo effects of antiplatelet agents and tyrosine kinase inhibitors on oxLDL-mediated platelet procoagulant activity

In Chapter 4, we explored the *ex vivo* effects of antiplatelet agents and tyrosine kinase inhibitors (TKIs) on oxidized low-density lipoprotein (oxLDL) enhanced platelet procoagulant activity. As a direct extension to the *ex vivo* work presented, ongoing and future studies will focus on *in vivo* murine and non-human primate (NHP) models to further investigate the effects of antiplatelet agents (e.g., ticagrelor, aspirin) and TKIs (e.g., ibrutinib) on oxLDL-enhanced platelet procoagulant activity.

To initially test the effects of antiplatelet agents and TKIs on oxLDL enhanced platelet procoagulant activity in a murine model, we first obtained wild-type mice and separated them into two groups: 1) control group and 2) oxLDL group. The oxLDL group received a retroorbital injection of 100 µl oxLDL at a concentration of 400 µg/ml. The control group did not receive any injections of oxLDL. We waited 10 minutes and then drew blood via the inferior vena cava, roughly ~50 µl was obtained. The collected blood was then treated with ticagrelor (1 µM), ibrutinib (10 µM), aspirin (1 mM), or vehicle (0.1% DMSO) and anti-mouse PE CD62P (1:25) and FITC lactadherin (2:25) to stain for P-selectin expression and phosphatidylserine exposure, respectively. Each platelet mixture was then stimulated with CRP-XL (0.1 µg/ml) or vehicle (0.1% DMSO) and incubated at 37 ^{o}C for 20 mins. Each sample was fixed in 2% paraformaldehyde, diluted with modified HEPES/Tyrode buffer, and analyzed using flow cytometry on a FACSCantoII

flow cytometer. Platelet populations were identified and gated based forward scatter and side scatter characteristics. Data was analyzed using the FlowJo software and the mean fluorescence intensity was recorded. The workflow is outlined in **Figure 5.1**.

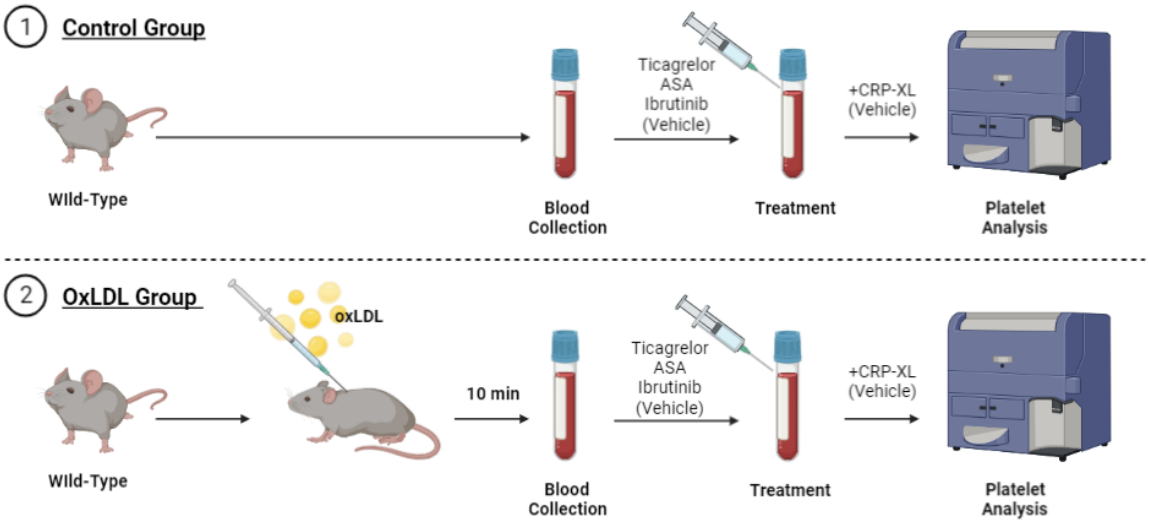

Figure 5.1. OxLDL murine model workflow – *ex vivo* treatment. Wild-type mice were separated into two groups: 1) control group and 2) oxLDL group. The oxLDL group received a retroorbital injection of 100 µl oxLDL at a concentration of 400 µg/ml. After 10 mins, blood was drawn via the inferior vena cava. The collected blood was then treated with ticagrelor (1 µM), ibrutinib (10 µM), aspirin (1 mM), or vehicle (0.1% DMSO) and treated with anti-mouse PE CD62P (1:25) and FITC lactadherin (2:25) to stain for P-selectin expression and phosphatidylserine exposure, respectively. Each platelet mixture was then stimulated with CRP-XL (0.1 µg/ml) or vehicle (0.1% DMSO) incubated at 37 ºC for 20 mins. FACSCantoII flow cytometer was used to measure the mean fluorescence intensity. Figure created in BioRender.com by Tony J. Zheng.

Preliminary results show that CRP-XL stimulation increased lactadherin exposure on murine platelets. In addition, oxLDL injected mice had greater lactadherin exposure on their platelets when stimulated with CRP-XL in comparison to unstimulated platelets, though not statistically significant. Lastly, preliminary results suggest that ticagrelor, aspirin, and ibrutinib treated murine platelets have a significantly decreased lactadherin exposure in comparison to untreated platelets even when stimulated with CRP-XL (**Figure 5.2**).

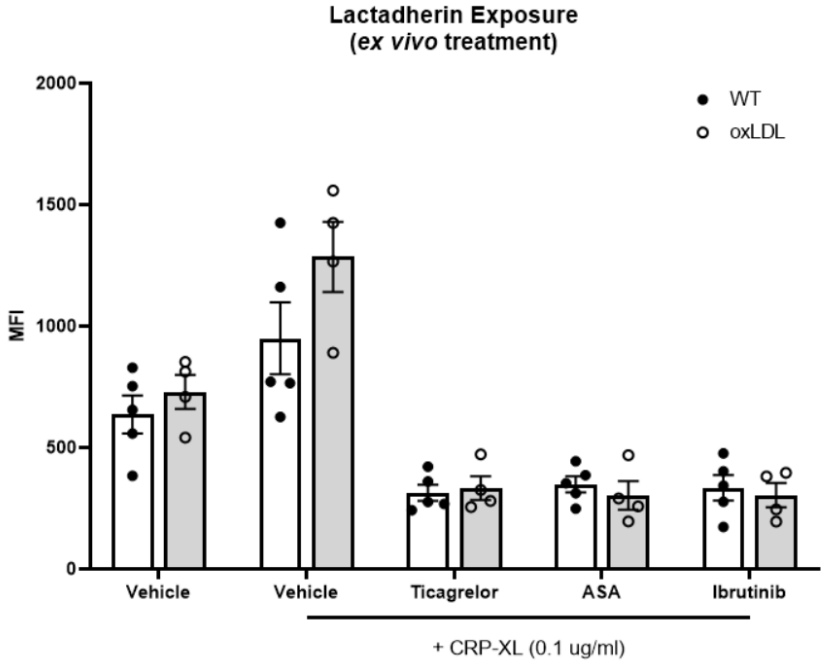

Figure 5.2. Ticagrelor, aspirin, and ibrutinib decrease lactadherin exposure on murine platelets *ex vivo*. Wild-type mice were separated into a control group (closed circle) and oxLDL group (opened circle). The oxLDL group received a retroorbital injection of 100 µl oxLDL at a concentration of 400 µg/ml. After 10 mins, blood was drawn via the inferior vena cava. The collected blood was then treated with ticagrelor (1 µM), ibrutinib (10 µM), aspirin (1 mM), or vehicle (0.1% DMSO) and anti-mouse PE CD62P (1:25) and FITC lactadherin (2:25) to stain for P-selectin expression and phosphatidylserine exposure, respectively. Each platelet mixture was then stimulated with CRP-XL (0.1 µg/ml) or vehicle (0.1% DMSO) incubated at 37 ^{o}C for 20 mins. FACSCantoII flow cytometer was used to measure the mean fluorescence intensity.

Next, wild-type mice were treated with ticagrelor (100 mg/kg), aspirin (30 mg/kg), and ibrutinib (10 mg/kg) in 100 µL PBS *in vivo* via an intraperitoneal injection. Each group of mice (n = 5) were injected with the respective inhibitor. After 30 minutes, each group received a retroorbital injection of 100 µl oxLDL at a concentration of 400 µg/ml. We waited 10 minutes and then drew blood via the inferior vena cava, roughly ~50 µl was obtained. The collected blood was then treated with anti-mouse PE CD62P (1:25) and FITC lactadherin (2:25) to stain for P-selectin expression and phosphatidylserine exposure, respectively. Each platelet mixture was then stimulated with CRP-XL (0.1 µg/ml) or vehicle (0.1% DMSO) and incubated at 37 ^{o}C for 20 mins. Each sample was fixed in 2% paraformaldehyde, diluted with modified HEPES/Tyrode buffer, and analyzed using flow cytometry on a FACSCantoII flow cytometer. Platelet populations were identified and gated based forward scatter and side scatter characteristics. Data was analyzed using the FlowJo software and the mean fluorescence intensity was recorded. The workflow is outlined in **Figure 5.3**.

Preliminary results show that CRP-XL stimulation increased P-selectin expression on murine platelets. In addition, oxLDL injected mice had greater P-selectin expression on their platelets when stimulated with CRP-XL in comparison to unstimulated platelets. Lastly, preliminary results suggest platelets from ticagrelor, aspirin, and ibrutinib injected mice have a significantly decreased P-selectin expression in comparison to untreated platelets even when stimulated with CRP-XL (**Figure 5.4**). Altogether, these results suggest that ticagrelor, aspirin, and ibrutinib decrease P-selectin expression and lactadherin exposure on murine platelets *in vivo* and *ex vivo,* respectively.

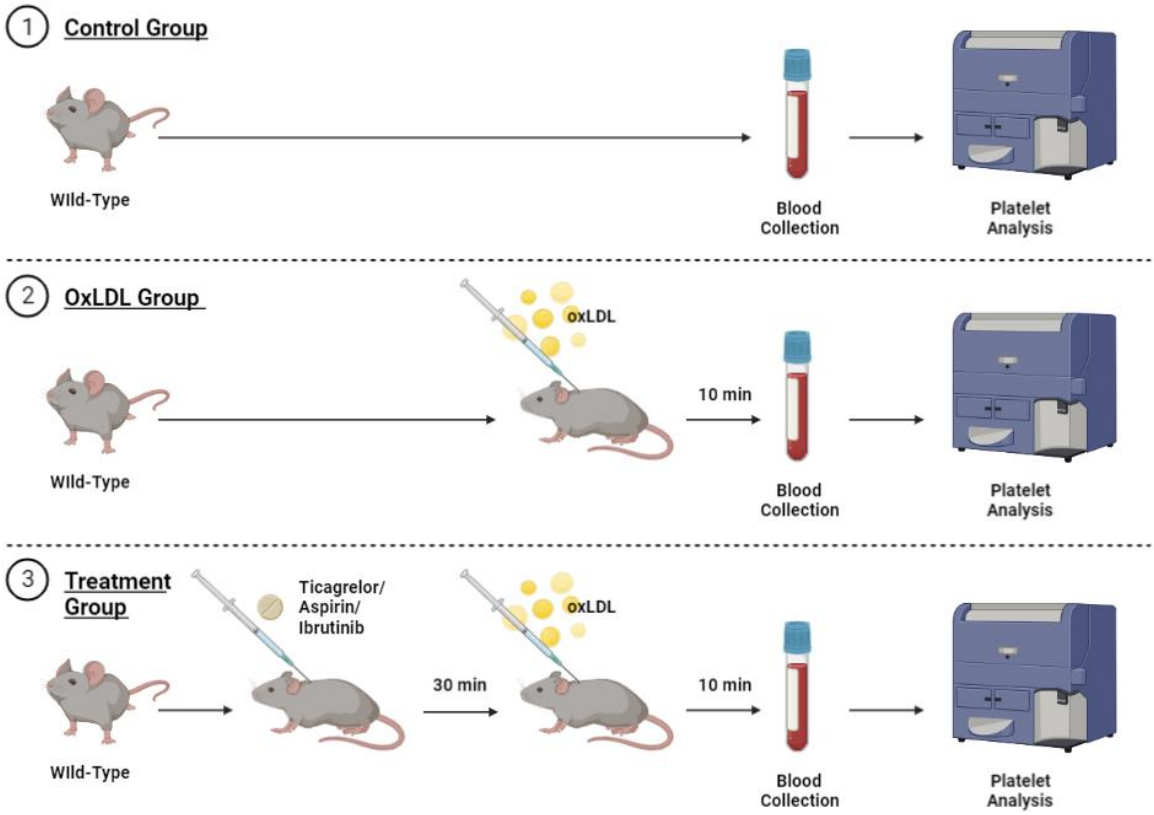

Figure 5.3. OxLDL murine model workflow – *in vivo* treatment. Wild-type mice were separated into five groups: 1) control group, 2) oxLDL group, and 3-5) ticagrelor (100 mg/kg), aspirin (30 mg/kg) and ibrutinib (10 mg/kg) treatment group. Each group of mice (n=5) were injected with inhibitor diluted in 100 µL PBS via an intraperitoneal injection. After 30 minutes, each group received a retroorbital injection of 100 µl oxLDL at a concentration of 400 µg/ml. After 10 mins, blood was drawn via the inferior vena cava. The collected blood was then treated with anti-mouse PE CD62P (1:25) and FITC lactadherin (2:25) to stain for P-selectin expression and phosphatidylserine exposure, respectively. Each platelet mixture was then stimulated with CRP-XL (0.1 µg/ml) or vehicle (0.1% DMSO) and incubated at 37 ºC for 20 mins. FACSCantoII flow cytometer was used to measure the mean fluorescence intensity. Figure created in BioRender.com by Tony J. Zheng.

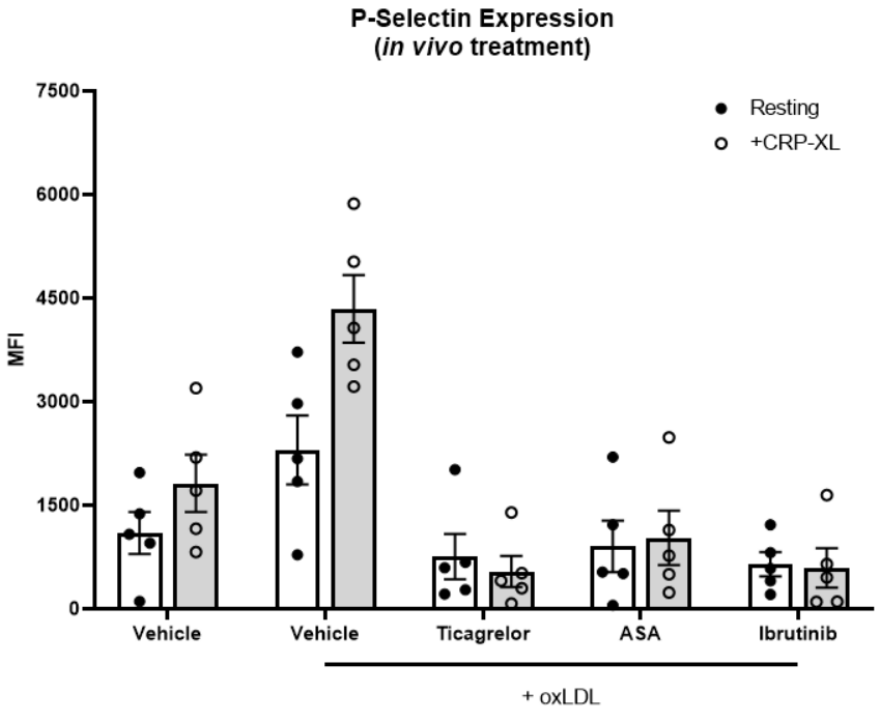

Figure 5.4. Ticagrelor, aspirin, and ibrutinib decrease P-selectin expression on murine platelets *in vivo*. Wild-type mice were treated with ticagrelor (100 mg/kg), aspirin (30 mg/kg), and ibrutinib (10 mg/kg) in 100 µL PBS *in vivo* via an intraperitoneal injection. After 30 minutes, each group received a retroorbital injection of 100 µl oxLDL at a concentration of 400 µg/ml. After 10 mins, blood was drawn via the inferior vena cava. The collected blood was then treated with anti-mouse PE CD62P (1:25) and FITC lactadherin (2:25) to stain for P-selectin expression and phosphatidylserine exposure, respectively. Each platelet mixture was then stimulated with CRP-XL (0.1 µg/ml) or vehicle (0.1% DMSO) and incubated at 37 ºC for 20 mins. FACSCantoII flow cytometer was used to measure the mean fluorescence intensity.

Future studies will focus on first analyzing these murine platelet samples to quantify the mean fluorescence intensity of P-selectin expression on platelets treated with the inhibitors *ex vivo* as well as lactadherin exposure on platelets treated with the inhibitors *in vivo*. Future studies will also extend into non-human primate models, in which NHPs will be subjected to a high fat diet, treated with ticagrelor, aspirin, and ibrutinib *ex vivo* and *in vivo*, and the procoagulant activity of platelets will be assessed.

5.3.2 Effects of trans-aortic valve replacements (TAVRs) on platelet function

Aortic stenosis is the most common valvular heart disease in the developed world, affecting over 20% of individuals 65 years old or greater (263, 264). Aortic stenosis is characterized by the narrowing of the aortic valve in the heart that prevents the valve from opening and closing fully, restricting blood flow from the heart to the rest of the body (263, 265). Aortic stenosis is most often caused by age-related progressive calcification of the valve and typically presents as chest pain, fatigue and shortness of breath in patients. Aortic stenosis is associated with other diseases and complications, including left ventricular hypertrophy and aortic regurgitation, leading ultimately to congestive heart failure and death if left untreated (264).

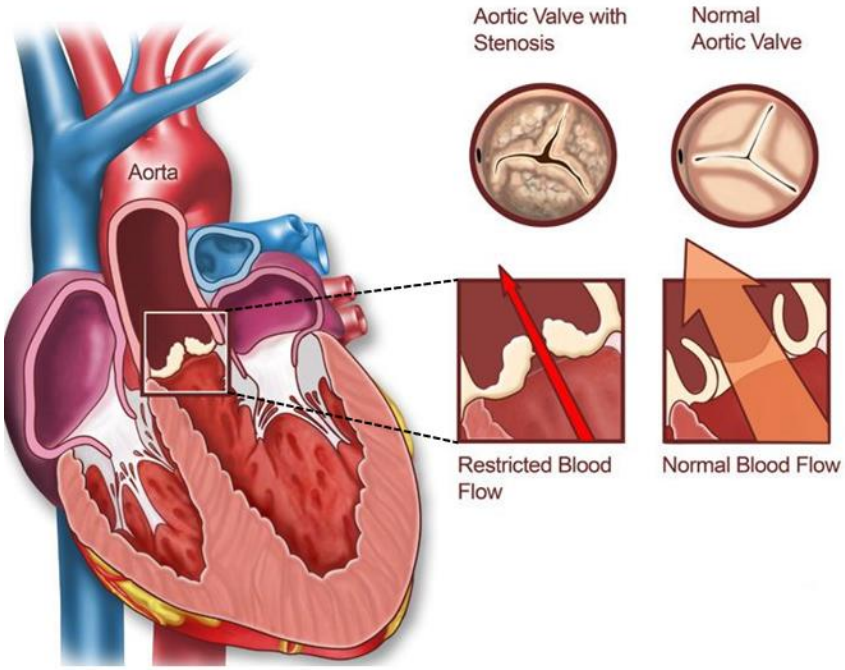

Figure 5.5. Aortic Stenosis. Aortic stenosis is characterized as the narrowing of the aortic value, as indicated by the box. Aortic stenosis is caused by progressive calcification of the valve that prevents the value from fully opening and closing, reducing the normal blood flow from the heart to the rest of the body. Reprinted with permission.

The traditional treatment for aortic stenosis is surgical aortic valve replacement (SAVR), which entails an open-heart surgery where the diseased valve is removed and replaced with a tissue/bioprosthetic valve (typically bovine pericardium or porcine pericardium) or a mechanical valve (typically titanium or pyrolytic carbon) (266). However, the magnitude of a SAVR procedure comes with increased complications of arrhythmia, bleeding, stroke, infection and cardiac failure and older patients with co-morbidities are at higher risk. In recent decades, trans-aortic valve replacement (TAVR) has been developed as a minimally invasive, catheter-based alternative procedure for high- and intermediate-risk patients with severe aortic stenosis. Despite the success, the major concern is leaflet thrombosis on the valves' biomaterial used in both SAVR and TAVR procedures (267-269). Thus, there is a need to better understand the factors and mechanisms that contribute to thrombosis on TAVR biomaterials.

Platelet Adhesion on Bovine Pericardium

To investigate the mechanisms that contribute to thrombosis, we first hypothesize that platelet adhesion is increased on the bovine pericardium biomaterial. Bovine pericardium was obtained from TissX, a company that sources, manufactures, and supplies a variety of tissue-based products for specifically for cardiac and vascular surgical applications. The bovine pericardium was cut into circular pieces of in diameter and placed in a microtiter plate. A 200 µl solution of washed purified platelets (5×10^8 platelets/ml) was incubated on the material surface for 1 hr at room temperature. A fibrinogen coated surface and a BSA coated surface was used for comparison. The samples were then washed and rinsed three times with PBS to remove non-adherent platelets. The total

number and concentration of platelets adhered to each surface was measured using a platelet acid phosphatase activity assay with a calibration curve using platelet solutions, ranging from 0 to 5×10^8 platelets/ml to set a standard curve (270). Preliminary results show that the concentration of platelets and total number of adhered platelets is greater on the bovine pericardium than compared to that on a BSA coated surface. The concentration and total number of platelets adhered on bovine pericardium was comparable to that adhered on a fibrinogen surface, approximately 4×10^7 platelets/ml (**Figure 5.2**).

Another common biomaterial used for valves is porcine pericardium. Future studies can be done to compare platelet adhesion on various TAVR materials, such as bovine pericardium vs. porcine pericardium. In addition, various agonists can be tested to evaluate their effects on platelet adhesion on TAVR surfaces. For instance, CRP-XL and/or oxLDL can be tested to investigate whether activated platelets in states of hyperlipidemia or atherosclerosis contribute to increased platelet adhesion on TAVR materials, such as bovine and porcine pericardium. Similarly, various inhibitors and antagonists can be tested to evaluate their ability in reducing platelet adhesion, platelet activation, and consequently thrombosis on TAVR materials. For instance, anti-platelet agents such as ticagrelor and aspirin or tyrosine kinase inhibitors such as ibrutinib and fostamatinib/R406 can be tested to investigate the mechanisms of platelet activation on these materials as well as their potential as antiplatelet agents in reducing thrombosis on TAVRs.

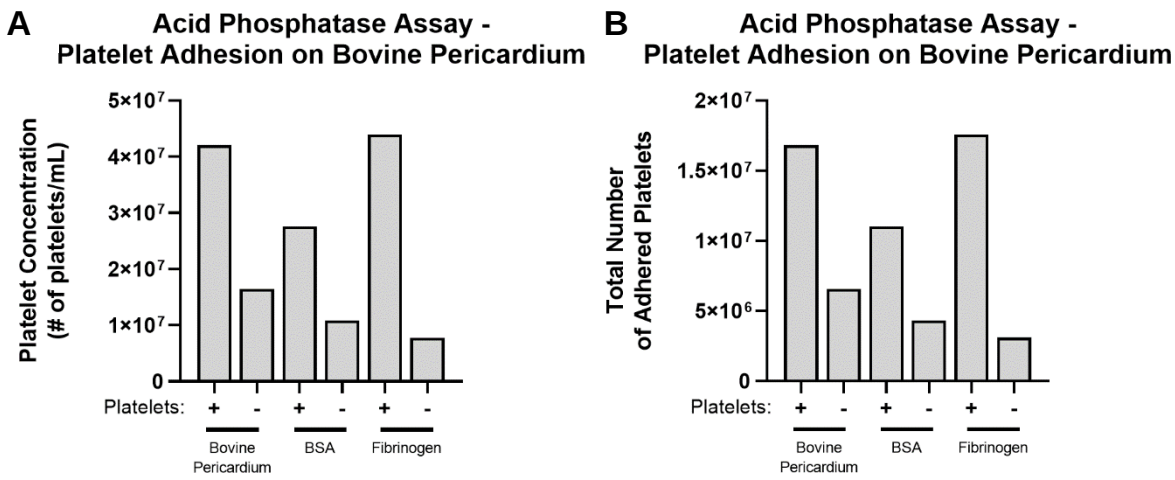

Figure 5.6. Platelet adhesion on bovine pericardium. Bovine pericardium was cut into circular pieces of in diameter and placed in a microtiter plate, along with BSA-coated and fibrinogen-coated surfaces. A 200 µl solution of washed purified platelets (5×10^8 platelets/ml) was incubated on each surface for 1 hr at room temperature. The samples were then rinsed three times with PBS to remove non-adherent platelets. **A)** The total number and **B)** concentration of platelets adhered to each surface was measured using a platelet acid phosphatase activity assay with a calibration curve using platelet solutions, ranging from 0 to 5×10^8 platelets/ml to set a standard curve.

Platelet Procoagulant Activity Pre-TAVR vs. Post-TAVR Procedure

To investigate the effects of the TAVR procedure itself on platelet procoagulant activity, whole blood samples were collected from patients immediately prior to the TAVR procedure (pre-TAVR) as well as immediately following the TAVR procedure (post-TAVR), accordingly to an approved Institutional Review Board by Oregon Health & Science University. We hypothesize that the introduction of the TAVR will cause platelets to be more procoagulant in comparison to platelets prior to TAVR placement.

Washed, purified platelets (2×10^7/ml) from pre-TAVR and post-TAVR samples were incubated with FITC bovine lactadherin (1:20) to stain for phosphatidylserine exposure. Each platelet mixture was stimulated with CRP-XL or vehicle (0.1% DMSO) and

incubated at 37 ^{o}C for 30 mins. Each sample was fixed in 2% paraformaldehyde, diluted with modified HEPES/Tyrode buffer, and analyzed using flow cytometry on a FACSCantoII flow cytometer (Becton Dickinson, Franklin Lakes, New Jersey, USA). Platelet populations were identified and gated based forward scatter and side scatter characteristics. Data was analyzed using FlowJo software in which the mean fluorescence intensity (MFI) was calculated. Preliminary data show that post-TAVR platelet samples stimulated with agonists exhibited higher phosphatidylserine exposure than pre-TAVR platelet samples, though not statistically significantly (**Figure 5.3**).

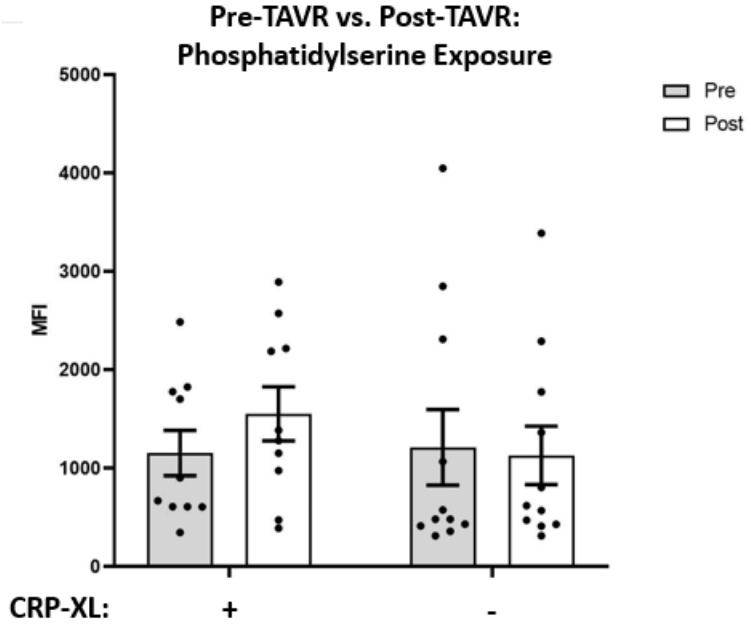

Figure 5.7. Phosphatidylserine exposure of pre-TAVR vs. post-TAVR platelet samples. Washed, purified platelets (2×10^7/ml) from pre-TAVR and post-TAVR samples were incubated with FITC bovine lactadherin (1:20) to stain for phosphatidylserine exposure. Each platelet mixture was stimulated with CRP-XL or vehicle (0.1% DMSO) and incubated at 37 ^{o}C for 30 mins. Each sample was fixed in 2% paraformaldehyde, diluted with modified HEPES/Tyrode buffer, and analyzed using flow cytometry. Data was analyzed using FlowJo software in which the mean fluorescence intensity (MFI) was calculated.

Patients' pre-TAVR and post-TAVR whole blood samples were obtained deidentified. Washed, purified platelets (1.5×10^8/ml) were prepared from each sample in a 96-well plate pre-blocked by 2% polyethylene glycol (PEG) 2000 for 1 h and washed with HEPES buffer saline (HBS, pH 7.4). Each platelet mixture (50 µl) was stimulated with GPVI specific agonist CRP-XL (0.5 µg/ml) and TRAP6 or vehicle (0.1% DMSO) and incubated for 10 mins at room temperature. Citrated platelet poor plasma (PPP, 50 µl) followed by $CaCl_2$ (25 mM, 50 µl) were added to each platelet mixture. Fibrin formation was measured as a change in turbidity at an absorbance of 405 nm at 1 min intervals over the course of 2 h using an Infinite M200 spectrophotometer (TECAN, Mannderdorf, Switzerland). The lag time and time to reach half of maximum turbidity were calculated. Preliminary data show that post-TAVR samples have a decreased normalized lag time and decreased normalized time to half max absorbance in comparison to pre-TAVR samples (**Figure 5.4**).

Future studies with pre-TAVR and post-TAVR patient samples can be done to analyze for other platelet functional responses, such as dense granule secretion, integrin receptor activation, alpha granule secretion, platelet aggregation, phosphoproteomics analyses, and other platelet protein signaling events in response to various agonists.

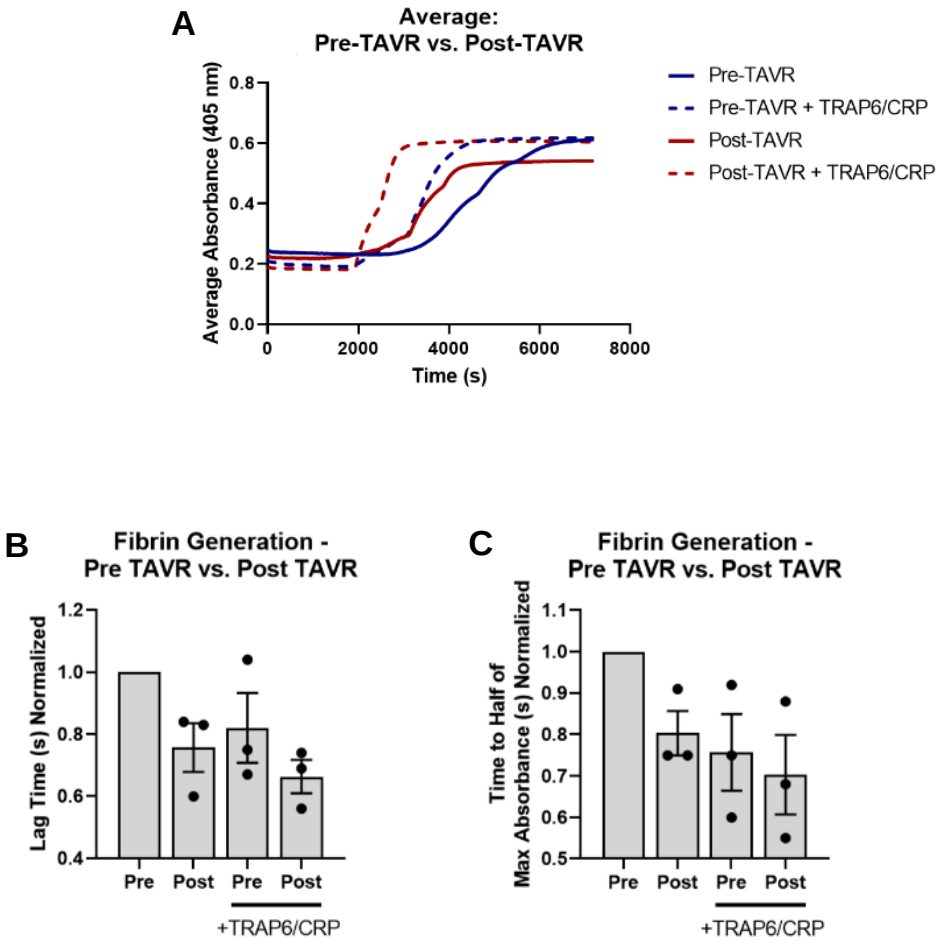

Figure 5.8. Fibrin generation of pre-TAVR vs. post-TAVR platelet samples. Washed, purified platelets (1.5×10^8/ml) were prepared from each pre-TAVR and post-TAVR patient sample in a 96-well plate pre-blocked by 2% polyethylene glycol (PEG) 2000 for 1 h and washed with HEPES buffer saline (HBS, pH 7.4). Each platelet mixture (50 µl) was stimulated with CRP-XL (0.5 µg/ml) and TRAP6 or vehicle (0.1% DMSO) and incubated for 10 mins at room temperature. Citrated platelet poor plasma (PPP, 50 µl) followed by $CaCl_2$ (25 mM, 50 µl) were added to each platelet mixture. **A)** Fibrin formation was measured as a change in turbidity at an absorbance of 405 nm at 1 min intervals over the course of 2 h using an Infinite M200 spectrophotometer (TECAN, Mannderdorf, Switzerland). The **B)** lag time and **C)** time to reach half of maximum turbidity were calculated.

Overall, this chapter details future directions focused on two main future studies, investigating: 1) *in vivo* effects of antiplatelet agents and tyrosine kinase inhibitors on oxLDL-mediated platelet procoagulant activity and 2) effects of trans-aortic valve replacements (TAVRs) on platelet function. This chapter provides preliminary results and future directions that extends current studies into *in vivo* murine models, non-human primate models, and human patients in the setting of transaortic valve replacements that will further explore the effects of tyrosine kinase inhibitors in a more physiological and clinical setting.

References

1. **Glass CK, and Witztum JL**. Atherosclerosis: the road ahead. *Cell* 104: 503-516, 2001.

2. **Libby P**. Inflammation in atherosclerosis. *Arteriosclerosis, thrombosis, and vascular biology* 32: 2045-2051, 2012.

3. **Frojmovic MM, and Milton JG**. Human platelet size, shape, and related functions in health and disease. *Physiological reviews* 62: 185-261, 1982.

4. **Paulus J-M**. Platelet size in man. 1975.

5. **Lenting PJ, Christophe OD, and Denis CV**. von Willebrand factor biosynthesis, secretion, and clearance: connecting the far ends. *Blood, The Journal of the American Society of Hematology* 125: 2019-2028, 2015.

6. **Zhou Y-F, Eng ET, Zhu J, Lu C, Walz T, and Springer TA**. Sequence and structure relationships within von Willebrand factor. *Blood, The Journal of the American Society of Hematology* 120: 449-458, 2012.

7. **Ruggeri ZM, and Mendolicchio GL**. Adhesion mechanisms in platelet function. *Circulation research* 100: 1673-1685, 2007.

8. **Mazzucato M, Spessotto P, Masotti A, De Appollonia L, Cozzi MR, Yoshioka A, Perris R, Colombatti A, and De Marco L**. Identification of domains responsible for von Willebrand factor type VI collagen interaction mediating platelet adhesion under high flow. *Journal of Biological Chemistry* 274: 3033-3041, 1999.

9. **van der Plas RM, Gomes L, Marquart JA, Vink T, Meijers JC, de Groot PG, Sixma JJ, and Huizinga EG**. Binding of von Willebrand factor to collagen type III: role of specific amino acids in the collagen binding domain of vWF and effects of neighboring domains. *Thrombosis and haemostasis* 84: 1005-1011, 2000.

10. **Springer TA**. von Willebrand factor, Jedi knight of the bloodstream. *Blood, The Journal of the American Society of Hematology* 124: 1412-1425, 2014.

11. **Dong J-f, Moake JL, Nolasco L, Bernardo A, Arceneaux W, Shrimpton CN, Schade AJ, McIntire LV, Fujikawa K, and López JA**. ADAMTS-13 rapidly cleaves newly secreted ultralarge von Willebrand factor multimers on the endothelial surface under flowing conditions. *Blood, The Journal of the American Society of Hematology* 100: 4033-4039, 2002.

12. **Ricard-Blum S**. The collagen family. *Cold Spring Harbor perspectives in biology* 3: a004978, 2011.

13. **Bergmeier W, and Hynes RO**. Extracellular matrix proteins in hemostasis and thrombosis. *Cold Spring Harbor perspectives in biology* 4: a005132, 2012.

14. **Henschen A, Lottspeich F, Kehl M, and Southan C**. Covalent structure of fibrinogen. *Annals of the New York Academy of Sciences* 408: 28-43, 1983.

15. **Blombäck B, Hessel B, and Hogg D**. Disulfide bridges in NH2-terminal part of human fibrinogen. *Thrombosis research* 8: 639-658, 1976.

16. **Huang S, Cao Z, and Davie E**. The role of amino-terminal disulfide bonds in the structure and assembly of human fibrinogen. *Biochemical and biophysical research communications* 190: 488-495, 1993.

17. **Zhang J-Z, and Redman C**. Identification of B beta chain domains involved in human fibrinogen assembly. *Journal of Biological Chemistry* 267: 21727-21732, 1992.

18. **Lakshmanan HHS, Melrose AR, Sepp A-LI, Mitrugno A, Ngo AT, Khader A, Thompson R, Sallee D, Pang J, and Mangin PH**. The basement membrane protein nidogen-1 supports platelet adhesion and activation. *Platelets* 32: 424-428, 2021.

19. **McCarty O, Zhao Y, Andrew N, Machesky L, Staunton D, Frampton J, and Watson S**. Evaluation of the role of platelet integrins in fibronectin-dependent spreading and adhesion. *Journal of thrombosis and haemostasis* 2: 1823-1833, 2004.

20. **Podor TJ, Campbell S, Chindemi P, Foulon DM, Farrell DH, Walton PD, Weitz JI, and Peterson CB**. Incorporation of vitronectin into fibrin clots: Evidence for a binding interaction between vitronectin and γA/γ′ fibrinogen. *Journal of Biological Chemistry* 277: 7520-7528, 2002.

21. **Konstantinides S, Schäfer K, Thinnes T, and Loskutoff DJ**. Plasminogen activator inhibitor-1 and its cofactor vitronectin stabilize arterial thrombi after vascular injury in mice. *Circulation* 103: 576-583, 2001.

22. **Kyriakides TR, Rojnuckarin P, Reidy MA, Hankenson KD, Papayannopoulou T, Kaushansky K, and Bornstein P**. Megakaryocytes require thrombospondin-2 for normal platelet formation and function. *Blood, The Journal of the American Society of Hematology* 101: 3915-3923, 2003.

23. **Jung SM, and Moroi M**. Platelet glycoprotein VI. *Multichain immune recognition receptor signaling* 53-63, 2008.

24. **Moroi M, and Jung SM**. Platelet glycoprotein VI: its structure and function. *Thrombosis research* 114: 221-233, 2004.

25. **Clemetson KJ, McGregor JL, James E, Dechavanne M, and Lüscher E**. Characterization of the platelet membrane glycoprotein abnormalities in Bernard-Soulier syndrome and comparison with normal by surface-labeling techniques and high-resolution two-dimensional gel electrophoresis. *The Journal of clinical investigation* 70: 304-311, 1982.

26. **Clemetson JM, Polgar J, Magnenat E, Wells TN, and Clemetson KJ**. The platelet collagen receptor glycoprotein VI is a member of the immunoglobulin superfamily closely related to FcαR and the natural killer receptors. *Journal of Biological Chemistry* 274: 29019-29024, 1999.

27. **Nieswandt B, and Watson SP**. Platelet-collagen interaction: is GPVI the central receptor? *Blood* 102: 449-461, 2003.

28. **Inoue O, Suzuki-Inoue K, McCarty OJ, Moroi M, Ruggeri ZM, Kunicki TJ, Ozaki Y, and Watson SP**. Laminin stimulates spreading of platelets through integrin α6β1–dependent activation of GPVI. *Blood* 107: 1405-1412, 2006.

29. **Watson S, Auger J, McCarty O, and Pearce A**. GPVI and integrin αIIbβ3 signaling in platelets. *Journal of Thrombosis and Haemostasis* 3: 1752-1762, 2005.

30. **Xu R-G, Gauer JS, Baker SR, Slater A, Martin EM, McPherson HR, Duval C, Manfield IW, Bonna AM, and Watson SP**. GPVI (Glycoprotein VI) Interaction With Fibrinogen Is Mediated by Avidity and the Fibrinogen αC-Region. *Arteriosclerosis, thrombosis, and vascular biology* 41: 1092-1104, 2021.

31. **Onselaer M-B, Hardy AT, Wilson C, Sanchez X, Babar AK, Miller JL, Watson CN, Watson SK, Bonna A, and Philippou H**. Fibrin and D-dimer bind to monomeric GPVI. *Blood advances* 1: 1495-1504, 2017.

32. **Moroi M, Induruwa I, Farndale RW, and Jung SM**. Dimers of the platelet collagen receptor Glycoprotein VI bind specifically to fibrin fibers during clot formation, but not to intact fibrinogen. *Journal of Thrombosis and Haemostasis* 2021.

33. **Ahmed MU, Kaneva V, Loyau S, Nechipurenko D, Receveur N, Le Bris M, Janus-Bell E, Didelot M, Rauch A, and Susen S**. Pharmacological blockade of glycoprotein VI promotes thrombus disaggregation in the absence of thrombin. *Arteriosclerosis, Thrombosis, and Vascular Biology* 40: 2127-2142, 2020.

34. **Courtney AH, Lo W-L, and Weiss A**. TCR signaling: mechanisms of initiation and propagation. *Trends in biochemical sciences* 43: 108-123, 2018.

35. **Ezumi Y, Shindoh K, Tsuji M, and Takayama H**. Physical and functional association of the Src family kinases Fyn and Lyn with the collagen receptor glycoprotein VI-Fc receptor γ chain complex on human platelets. *The Journal of experimental medicine* 188: 267-276, 1998.

36. **Quek L, Bolen J, and Watson S**. A role for Bruton's tyrosine kinase (Btk) in platelet activation by collagen. *Current biology* 8: 1137-S1131, 1998.

37. **Manne BK, Badolia R, Dangelmaier C, Eble JA, Ellmeier W, Kahn M, and Kunapuli SP**. Distinct pathways regulate Syk protein activation downstream of immune tyrosine activation motif (ITAM) and hemITAM receptors in platelets. *Journal of Biological Chemistry* 290: 11557-11568, 2015.

38. **Rayes J, Watson SP, and Nieswandt B**. Functional significance of the platelet immune receptors GPVI and CLEC-2. *The Journal of clinical investigation* 129: 12-23, 2019.

39. **Babur Ö, Melrose AR, Cunliffe JM, Klimek J, Pang J, Sepp A-LI, Zilberman-Rudenko J, Tassi Yunga S, Zheng T, and Parra-Izquierdo I**. Phosphoproteomic quantitation and causal analysis reveal pathways in GPVI/ITAM-mediated platelet activation programs. *Blood* 136: 2346-2358, 2020.

40. **Aslan JE**. Platelet proteomes, pathways, and phenotypes as informants of vascular wellness and disease. *Arteriosclerosis, thrombosis, and vascular biology* 41: 999-1011, 2021.

41. **Kato K, Kanaji T, Russell S, Kunicki TJ, Furihata K, Kanaji S, Marchese P, Reininger A, Ruggeri ZM, and Ware J**. The contribution of glycoprotein VI to stable platelet adhesion and thrombus formation illustrated by targeted gene deletion. *Blood* 102: 1701-1707, 2003.

42. **Arthur JF, Dunkley S, and Andrews RK**. Platelet glycoprotein VI-related clinical defects. *British journal of haematology* 139: 363-372, 2007.

43. **Inoue O, Suzuki-Inoue K, Dean WL, Frampton J, and Watson SP**. Integrin α2β1 mediates outside-in regulation of platelet spreading on collagen through activation of Src kinases and PLCγ2. *The Journal of cell biology* 160: 769-780, 2003.

44. **Bennett JS**. Structure and function of the platelet integrin α IIb β 3. *The Journal of clinical investigation* 115: 3363-3369, 2005.

45. **Ma YQ, Qin J, and Plow E**. Platelet integrin αIIbβ3: activation mechanisms. *Journal of Thrombosis and Haemostasis* 5: 1345-1352, 2007.

46. **Shattil SJ**. Signaling through platelet integrin αIIbβ3: inside-out, outside-in, and sideways. *Thrombosis and haemostasis* 82: 318-325, 1999.

47. **Huang J, Li X, Shi X, Zhu M, Wang J, Huang S, Huang X, Wang H, Li L, and Deng H**. Platelet integrin αIIbβ3: signal transduction, regulation, and its therapeutic targeting. *Journal of hematology & oncology* 12: 1-22, 2019.

48. **Mccarty OJ, Calaminus S, Berndt MC, Machesky L, and Watson SP**. von Willebrand factor mediates platelet spreading through glycoprotein Ib and αIIbβ3 in the presence of botrocetin and ristocetin, respectively. *Journal of thrombosis and haemostasis* 4: 1367-1378, 2006.

49. **Thornber K, McCarty OJ, Watson SP, and Pears CJ**. Distinct but critical roles for integrin αIIbβ3 in platelet lamellipodia formation on fibrinogen, collagen-related peptide and thrombin. *The FEBS journal* 273: 5032-5043, 2006.

50. **Woodside DG, Obergfell A, Leng L, Wilsbacher JL, Miranti CK, Brugge JS, Shattil SJ, and Ginsberg MH**. Activation of Syk protein tyrosine kinase through interaction with integrin β cytoplasmic domains. *Current Biology* 11: 1799-1804, 2001.

51. **Woodside DG, Obergfell A, Talapatra A, Calderwood DA, Shattil SJ, and Ginsberg MH**. The N-terminal SH2 domains of Syk and ZAP-70 mediate phosphotyrosine-independent binding to integrin β cytoplasmic domains. *Journal of Biological Chemistry* 277: 39401-39408, 2002.

52. **Boylan B, Gao C, Rathore V, Gill JC, Newman DK, and Newman PJ**. Identification of FcγRIIa as the ITAM-bearing receptor mediating αIIbβ3 outside-in integrin signaling in human platelets. *Blood, The Journal of the American Society of Hematology* 112: 2780-2786, 2008.

53. **Zhi H, Rauova L, Hayes V, Gao C, Boylan B, Newman DK, McKenzie SE, Cooley BC, Poncz M, and Newman PJ**. Cooperative integrin/ITAM signaling in platelets enhances thrombus formation in vitro and in vivo. *Blood, The Journal of the American Society of Hematology* 121: 1858-1867, 2013.

54. **Stalker TJ, Newman DK, Ma P, Wannemacher KM, and Brass LF**. Platelet Signaling. In: *Antiplatelet Agents*, edited by Gresele P, Born GVR, Patrono C, and Page CP. Berlin, Heidelberg: Springer Berlin Heidelberg, 2012, p. 59-85.

55. **Offermanns S**. Activation of Platelet Function Through G Protein–Coupled Receptors. *Circulation Research* 99: 1293-1304, 2006.

56. **Larsen JB, and Hvas AM**. Thrombin: A Pivotal Player in Hemostasis and Beyond. *Semin Thromb Hemost* 47: 759-774, 2021.

57. **Mattheij NJ, Swieringa F, Mastenbroek TG, Berny-Lang MA, May F, Baaten CC, van der Meijden PE, Henskens YM, Beckers EA, and Suylen DP**. Coated platelets function in platelet-dependent fibrin formation via integrin αIIbβ3 and transglutaminase factor XIII. *Haematologica* 101: 427, 2016.

58. **Rigg RA, Healy LD, Chu TT, Ngo AT, Mitrugno A, Zilberman-Rudenko J, Aslan JE, Hinds MT, Vecchiarelli LD, and Morgan TK**. Protease-activated receptor 4 activity promotes platelet granule release and platelet-leukocyte interactions. *Platelets* 30: 126-135, 2019.

59. **Mitrugno A, Rigg RA, Laschober NB, Ngo AT, Pang J, Williams CD, Aslan JE, and McCarty OJ**. Potentiation of TRAP-6-induced platelet dense granule release by blockade of P2Y12 signaling with MRS2395. *Platelets* 29: 383-394, 2018.

60. **Heuberger DM, and Schuepbach RA**. Protease-activated receptors (PARs): mechanisms of action and potential therapeutic modulators in PAR-driven inflammatory diseases. *Thrombosis Journal* 17: 4, 2019.

61. **Han X, Nieman MT, and Kerlin BA**. Protease-activated receptors: An illustrated review. *Research and Practice in Thrombosis and Haemostasis* 5: 17-26, 2021.

62. **Nieman MT, and Schmaier AH**. Interaction of thrombin with PAR1 and PAR4 at the thrombin cleavage site. *Biochemistry* 46: 8603-8610, 2007.

63. **Ngo AT, Parra-Izquierdo I, Aslan JE, and McCarty OJ**. Rho GTPase regulation of reactive oxygen species generation and signalling in platelet function and disease. *Small GTPases* 1-18, 2021.

64. **Stegner D, and Nieswandt B**. Platelet receptor signaling in thrombus formation. *Journal of Molecular Medicine* 89: 109-121, 2011.

65. **Murugappan S, Shankar H, Bhamidipati S, Dorsam RT, Jin J, and Kunapuli SP**. Molecular mechanism and functional implications of thrombin-mediated tyrosine phosphorylation of PKCdelta in platelets. *Blood* 106: 550-557, 2005.

66. **Senis YA, Craig AW, and Greer PA**. Fps/Fes and Fer protein-tyrosinekinases play redundant roles in regulating hematopoiesis. *Exp Hematol* 31: 673-681, 2003.

67. **Lipsky AH, Farooqui MZ, Tian X, Martyr S, Cullinane AM, Nghiem K, Sun C, Valdez J, Niemann CU, and Herman SE**. Incidence and risk factors of bleeding-related adverse events in patients with chronic lymphocytic leukemia treated with ibrutinib. *Haematologica* 100: 1571, 2015.

68. **Byrd JC, Furman RR, Coutre SE, Flinn IW, Burger JA, Blum KA, Grant B, Sharman JP, Coleman M, and Wierda WG**. Targeting BTK with ibrutinib in relapsed chronic lymphocytic leukemia. *New England Journal of Medicine* 369: 32-42, 2013.

69. **Byrd JC, Brown JR, O'Brien S, Barrientos JC, Kay NE, Reddy NM, Coutre S, Tam CS, Mulligan SP, and Jaeger U**. Ibrutinib versus ofatumumab in previously treated chronic lymphoid leukemia. *New England Journal of Medicine* 371: 213-223, 2014.

70. **Akinleye A, Chen Y, Mukhi N, Song Y, and Liu D**. Ibrutinib and novel BTK inhibitors in clinical development. *Journal of hematology & oncology* 6: 1-9, 2013.

71. **Burger JA, Tedeschi A, Barr PM, Robak T, Owen C, Ghia P, Bairey O, Hillmen P, Bartlett NL, and Li J**. Ibrutinib as initial therapy for patients with chronic lymphocytic leukemia. *New England Journal of Medicine* 373: 2425-2437, 2015.

72. **Treon SP, Tripsas CK, Meid K, Warren D, Varma G, Green R, Argyropoulos KV, Yang G, Cao Y, and Xu L**. Ibrutinib in previously treated Waldenström's macroglobulinemia. *New England Journal of Medicine* 372: 1430-1440, 2015.

73. **Shatzel JJ, Olson SR, Tao DL, McCarty OJ, Danilov AV, and DeLoughery TG**. Ibrutinib-associated bleeding: pathogenesis, management and risk reduction strategies. *Journal of thrombosis and haemostasis* 15: 835-847, 2017.

74. **Stephens DM, and Byrd JC**. How I manage ibrutinib intolerance and complications in patients with chronic lymphocytic leukemia. *Blood, The Journal of the American Society of Hematology* 133: 1298-1307, 2019.

75. **Brown JR, Moslehi J, O'Brien S, Ghia P, Hillmen P, Cymbalista F, Shanafelt TD, Fraser G, Rule S, and Kipps TJ**. Characterization of atrial fibrillation adverse events reported in ibrutinib randomized controlled registration trials. *Haematologica* 102: 1796, 2017.

76. **Mócsai A, Ruland J, and Tybulewicz VL**. The SYK tyrosine kinase: a crucial player in diverse biological functions. *Nature Reviews Immunology* 10: 387-402, 2010.

77. **Riccaboni M, Bianchi I, and Petrillo P**. Spleen tyrosine kinases: biology, therapeutic targets and drugs. *Drug discovery today* 15: 517-530, 2010.

78. **Pearce AC, Mccarty OJ, Calaminus SD, Vigorito E, Turner M, and Watson SP**. Vav family proteins are required for optimal regulation of PLCγ2 by integrin αIIbβ3. *Biochemical Journal* 401: 753-761, 2007.

79. **Hoellenriegel J, Coffey GP, Sinha U, Pandey A, Sivina M, Ferrajoli A, Ravandi F, Wierda WG, O'Brien S, and Keating MJ**. Selective, novel spleen tyrosine kinase (Syk) inhibitors suppress chronic lymphocytic leukemia B-cell activation and migration. *Leukemia* 26: 1576-1583, 2012.

80. **Weinblatt ME, Kavanaugh A, Genovese MC, Musser TK, Grossbard EB, and Magilavy DB**. An oral spleen tyrosine kinase (Syk) inhibitor for rheumatoid arthritis. *New England Journal of Medicine* 363: 1303-1312, 2010.

81. **Buchner M, Fuchs S, Prinz G, Pfeifer D, Bartholomé K, Burger M, Chevalier N, Vallat L, Timmer J, and Gribben JG**. Spleen tyrosine kinase is overexpressed and represents a potential therapeutic target in chronic lymphocytic leukemia. *Cancer research* 69: 5424-5432, 2009.

82. **Tullemans B, Heemskerk J, and Kuijpers M**. Acquired platelet antagonism: off-target antiplatelet effects of malignancy treatment with tyrosine kinase inhibitors. *Journal of thrombosis and haemostasis* 16: 1686-1699, 2018.

83. **Zheng TJ, Lofurno ER, Melrose AR, Lakshmanan HHS, Pang J, Phillips KG, Fallon ME, Kohs TC, Ngo AT, and Shatzel JJ**. Assessment of the effects of Syk and BTK inhibitors on GPVI-mediated platelet signaling and function. *American Journal of Physiology-Cell Physiology* 320: C902-C915, 2021.

84. **Spalton JC, Mori J, Pollitt AY, Hughes CE, Eble JA, and Watson SP**. The novel Syk inhibitor R406 reveals mechanistic differences in the initiation of GPVI and CLEC-2 signaling in platelets. *Journal of Thrombosis and Haemostasis* 7: 1192-1199, 2009.

85. **Andre P, Morooka T, Sim D, Abe K, Lowell C, Nanda N, Delaney S, Siu G, Yan Y, and Hollenbach S**. Critical role for Syk in responses to vascular injury. *Blood, The Journal of the American Society of Hematology* 118: 5000-5010, 2011.

86. **Friedberg JW, Sharman J, Sweetenham J, Johnston PB, Vose JM, LaCasce A, Schaefer-Cutillo J, De Vos S, Sinha R, and Leonard JP**. Inhibition of Syk with fostamatinib disodium has significant clinical activity in non-Hodgkin lymphoma and chronic lymphocytic leukemia. *Blood, The Journal of the American Society of Hematology* 115: 2578-2585, 2010.

87. **Bussel J, Arnold DM, Grossbard E, Mayer J, Treliński J, Homenda W, Hellmann A, Windyga J, Sivcheva L, and Khalafallah AA**. Fostamatinib for the treatment of adult persistent and chronic immune thrombocytopenia: results of two phase 3, randomized, placebo-controlled trials. *American journal of hematology* 93: 921-930, 2018.

88. **Bajpai M**. Fostamatinib, a Syk inhibitor prodrug for the treatment of inflammatory diseases. *IDrugs: the investigational drugs journal* 12: 174-185, 2009.

89. **Sharman J, Hawkins M, Kolibaba K, Boxer M, Klein L, Wu M, Hu J, Abella S, and Yasenchak C**. An open-label phase 2 trial of entospletinib (GS-9973), a selective spleen tyrosine kinase inhibitor, in chronic lymphocytic leukemia. *Blood, The Journal of the American Society of Hematology* 125: 2336-2343, 2015.

90. **Barr PM, Saylors GB, Spurgeon SE, Cheson BD, Greenwald DR, O'Brien SM, Liem AK, Mclntyre RE, Joshi A, and Abella-Dominicis E**. Phase 2 study of idelalisib and entospletinib: pneumonitis limits combination therapy in relapsed refractory CLL and NHL. *Blood, The Journal of the American Society of Hematology* 127: 2411-2415, 2016.

91. **Sharman J, and Di Paolo J**. Targeting B-cell receptor signaling kinases in chronic lymphocytic leukemia: the promise of entospletinib. *Therapeutic advances in hematology* 7: 157-170, 2016.

92. **Currie KS, Kropf JE, Lee T, Blomgren P, Xu J, Zhao Z, Gallion S, Whitney JA, Maclin D, and Lansdon EB**. Discovery of GS-9973, a selective and orally efficacious inhibitor of spleen tyrosine kinase. *Journal of medicinal chemistry* 57: 3856-3873, 2014.

93. **Burke RT, Meadows S, Loriaux MM, Currie KS, Mitchell SA, Maciejewski P, Clarke AS, Dipaolo JA, Druker BJ, and Lannutti BJ**. A potential therapeutic strategy for chronic lymphocytic leukemia by combining Idelalisib and GS-9973, a novel spleen tyrosine kinase (Syk) inhibitor. *Oncotarget* 5: 908, 2014.

94. **Series J, Ribes A, Garcia C, Souleyreau P, Bauters A, Morschhauser F, Jürgensmeier JM, Sié P, Ysebaert L, and Payrastre B**. Effects of novel Btk and Syk inhibitors on platelet functions alone and in combination in vitro and in vivo. *Journal of Thrombosis and Haemostasis* 18: 3336-3351, 2020.

95. **Zhang Y, and Diamond SL**. Src family kinases inhibition by dasatinib blocks initial and subsequent platelet deposition on collagen under flow, but lacks efficacy with thrombin generation. *Thrombosis Research* 192: 141-151, 2020.

96. **Perrella G, Montague SJ, Brown HC, Garcia Quintanilla L, Slater A, Stegner D, Thomas M, Heemskerk JW, and Watson SP**. Role of Tyrosine Kinase Syk in Thrombus Stabilisation at High Shear. *International Journal of Molecular Sciences* 23: 493, 2022.

97. **Harbi MH, Smith CW, Nicolson PL, Watson SP, and Thomas MR**. Novel antiplatelet strategies targeting GPVI, CLEC-2 and tyrosine kinases. *Platelets* 32: 29-41, 2021.

98. **Clarke AS, Rousseau E, Wang K, Kim J-Y, Murray BP, Bannister R, Matzkies F, Currie KS, and Di Paolo JA**. Effects of GS-9876, a novel spleen tyrosine kinase inhibitor, on platelet function and systemic hemostasis. *Thrombosis research* 170: 109-118, 2018.

99. **Bye AP, Hoepel W, Mitchell JL, Jégouic S, Loureiro S, Sage T, Vidarsson G, Nouta J, Wuhrer M, and de Taeye S**. Aberrant glycosylation of anti-SARS-CoV-2 spike IgG is a prothrombotic stimulus for platelets. *Blood, The Journal of the American Society of Hematology* 138: 1481-1489, 2021.

100. **Nicolson PL, Welsh JD, Chauhan A, Thomas MR, Kahn ML, and Watson SP**. A rationale for blocking thromboinflammation in COVID-19 with Btk inhibitors. *Platelets* 31: 685-690, 2020.

101. **Boggon TJ, and Eck MJ**. Structure and regulation of Src family kinases. *Oncogene* 23: 7918-7927, 2004.

102. **Parsons SJ, and Parsons JT**. Src family kinases, key regulators of signal transduction. *Oncogene* 23: 7906-7909, 2004.

103. **Senis YA, Mazharian A, and Mori J**. Src family kinases: at the forefront of platelet activation. *Blood, The Journal of the American Society of Hematology* 124: 2013-2024, 2014.

104. **Getz TM, Mayanglambam A, Daniel JL, and Kunapuli SP**. Go6976 abrogates GPVI-mediated platelet functional responses in human platelets through inhibition of Syk. *Journal of thrombosis and haemostasis: JTH* 9: 608, 2011.

105. **Li Z, Zhang G, Liu J, Stojanovic A, Ruan C, Lowell CA, and Du X**. An important role of the SRC family kinase Lyn in stimulating platelet granule secretion. *Journal of Biological Chemistry* 285: 12559-12570, 2010.

106. **Polanowska-Grabowska R, Gibbins JM, and Gear AR**. Platelet adhesion to collagen and collagen-related peptide under flow: roles of the α2β1 integrin, GPVI, and Src tyrosine kinases. *Arteriosclerosis, thrombosis, and vascular biology* 23: 1934-1940, 2003.

107. **Xiang B, Zhang G, Stefanini L, Bergmeier W, Gartner TK, Whiteheart SW, and Li Z**. The Src family kinases and protein kinase C synergize to mediate Gq-dependent platelet activation. *Journal of Biological Chemistry* 287: 41277-41287, 2012.

108. **Talpaz M, Shah NP, Kantarjian H, Donato N, Nicoll J, Paquette R, Cortes J, O'Brien S, Nicaise C, and Bleickardt E**. Dasatinib in imatinib-resistant Philadelphia chromosome–positive leukemias. *New England Journal of Medicine* 354: 2531-2541, 2006.

109. **Schittenhelm MM, Shiraga S, Schroeder A, Corbin AS, Griffith D, Lee FY, Bokemeyer C, Deininger MW, Druker BJ, and Heinrich MC**. Dasatinib (BMS-354825), a dual SRC/ABL kinase inhibitor, inhibits the kinase activity of wild-type, juxtamembrane, and activation loop mutant KIT isoforms associated with human malignancies. *Cancer research* 66: 473-481, 2006.

110. **Gratacap M-P, Martin V, Valéra M-C, Allart S, Garcia C, Sié P, Recher C, and Payrastre B**. The new tyrosine-kinase inhibitor and anticancer drug dasatinib reversibly affects platelet activation in vitro and in vivo. *Blood, The Journal of the American Society of Hematology* 114: 1884-1892, 2009.

111. **Quintás-Cardama A, Han X, Kantarjian H, and Cortes J**. Tyrosine kinase inhibitor–induced platelet dysfunction in patients with chronic myeloid leukemia. *Blood, The Journal of the American Society of Hematology* 114: 261-263, 2009.

112. **Beke Debreceni I, Mezei G, Batár P, Illés Á, and Kappelmayer J**. Dasatinib inhibits procoagulant and clot retracting activities of human platelets. *International journal of molecular sciences* 20: 5430, 2019.

113. **Aaronson DS, and Horvath CM**. A road map for those who don't know JAK-STAT. *Science* 296: 1653-1655, 2002.

114. **Subramaniam PS, Torres BA, and Johnson HM**. So many ligands, so few transcription factors: a new paradigm for signaling through the STAT transcription factors. *Cytokine* 15: 175-187, 2001.

115. **Yamaoka K, Saharinen P, Pesu M, Holt VE, 3rd, Silvennoinen O, and O'Shea JJ**. The Janus kinases (Jaks). *Genome Biol* 5: 253, 2004.

116. **Bousoik E, and Montazeri Aliabadi H**. "Do We Know Jack" About JAK? A Closer Look at JAK/STAT Signaling Pathway. *Front Oncol* 8: 287, 2018.

117. **Kontzias A, Kotlyar A, Laurence A, Changelian P, and O'Shea JJ**. Jakinibs: a new class of kinase inhibitors in cancer and autoimmune disease. *Curr Opin Pharmacol* 12: 464-470, 2012.

118. **McKeage K**. Ruxolitinib: A Review in Polycythaemia Vera. *Drugs* 75: 1773-1781, 2015.

119. **Plosker GL**. Ruxolitinib: a review of its use in patients with myelofibrosis. *Drugs* 75: 297-308, 2015.

120. **Tanaka Y**. Recent progress and perspective in JAK inhibitors for rheumatoid arthritis: from bench to bedside. *J Biochem* 158: 173-179, 2015.

121. **Genovese MC, Fleischmann R, Combe B, Hall S, Rubbert-Roth A, Zhang Y, Zhou Y, Mohamed MF, Meerwein S, and Pangan AL**. Safety and efficacy of upadacitinib in patients with active rheumatoid arthritis refractory to biologic disease-modifying anti-rheumatic drugs (SELECT-BEYOND): a double-blind, randomised controlled phase 3 trial. *Lancet* 391: 2513-2524, 2018.

122. **Markham A**. Baricitinib: First Global Approval. *Drugs* 77: 697-704, 2017.

123. **Rajasimhan S, Pamuk O, and Katz JD**. Safety of Janus Kinase Inhibitors in Older Patients: A Focus on the Thromboembolic Risk. *Drugs Aging* 37: 551-558, 2020.

124. **Verden A, Dimbil M, Kyle R, Overstreet B, and Hoffman KB**. Analysis of Spontaneous Postmarket Case Reports Submitted to the FDA Regarding Thromboembolic Adverse Events and JAK Inhibitors. *Drug Saf* 41: 357-361, 2018.

125. **Mehta P, Ciurtin C, Scully M, Levi M, and Chambers RC**. JAK inhibitors in COVID-19: the need for vigilance regarding increased inherent thrombotic risk. *Eur Respir J* 56: 2020.

126. **Barraco F, Greil R, Herbrecht R, Schmidt B, Reiter A, Willenbacher W, Raymakers R, Liersch R, Wroclawska M, Pack R, Burock K, Karumanchi D, and Gisslinger H**. Real-world non-interventional long-term post-authorisation safety study of ruxolitinib in myelofibrosis. *Br J Haematol* 191: 764-774, 2020.

127. **Woods B, Chen W, Chiu S, Marinaccio C, Fu C, Gu L, Bulic M, Yang Q, Zouak A, and Jia S**. Activation of JAK/STAT signaling in megakaryocytes sustains myeloproliferation in vivo. *Clinical Cancer Research* 25: 5901-5912, 2019.

128. **Levade M, David E, Garcia C, Laurent P-A, Cadot S, Michallet A-S, Bordet J-C, Tam C, Sié P, and Ysebaert L**. Ibrutinib treatment affects collagen and von Willebrand factor-dependent platelet functions. *Blood, The Journal of the American Society of Hematology* 124: 3991-3995, 2014.

129. Initial safety trial results find increased risk of serious heart-related problems and cancer with arthritis and ulcerative colitis medicine Xeljanz, Xeljanz XR (tofacitinib). 2021.

130. **Mezei G, Debreceni IB, Kerenyi A, Remenyi G, Szasz R, Illes A, Kappelmayer J, and Batar P**. Dasatinib inhibits coated-platelet generation in patients with chronic myeloid leukemia. *Platelets* 30: 836-843, 2019.

131. **Hobbs CM, Manning H, Bennett C, Vasquez L, Severin S, Brain L, Mazharian A, Guerrero JA, Li J, Soranzo N, Green AR, Watson SP, and Ghevaert C**. JAK2V617F leads to intrinsic changes in platelet formation and reactivity in a knock-in mouse model of essential thrombocythemia. *Blood* 122: 3787-3797, 2013.

132. **Houck KL, Yuan H, Tian Y, Solomon M, Cramer D, Liu K, Zhou Z, Wu X, Zhang J, Oehler V, and Dong JF**. Physical proximity and functional cooperation of glycoprotein 130 and glycoprotein VI in platelet membrane lipid rafts. *J Thromb Haemost* 17: 1500-1510, 2019.

133. **Eaton N, Subramaniam S, Schulte ML, Drew C, Jakab D, Haberichter SL, Weiler H, and Falet H**. Bleeding diathesis in mice lacking JAK2 in platelets. *Blood Adv* 5: 2969-2981, 2021.

134. **Olson SR, Koprowski S, Hum J, McCarty OJ, DeLoughery TG, and Shatzel JJ**. Chronic liver disease, thrombocytopenia and procedural bleeding risk; are novel thrombopoietin mimetics the solution? *Platelets* 30: 796-798, 2019.

135. **Lindquist I, Olson SR, Li A, Al-Samkari H, Jou JH, McCarty OJ, and Shatzel JJ**. The efficacy and safety of thrombopoietin receptor agonists in patients with chronic liver disease undergoing elective procedures: a systematic review and meta-analysis. *Platelets* 1-7, 2021.

136. **Miyakawa Y, Oda A, Druker BJ, Kato T, Miyazaki H, Handa M, and Ikeda Y**. Recombinant thrombopoietin induces rapid protein tyrosine phosphorylation of Janus kinase 2 and Shc in human blood platelets. *Blood* 86: 23-27, 1995.

137. **Chen J, Herceg-Harjacek L, Groopman JE, and Grabarek J**. Regulation of platelet activation in vitro by the c-Mpl ligand, thrombopoietin. *Blood* 86: 4054-4062, 1995.

138. **Akinleye A, Furqan M, and Adekunle O**. Ibrutinib and indolent B-cell lymphomas. *Clin Lymphoma Myeloma Leuk* 14: 253-260, 2014.

139. **Yuan H, Houck KL, Tian Y, Bharadwaj U, Hull K, Zhou Z, Zhu M, Wu X, Tweardy DJ, Romo D, Fu X, Zhang Y, Zhang J, and Dong JF**. Piperlongumine Blocks JAK2-STAT3 to Inhibit Collagen-Induced Platelet Reactivity Independent of Reactive Oxygen Species. *PLoS One* 10: e0143964, 2015.

140. **Parra-Izquierdo I, Melrose AR, Pang J, Lakshmanan HHS, Reitsma SE, Vavilapalli SH, Larson MK, Shatzel JJ, McCarty OJT, and Aslan JE**. Janus kinase inhibitors ruxolitinib and baricitinib impair glycoprotein-VI mediated platelet function. *Platelets* 1-12, 2021.

141. **Parra-Izquierdo I, Lakshmanan HHS, Melrose AR, Pang J, Zheng TJ, Jordan KR, Reitsma SE, McCarty OJ, and Aslan JE**. The Toll-Like Receptor 2 Ligand Pam2CSK4 Activates Platelet Nuclear Factor-κB and Bruton's Tyrosine Kinase Signaling to Promote Platelet-Endothelial Cell Interactions. *Frontiers in immunology* 3492, 2021.

142. **A TV, Haikarainen T, Raivola J, and Silvennoinen O**. Selective JAKinibs: Prospects in Inflammatory and Autoimmune Diseases. *BioDrugs* 33: 15-32, 2019.

143. **Colicelli J**. ABL tyrosine kinases: evolution of function, regulation, and specificity. *Sci Signal* 3: re6, 2010.

144. **Cohen MH, Williams G, Johnson JR, Duan J, Gobburu J, Rahman A, Benson K, Leighton J, Kim SK, Wood R, Rothmann M, Chen G, U KM, Staten AM, and Pazdur R**. Approval summary for imatinib mesylate capsules in the treatment of chronic myelogenous leukemia. *Clin Cancer Res* 8: 935-942, 2002.

145. **Malik S, Hassan S, and Eşkazan AE**. Novel BCR-ABL1 tyrosine kinase inhibitors in the treatment of chronic myeloid leukemia. *Expert Rev Hematol* 14: 975-978, 2021.

146. **Nair RR, Chauhan R, Harankhedkar S, Mahapatra M, and Saxena R**. Imatinib-induced platelet dysfunction and hypofibrinogenemia in chronic myeloid leukemia. *Blood Coagul Fibrinolysis* 30: 246-248, 2019.

147. **Loren CP, Aslan JE, Rigg RA, Nowak MS, Healy LD, Gruber A, Druker BJ, and McCarty OJ**. The BCR-ABL inhibitor ponatinib inhibits platelet immunoreceptor tyrosine-based activation motif (ITAM) signaling, platelet activation and aggregate formation under shear. *Thromb Res* 135: 155-160, 2015.

148. **Neelakantan P, Marin D, Laffan M, Goldman J, Apperley J, and Milojkovic D**. Platelet dysfunction associated with ponatinib, a new pan BCR-ABL inhibitor with efficacy for chronic myeloid leukemia resistant to multiple tyrosine kinase inhibitor therapy. *Haematologica* 97: 1444, 2012.

149. **Mezei G, Batár P, Kozma L, Illes A, Kappelmayer J, and Debreceni IB**. Ponatinib Exerts an Inhibitory Effect on Collagen-induced Platelet Aggregation and Generation of Coated-Platelets. *Anticancer Research* 41: 4867-4874, 2021.

150. **Deb S, Boknas N, Sjostrom C, Tharmakulanathan A, Lotfi K, and Ramstrom S**. Varying effects of tyrosine kinase inhibitors on platelet function-A need for individualized CML treatment to minimize the risk for hemostatic and thrombotic complications? *Cancer Med* 9: 313-323, 2020.

151. **Latifi Y, Moccetti F, Wu M, Xie A, Packwood W, Qi Y, Ozawa K, Shentu W, Brown E, and Shirai T**. Thrombotic microangiopathy as a cause of cardiovascular toxicity from the BCR-ABL1 tyrosine kinase inhibitor ponatinib. *Blood, The Journal of the American Society of Hematology* 133: 1597-1606, 2019.

152. **Moslehi JJ, and Deininger M**. Tyrosine kinase inhibitor–associated cardiovascular toxicity in chronic myeloid leukemia. *Journal of clinical oncology* 33: 4210, 2015.

153. **Cortes JE, Kim D-W, Pinilla-Ibarz J, le Coutre PD, Paquette R, Chuah C, Nicolini FE, Apperley JF, Khoury HJ, and Talpaz M**. Ponatinib efficacy and safety in Philadelphia chromosome–positive leukemia: final 5-year results of the phase 2 PACE trial. *Blood, The Journal of the American Society of Hematology* 132: 393-404, 2018.

154. **Murphy JM, Rodriguez YAR, Jeong K, Ahn EE, and Lim SS**. Targeting focal adhesion kinase in cancer cells and the tumor microenvironment. *Exp Mol Med* 52: 877-886, 2020.

155. **Hitchcock IS, Fox NE, Prévost N, Sear K, Shattil SJ, and Kaushansky K**. Roles of focal adhesion kinase (FAK) in megakaryopoiesis and platelet function: studies using a megakaryocyte lineage specific FAK knockout. *Blood* 111: 596-604, 2008.

156. **Guidetti GF, Torti M, and Canobbio I**. Focal Adhesion Kinases in Platelet Function and Thrombosis. *Arterioscler Thromb Vasc Biol* 39: 857-868, 2019.

157. **Relou IA, Bax LA, van Rijn HJ, and Akkerman JW**. Site-specific phosphorylation of platelet focal adhesion kinase by low-density lipoprotein. *Biochem J* 369: 407-416, 2003.

158. **Jones ML, Shawe-Taylor AJ, Williams CM, and Poole AW**. Characterization of a novel focal adhesion kinase inhibitor in human platelets. *Biochem Biophys Res Commun* 389: 198-203, 2009.

159. **Carrim N, Walsh TG, Consonni A, Torti M, Berndt MC, and Metharom P**. Role of focal adhesion tyrosine kinases in GPVI-dependent platelet activation and reactive oxygen species formation. *PLoS One* 9: e113679, 2014.

160. **Roh ME, Cosgrove M, Gorski K, and Hitchcock IS**. Off-targets effects underlie the inhibitory effect of FAK inhibitors on platelet activation: studies using Fak-deficient mice. *J Thromb Haemost* 11: 1776-1778, 2013.

161. **Homsi J, and Daud AI**. Spectrum of activity and mechanism of action of VEGF/PDGF inhibitors. *Cancer Control* 14: 285-294, 2007.

162. **Yang JG, Wang LL, and Ma DC**. Effects of vascular endothelial growth factors and their receptors on megakaryocytes and platelets and related diseases. *Br J Haematol* 180: 321-334, 2018.

163. **Vassbotn FS, Havnen OK, Heldin CH, and Holmsen H**. Negative feedback regulation of human platelets via autocrine activation of the platelet-derived growth factor alpha-receptor. *J Biol Chem* 269: 13874-13879, 1994.

164. **McCormack PL**. Pazopanib: a review of its use in the management of advanced renal cell carcinoma. *Drugs* 74: 1111-1125, 2014.

165. **Tullemans BM, Nagy M, Sabrkhany S, Griffioen AW, Aarts M, Heemskerk JW, and Kuijpers MJ**. Tyrosine kinase inhibitor pazopanib inhibits platelet procoagulant activity in renal cell carcinoma patients. *Frontiers in cardiovascular medicine* 5: 142, 2018.

166. **Mori J, Nagy Z, Di Nunzio G, Smith CW, Geer MJ, Al Ghaithi R, van Geffen JP, Heising S, Boothman L, Tullemans BME, Correia JN, Tee L, Kuijpers MJE, Harrison P, Heemskerk JWM, Jarvis GE, Tarakhovsky A, Weiss A, Mazharian A, and Senis YA**. Maintenance of murine platelet homeostasis by the kinase Csk and phosphatase CD148. *Blood* 131: 1122-1144, 2018.

167. **Tullemans BM, Veninga A, Fernandez DI, Aarts MJ, Eble JA, van der Meijden PE, Heemskerk JW, and Kuijpers MJ**. Multiparameter Evaluation of the Platelet-Inhibitory Effects of Tyrosine Kinase Inhibitors Used for Cancer Treatment. *International journal of molecular sciences* 22: 11199, 2021.

168. **Senis YA, Nagy Z, Mori J, Lane S, and Lane P**. Platelet Src family kinases: A tale of reversible phosphorylation. *Research and practice in thrombosis and haemostasis* 5: 376-389, 2021.

169. **Chong YP, Mulhern TD, and Cheng HC**. C-terminal Src kinase (CSK) and CSK-homologous kinase (CHK)--endogenous negative regulators of Src-family protein kinases. *Growth Factors* 23: 233-244, 2005.

170. **Nagy Z, Mori J, Ivanova VS, Mazharian A, and Senis YA**. Interplay between the tyrosine kinases Chk and Csk and phosphatase PTPRJ is critical for regulating platelets in mice. *Blood* 135: 1574-1587, 2020.

171. **Mendez JS, and Grommes C**. Treatment of Primary Central Nervous System Lymphoma: From Chemotherapy to Small Molecules. *Am Soc Clin Oncol Educ Book* 38: 604-615, 2018.

172. **O'Malley DP, Ahuja V, Fink B, Cao C, Wang C, Swanson J, Wee S, Gavai AV, Tokarski J, Critton D, Paiva AA, Johnson BM, Szapiel N, and Xie D**. Discovery of Pyridazinone and Pyrazolo[1,5-a]pyridine Inhibitors of C-Terminal Src Kinase. *ACS Med Chem Lett* 10: 1486-1491, 2019.

173. **Craig AW**. FES/FER kinase signaling in hematopoietic cells and leukemias. *Front Biosci (Landmark Ed)* 17: 861-875, 2012.

174. **Taniguchi T, Inagaki H, Baba D, Yasumatsu I, Toyota A, Kaneta Y, Kiga M, Iimura S, Odagiri T, Shibata Y, Ueda K, Seo M, Shimizu H, Imaoka T, and Nakayama K**. Discovery of Novel Pyrido-pyridazinone Derivatives as FER Tyrosine Kinase Inhibitors with Antitumor Activity. *ACS Med Chem Lett* 10: 737-742, 2019.

175. **Mohamed AJ, Yu L, Bäckesjö CM, Vargas L, Faryal R, Aints A, Christensson B, Berglöf A, Vihinen M, and Nore BF**. Bruton's tyrosine kinase (Btk): function, regulation, and transformation with special emphasis on the PH domain. *Immunological reviews* 228: 58-73, 2009.

176. **Packham MA**. Role of platelets in thrombosis and hemostasis. *Canadian journal of physiology and pharmacology* 72: 278-284, 1994.

177. **Rayes J, Watson SP, and Nieswandt B**. Functional significance of the platelet immune receptors GPVI and CLEC-2. *J Clin Invest* 129: 12-23, 2019.

178. **Manne BK, Badolia R, Dangelmaier C, Eble JA, Ellmeier W, Kahn M, and Kunapuli SP**. Distinct pathways regulate Syk protein activation downstream of immune tyrosine activation motif (ITAM) and hemITAM receptors in platelets. *J Biol Chem* 290: 11557-11568, 2015.

179. **Geahlen RL**. Getting Syk: spleen tyrosine kinase as a therapeutic target. *Trends in pharmacological sciences* 35: 414-422, 2014.

180. **Liang C, Tian D, Ren X, Ding S, Jia M, Xin M, and Thareja S**. The development of Bruton's tyrosine kinase (BTK) inhibitors from 2012 to 2017: a mini-review. *European journal of medicinal chemistry* 151: 315-326, 2018.

181. **Hendriks RW, Yuvaraj S, and Kil LP**. Targeting Bruton's tyrosine kinase in B cell malignancies. *Nature Reviews Cancer* 14: 219-232, 2014.

182. **Byrd JC, Furman RR, Coutre SE, Flinn IW, Burger JA, Blum KA, Grant B, Sharman JP, Coleman M, Wierda WG, Jones JA, Zhao W, Heerema NA, Johnson AJ, Sukbuntherng J, Chang BY, Clow F, Hedrick E, Buggy JJ, James DF, and O'Brien S**. Targeting BTK with ibrutinib in relapsed chronic lymphocytic leukemia. *N Engl J Med* 369: 32-42, 2013.

183. **Wang ML, Rule S, Martin P, Goy A, Auer R, Kahl BS, Jurczak W, Advani RH, Romaguera JE, Williams ME, Barrientos JC, Chmielowska E, Radford J, Stilgenbauer S, Dreyling M, Jedrzejczak WW, Johnson P, Spurgeon SE, Li L, Zhang L, Newberry K, Ou Z, Cheng N, Fang B, McGreivy J, Clow F, Buggy JJ, Chang BY, Beaupre DM, Kunkel LA, and Blum KA**. Targeting BTK with ibrutinib in relapsed or refractory mantle-cell lymphoma. *N Engl J Med* 369: 507-516, 2013.

184. **Krause DS, and Van Etten RA**. Tyrosine kinases as targets for cancer therapy. *N Engl J Med* 353: 172-187, 2005.

185. **McAdoo SP, and Tam FW**. Fostamatinib disodium. *Drugs of the future* 36: 273, 2011.

186. **Babur O, Melrose AR, Cunliffe JM, Klimek J, Pang J, Sepp AI, Zilberman-Rudenko J, Tassi Yunga S, Zheng T, Parra-Izquierdo I, Minnier J, McCarty OJT, Demir E, Reddy AP, Wilmarth PA, David LL, and Aslan JE**. Phosphoproteomic quantitation and causal analysis reveal pathways in GPVI/ITAM-mediated platelet activation programs. *Blood* 136: 2346-2358, 2020.

187. **Rigg RA, Aslan JE, Healy LD, Wallisch M, Thierheimer ML, Loren CP, Pang J, Hinds MT, Gruber A, and McCarty OJ**. Oral administration of Bruton's tyrosine kinase inhibitors impairs GPVI-mediated platelet function. *Am J Physiol Cell Physiol* 310: C373-380, 2016.

188. **Aslan JE**. Platelet Rho GTPase regulation in physiology and disease. *Platelets* 30: 17-22, 2019.

189. **Aslan JE, Itakura A, Gertz JM, and McCarty OJ**. Platelet shape change and spreading. *Methods Mol Biol* 788: 91-100, 2012.

190. **Ngo AT, Thierheimer ML, Babur Ö, Rocheleau AD, Huang T, Pang J, Rigg RA, Mitrugno A, Theodorescu D, and Burchard J**. Assessment of roles for the Rho-specific guanine nucleotide dissociation inhibitor Ly-GDI in platelet

function: a spatial systems approach. *American Journal of Physiology-Cell Physiology* 312: C527-C536, 2017.

191. **Bolte S, and Cordelières FP**. A guided tour into subcellular colocalization analysis in light microscopy. *Journal of microscopy* 224: 213-232, 2006.

192. **Manders E, Stap J, Brakenhoff G, Van Driel R, and Aten J**. Dynamics of three-dimensional replication patterns during the S-phase, analysed by double labelling of DNA and confocal microscopy. *Journal of cell science* 103: 857-862, 1992.

193. **Peters CG, Michelson AD, and Flaumenhaft R**. Granule exocytosis is required for platelet spreading: differential sorting of α-granules expressing VAMP-7. *Blood, The Journal of the American Society of Hematology* 120: 199-206, 2012.

194. **Itakura A, Aslan JE, Kusanto BT, Phillips KG, Porter JE, Newton PK, Nan X, Insall RH, Chernoff J, and McCarty OJ**. p21-Activated kinase (PAK) regulates cytoskeletal reorganization and directional migration in human neutrophils. *PLoS One* 8: e73063, 2013.

195. **Aslan JE, Itakura A, Haley KM, Tormoen GW, Loren CP, Baker SM, Pang J, Chernoff J, and McCarty OJ**. P21 activated kinase signaling coordinates glycoprotein receptor VI–mediated platelet aggregation, lamellipodia formation, and aggregate stability under shear. *Arteriosclerosis, thrombosis, and vascular biology* 33: 1544-1551, 2013.

196. **Aslan JE, Tormoen GW, Loren CP, Pang J, and McCarty OJT**. S6K1 and mTOR regulate Rac1-driven platelet activation and aggregation. *Blood* 118: 3129-3136, 2011.

197. **Wallisch M, Lorentz CU, Lakshmanan HH, Johnson J, Carris MR, Puy C, Gailani D, Hinds MT, McCarty OJ, and Gruber A**. Antibody inhibition of contact factor XII reduces platelet deposition in a model of extracorporeal membrane oxygenator perfusion in nonhuman primates. *Research and Practice in Thrombosis and Haemostasis* 4: 205-216, 2020.

198. **Baker SM, Phillips KG, and McCarty OJ**. Development of a label-free imaging technique for the quantification of thrombus formation. *Cellular and molecular bioengineering* 5: 488-492, 2012.

199. **Baker-Groberg SM, Phillips KG, and McCarty OJ**. Quantification of volume, mass, and density of thrombus formation using brightfield and differential interference contrast microscopy. *Journal of biomedical optics* 18: 016014, 2013.

200. **Sittampalam GS, Grossman A, Brimacombe K, Arkin M, Auld D, Austin CP, Baell J, Bejcek B, Caaveiro JM, and Chung TD**. Assay guidance manual [Internet]. 2004.

201. **Denzinger V, Busygina K, Jamasbi J, Pekrul I, Spannagl M, Weber C, Lorenz R, and Siess W**. Optimizing Platelet GPVI Inhibition versus Haemostatic Impairment by the Btk Inhibitors Ibrutinib, Acalabrutinib, ONO/GS-4059, BGB-3111 and Evobrutinib. *Thrombosis and haemostasis* 119: 397-406, 2019.

202. **Levade M, David E, Garcia C, Laurent PA, Cadot S, Michallet AS, Bordet JC, Tam C, Sie P, Ysebaert L, and Payrastre B**. Ibrutinib treatment affects collagen and von Willebrand factor-dependent platelet functions. *Blood* 124: 3991-3995, 2014.

203. **Li Z, Delaney MK, O'Brien KA, and Du X**. Signaling during platelet adhesion and activation. *Arteriosclerosis, thrombosis, and vascular biology* 30: 2341-2349, 2010.

204. **Bouaziz A, Amor NB, Woodard GE, Zibidi H, Lopez JJ, Bartegi A, Salido GM, and Rosado JA**. Tyrosine phosphorylation / dephosphorylation balance is involved in thrombin-evoked microtubular reorganisation in human platelets. *Thromb Haemost* 98: 375-384, 2007.

205. **Aslan JE, Phillips KG, Healy LD, Itakura A, Pang J, and McCarty OJ**. Histone deacetylase 6-mediated deacetylation of alpha-tubulin coordinates cytoskeletal and signaling events during platelet activation. *Am J Physiol Cell Physiol* 305: C1230-1239, 2013.

206. **Sadoul K**. New explanations for old observations: marginal band coiling during platelet activation. *J Thromb Haemost* 13: 333-346, 2015.

207. **Redondo PC, Harper AG, Sage SO, and Rosado JA**. Dual role of tubulin-cytoskeleton in store-operated calcium entry in human platelets. *Cell Signal* 19: 2147-2154, 2007.

208. **Cimmino G, Tarallo R, Conte S, Morello A, Pellegrino G, Loffredo FS, Cali G, De Luca N, Golino P, Trimarco B, and Cirillo P**. Colchicine reduces platelet aggregation by modulating cytoskeleton rearrangement via inhibition of cofilin and LIM domain kinase 1. *Vascul Pharmacol* 111: 62-70, 2018.

209. **Aslan JE, and McCarty OJ**. Rho GTPases in platelet function. *J Thromb Haemost* 11: 35-46, 2013.

210. **Kapeller R, Chakrabarti R, Cantley L, Fay F, and Corvera S**. Internalization of activated platelet-derived growth factor receptor-phosphatidylinositol-3' kinase complexes: potential interactions with the microtubule cytoskeleton. *Mol Cell Biol* 13: 6052-6063, 1993.

211. **Kapeller R, Toker A, Cantley LC, and Carpenter CL**. Phosphoinositide 3-kinase binds constitutively to alpha/beta-tubulin and binds to gamma-tubulin in response to insulin. *J Biol Chem* 270: 25985-25991, 1995.

212. **Bershadsky A, Chausovsky A, Becker E, Lyubimova A, and Geiger B**. Involvement of microtubules in the control of adhesion-dependent signal transduction. *Curr Biol* 6: 1279-1289, 1996.

213. **Zhang J, Fry MJ, Waterfield MD, Jaken S, Liao L, Fox JE, and Rittenhouse SE**. Activated phosphoinositide 3-kinase associates with membrane skeleton in thrombin-exposed platelets. *J Biol Chem* 267: 4686-4692, 1992.

214. **Aslan JE**. Platelet shape change. In: *Platelets in Thrombotic and Non-Thrombotic Disorders*, edited by Gresele P, López J, Kleiman N, and Page CSpringer, 2017.

215. **Tan S-L, Liao C, Lucas MC, Stevenson C, and DeMartino JA**. Targeting the SYK–BTK axis for the treatment of immunological and hematological disorders: recent progress and therapeutic perspectives. *Pharmacology & therapeutics* 138: 294-309, 2013.

216. **Matsubara S, Koya T, Takeda K, Joetham A, Miyahara N, Pine P, Masuda ES, Swasey CH, and Gelfand EW**. Syk activation in dendritic cells is essential for airway hyperresponsiveness and inflammation. *Am J Respir Cell Mol Biol* 34: 426-433, 2006.

217. **Honigberg LA, Smith AM, Sirisawad M, Verner E, Loury D, Chang B, Li S, Pan Z, Thamm DH, Miller RA, and Buggy JJ**. The Bruton tyrosine kinase inhibitor PCI-32765 blocks B-cell activation and is efficacious in models of autoimmune disease and B-cell malignancy. *Proc Natl Acad Sci U S A* 107: 13075-13080, 2010.

218. **Ghia P, Pluta A, Wach M, Lysak D, Kozak T, Simkovic M, Kaplan P, Kraychok I, Illes A, de la Serna J, Dolan S, Campbell P, Musuraca G, Jacob A, Avery E, Lee JH, Liang W, Patel P, Quah C, and Jurczak W**. ASCEND: Phase III, Randomized Trial of Acalabrutinib Versus Idelalisib Plus Rituximab or Bendamustine Plus Rituximab in Relapsed or Refractory Chronic Lymphocytic Leukemia. *J Clin Oncol* JCO1903355, 2020.

219. **Nicolson PLR, Hughes CE, Watson S, Nock SH, Hardy AT, Watson CN, Montague SJ, Clifford H, Huissoon AP, Malcor JD, Thomas MR, Pollitt AY, Tomlinson MG, Pratt G, and Watson SP**. Inhibition of Btk by Btk-specific concentrations of ibrutinib and acalabrutinib delays but does not block platelet aggregation mediated by glycoprotein VI. *Haematologica* 103: 2097-2108, 2018.

220. **Watson SP, Auger JM, McCarty OJ, and Pearce AC**. GPVI and integrin alphaIIb beta3 signaling in platelets. *J Thromb Haemost* 3: 1752-1762, 2005.

221. **Connell NT, and Berliner N**. Fostamatinib for the treatment of chronic immune thrombocytopenia. *Blood* 133: 2027-2030, 2019.

222. **Thorp BC, and Badoux X**. Atrial fibrillation as a complication of ibrutinib therapy: clinical features and challenges of management. *Leuk Lymphoma* 59: 311-320, 2018.

223. **Poole A, Gibbins J, Turner M, Van Vugt M, Van de Winkel J, Saito T, Tybulewicz V, and Watson S**. The Fc receptor γ-chain and the tyrosine kinase Syk are essential for activation of mouse platelets by collagen. *The EMBO journal* 16: 2333-2341, 1997.

224. **Kim E, Zhang H, Sivina M, Vaca A, Thompson PA, Jain N, Ferrajoli A, Estrov ZE, Keating MJ, Wierda WG, Rice WG, Andreeff M, and Burger JA**. CG-806, a First-in-Class Pan-FLT3/Pan-BTK Inhibitor, Exhibits Broad Signaling Inhibition in Chronic Lymphocytic Leukemia Cells. *Blood* 134: 3051-3051, 2019.

225. **Pasquet J-M, Gross B, Quek L, Asazuma N, Zhang W, Sommers CL, Schweighoffer E, Tybulewicz V, Judd B, and Lee JR**. LAT is required for tyrosine phosphorylation of phospholipase Cγ2 and platelet activation by the collagen receptor GPVI. *Molecular and cellular biology* 19: 8326-8334, 1999.

226. **Goldmann L, Duan R, Kragh T, Wittmann G, Weber C, Lorenz R, von Hundelshausen P, Spannagl M, and Siess W**. Oral Bruton tyrosine kinase inhibitors block activation of the platelet Fc receptor CD32a (FcgammaRIIA): a new option in HIT? *Blood Adv* 3: 4021-4033, 2019.

227. **Gross BS, Lee JR, Clements JL, Turner M, Tybulewicz VL, Findell PR, Koretzky GA, and Watson SP**. Tyrosine phosphorylation of SLP-76 is downstream of Syk following stimulation of the collagen receptor in platelets. *Journal of Biological Chemistry* 274: 5963-5971, 1999.

228. **Zaro BW, Vinogradova EV, Lazar DC, Blewett MM, Suciu RM, Takaya J, Studer S, de la Torre JC, Casanova JL, Cravatt BF, and Teijaro JR**. Dimethyl Fumarate Disrupts Human Innate Immune Signaling by Targeting the IRAK4-MyD88 Complex. *J Immunol* 202: 2737-2746, 2019.

229. **Walford T, Musa FI, and Harper AG**. Nicergoline inhibits human platelet Ca(2+) signalling through triggering a microtubule-dependent reorganization of the platelet ultrastructure. *Br J Pharmacol* 173: 234-247, 2016.

230. **Tardif JC, Kouz S, Waters DD, Bertrand OF, Diaz R, Maggioni AP, Pinto FJ, Ibrahim R, Gamra H, Kiwan GS, Berry C, Lopez-Sendon J, Ostadal P, Koenig W, Angoulvant D, Gregoire JC, Lavoie MA, Dube MP, Rhainds D, Provencher M, Blondeau L, Orfanos A, L'Allier PL, Guertin MC, and Roubille F**. Efficacy and Safety of Low-Dose Colchicine after Myocardial Infarction. *N Engl J Med* 381: 2497-2505, 2019.

231. **Shah B, Allen N, Harchandani B, Pillinger M, Katz S, Sedlis SP, Echagarruga C, Samuels SK, Morina P, Singh P, Karotkin L, and Berger JS**. Erratum to:

Effect of Colchicine on Platelet-Platelet and Platelet-Leukocyte Interactions: a Pilot Study in Healthy Subjects. *Inflammation* 39: 501, 2016.

232. **Pandey MK, Gowda K, Sung SS, Abraham T, Budak-Alpdogan T, Talamo G, Dovat S, and Amin S**. A novel dual inhibitor of microtubule and Bruton's tyrosine kinase inhibits survival of multiple myeloma and osteoclastogenesis. *Exp Hematol* 53: 31-42, 2017.

233. **Zorba A, Nguyen C, Xu Y, Starr J, Borzilleri K, Smith J, Zhu H, Farley KA, Ding W, Schiemer J, Feng X, Chang JS, Uccello DP, Young JA, Garcia-Irrizary CN, Czabaniuk L, Schuff B, Oliver R, Montgomery J, Hayward MM, Coe J, Chen J, Niosi M, Luthra S, Shah JC, El-Kattan A, Qiu X, West GM, Noe MC, Shanmugasundaram V, Gilbert AM, Brown MF, and Calabrese MF**. Delineating the role of cooperativity in the design of potent PROTACs for BTK. *Proc Natl Acad Sci U S A* 115: E7285-E7292, 2018.

234. **Gabizon R, Shraga A, Gehrtz P, Livnah E, Shorer Y, Gurwicz N, Avram L, Unger T, Aharoni H, Albeck S, Brandis A, Shulman Z, Katz BZ, Herishanu Y, and London N**. Efficient Targeted Degradation via Reversible and Irreversible Covalent PROTACs. *J Am Chem Soc* 2020.

235. **Busygina K, Jamasbi J, Seiler T, Deckmyn H, Weber C, Brandl R, Lorenz R, and Siess W**. Oral Bruton tyrosine kinase inhibitors selectively block atherosclerotic plaque-triggered thrombus formation in humans. *Blood* 131: 2605-2616, 2018.

236. **Aslan JE**. Platelet Proteomes, Pathways, and Phenotypes as Informants of Vascular Wellness and Disease. *Arterioscler Thromb Vasc Biol* ATVBAHA120314647, 2021.

237. **Parra-Izquierdo I, and Aslan JE**. Perspectives on platelet heterogeneity and host immune response in COVID-19. *Seminars in Thrombosis and Hemostasis* 2020.

238. **Wendelboe AM, and Raskob GE**. Global burden of thrombosis: epidemiologic aspects. *Circulation research* 118: 1340-1347, 2016.

239. **Herrington W, Lacey B, Sherliker P, Armitage J, and Lewington S**. Epidemiology of atherosclerosis and the potential to reduce the global burden of atherothrombotic disease. *Circulation research* 118: 535-546, 2016.

240. **Ahmad FB, and Anderson RN**. The leading causes of death in the US for 2020. *JAMA* 325: 1829-1830, 2021.

241. **Tomaiuolo M, Brass LF, and Stalker TJ**. Regulation of platelet activation and coagulation and its role in vascular injury and arterial thrombosis. *Interventional cardiology clinics* 6: 1, 2017.

242. **Podrez EA, Byzova TV, Febbraio M, Salomon RG, Ma Y, Valiyaveettil M, Poliakov E, Sun M, Finton PJ, and Curtis BR**. Platelet CD36 links hyperlipidemia, oxidant stress and a prothrombotic phenotype. *Nature medicine* 13: 1086-1095, 2007.

243. **Yang M, Li W, Harberg C, Chen W, Yue H, Ferreira RB, Wynia-Smith SL, Carroll KS, Zielonka J, Flaumenhaft R, Silverstein RL, and Smith BC**. Cysteine sulfenylation by CD36 signaling promotes arterial thrombosis in dyslipidemia. *Blood Advances* 4: 4494-4507, 2020.

244. **Yang M, Kholmukhamedov A, Schulte ML, Cooley BC, Scoggins NiO, Wood JP, Cameron SJ, Morrell CN, Jobe SM, and Silverstein RL**. Platelet CD36 signaling through ERK5 promotes caspase-dependent procoagulant activity and fibrin deposition in vivo. *Blood Advances* 2: 2848-2861, 2018.

245. **Ghosh A, Li W, Febbraio M, Espinola RG, McCrae KR, Cockrell E, and Silverstein RL**. Platelet CD36 mediates interactions with endothelial cell–derived microparticles and contributes to thrombosis in mice. *The Journal of clinical investigation* 118: 1934-1943, 2008.

246. **Chen K, Febbraio M, Li W, and Silverstein RL**. A specific CD36-dependent signaling pathway is required for platelet activation by oxidized low-density lipoprotein. *Circulation research* 102: 1512-1519, 2008.

247. **Magwenzi S, Woodward C, Wraith KS, Aburima A, Raslan Z, Jones H, McNeil C, Wheatcroft S, Yuldasheva N, and Febbriao M**. Oxidized LDL activates blood platelets through CD36/NOX2–mediated inhibition of the cGMP/protein kinase G signaling cascade. *Blood, The Journal of the American Society of Hematology* 125: 2693-2703, 2015.

248. **Wraith KS, Magwenzi S, Aburima A, Wen Y, Leake D, and Naseem KM**. Oxidized low-density lipoproteins induce rapid platelet activation and shape change through tyrosine kinase and Rho kinase–signaling pathways. *Blood, The Journal of the American Society of Hematology* 122: 580-589, 2013.

249. **Schoenwaelder SM, Yuan Y, Josefsson EC, White MJ, Yao Y, Mason KD, O'Reilly LA, Henley KJ, Ono A, and Hsiao S**. Two distinct pathways regulate platelet phosphatidylserine exposure and procoagulant function. *Blood, The Journal of the American Society of Hematology* 114: 663-666, 2009.

250. **Thiagarajan P, and Tait J**. Binding of annexin V/placental anticoagulant protein I to platelets. Evidence for phosphatidylserine exposure in the procoagulant response of activated platelets. *Journal of Biological Chemistry* 265: 17420-17423, 1990.

251. **Patrono C, Morais J, Baigent C, Collet J-P, Fitzgerald D, Halvorsen S, Rocca B, Siegbahn A, Storey RF, and Vilahur G**. Antiplatelet agents for the treatment

and prevention of coronary atherothrombosis. *Journal of the American College of Cardiology* 70: 1760-1776, 2017.

252. **Mehran R, Baber U, Sharma SK, Cohen DJ, Angiolillo DJ, Briguori C, Cha JY, Collier T, Dangas G, and Dudek D**. Ticagrelor with or without aspirin in high-risk patients after PCI. *New England Journal of Medicine* 381: 2032-2042, 2019.

253. **Johnston SC, Amarenco P, Denison H, Evans SR, Himmelmann A, James S, Knutsson M, Ladenvall P, Molina CA, and Wang Y**. Ticagrelor and aspirin or aspirin alone in acute ischemic stroke or TIA. *New England Journal of Medicine* 383: 207-217, 2020.

254. **McFadyen JD, Schaff M, and Peter K**. Current and future antiplatelet therapies: emphasis on preserving haemostasis. *Nature Reviews Cardiology* 15: 181-191, 2018.

255. **Mitrugno A, Sylman JL, Ngo AT, Pang J, Sears RC, Williams CD, and McCarty OJ**. Aspirin therapy reduces the ability of platelets to promote colon and pancreatic cancer cell proliferation: Implications for the oncoprotein c-MYC. *American Journal of Physiology-Cell Physiology* 2017.

256. **Aslan JE, Tormoen GW, Loren CP, Pang J, and McCarty OJ**. S6K1 and mTOR regulate Rac1-driven platelet activation and aggregation. *Blood, The Journal of the American Society of Hematology* 118: 3129-3136, 2011.

257. **Korporaal SJ, Van Eck M, Adelmeijer J, Ijsseldijk M, Out R, Lisman T, Lenting PJ, Van Berkel TJ, and Akkerman J-WN**. Platelet activation by oxidized low density lipoprotein is mediated by CD36 and scavenger receptor-A. *Arteriosclerosis, thrombosis, and vascular biology* 27: 2476-2483, 2007.

258. **Huang M-M, Bolen JB, Barnwell JW, Shattil SJ, and Brugge JS**. Membrane glycoprotein IV (CD36) is physically associated with the Fyn, Lyn, and Yes protein-tyrosine kinases in human platelets. *Proceedings of the National Academy of Sciences* 88: 7844-7848, 1991.

259. **Yang M, Cooley BC, Li W, Chen Y, Vasquez-Vivar J, Scoggins NiO, Cameron SJ, Morrell CN, and Silverstein RL**. Platelet CD36 promotes thrombosis by activating redox sensor ERK5 in hyperlipidemic conditions. *Blood, The Journal of the American Society of Hematology* 129: 2917-2927, 2017.

260. **Busygina K, Denzinger V, Bernlochner I, Weber C, Lorenz R, and Siess W**. Btk Inhibitors as First Oral Atherothrombosis-Selective Antiplatelet Drugs? *Thromb Haemost* 119: 1212-1221, 2019.

261. **Nemerovski CW, Salinitri FD, Morbitzer KA, and Moser LR**. Aspirin for primary prevention of cardiovascular disease events. *Pharmacotherapy: The Journal of Human Pharmacology and Drug Therapy* 32: 1020-1035, 2012.

262. **Johnson TW, Baos S, Collett L, Hutchinson JL, Nkau M, Molina M, Aungraheeta R, Reilly-Stitt C, Bowles R, and Reeves BC**. Pharmacodynamic comparison of ticagrelor monotherapy versus ticagrelor and aspirin in patients after percutaneous coronary intervention: the TEMPLATE (Ticagrelor Monotherapy and Platelet Reactivity) randomized controlled trial. *Journal of the American Heart Association* 9: e016495, 2020.

263. **Carabello BA, and Paulus WJ**. Aortic stenosis. *The lancet* 373: 956-966, 2009.

264. **Chambers J**. Aortic stenosis. British Medical Journal Publishing Group, 2005, p. 801-802.

265. **Carabello BA**. Introduction to aortic stenosis. *Circulation research* 113: 179-185, 2013.

266. **Patrick PH**. TAVR and SAVR: current treatment of aortic stenosis. *Clinical Medicine Insights: Cardiology* 6: CMC. S7540, 2012.

267. **De Marchena E, Mesa J, Pomenti S, Marin y Kall C, Marincic X, Yahagi K, Ladich E, Kutys R, Aga Y, and Ragosta M**. Thrombus formation following transcatheter aortic valve replacement. *JACC: Cardiovascular Interventions* 8: 728-739, 2015.

268. **Puri R, Auffret V, and Rodés-Cabau J**. Bioprosthetic valve thrombosis. *Journal of the American College of Cardiology* 69: 2193-2211, 2017.

269. **Chakravarty T, Søndergaard L, Friedman J, De Backer O, Berman D, Kofoed KF, Jilaihawi H, Shiota T, Abramowitz Y, and Jørgensen TH**. Subclinical leaflet thrombosis in surgical and transcatheter bioprosthetic aortic valves: an observational study. *The Lancet* 389: 2383-2392, 2017.

270. **Bates NM, Puy C, Jurney PL, McCarty OJ, and Hinds MT**. Evaluation of the effect of crosslinking method of poly (vinyl alcohol) hydrogels on thrombogenicity. *Cardiovascular engineering and technology* 11: 448-455, 2020.

Biographical Sketch

NAME: Tony Zheng

eRA COMMONS USERNAME: zhengto

POSITION TITLE: MD/PhD Candidate

EDUCATION/TRAINING

INSTITUTION AND LOCATION	DEGREE	COMPLETION
Johns Hopkins University; Baltimore, MD	Bachelor	06/2015
Johns Hopkins University; Baltimore, MD	Masters	06/2017
Oregon Health & Science University; Portland, OR	MD/PhD	06/2022 (PhD) In Progress (MD)

Personal Statement

As a future physician scientist (MD/PhD), it is my greatest desire to dedicate my career and life working at the intersection of medicine and research as a leader in academic medicine. I aspire to not only make new discoveries as a scientist, but to utilize such discoveries as an engineer and physician to innovate biomedical tools to treat patients. My goal is to bridge such scientific advances into the clinic and improve patient care through new technologies and scientific knowledge for diagnosis, therapeutics, and treatment.

My interest in research and medicine began during my undergraduate studies at Johns Hopkins University. As a biomedical engineering student, I conducted research with Dr. Steven Zeiler MD PhD, investigating post-stroke recovery and brain plasticity. I learned about the scientific process and was also fortunate to have the opportunity to shadow Dr. Zeiler and his team in the neurology intensive care unit, tending to stroke patients. This culminated into not only a publication (Zeiler et al. *Neurorehabilitation and Neural Repair* 2016), but more importantly a strong desire to treat patients and do research. This dual experience sparked my aspiration for a career path as a physician scientist. I was drawn to the harmonizing relationship of a dual degree as patient interactions raise important questions and shine a new light on critical medical issues. And in turn, research strives to directly improve our scientific knowledge to answer these questions and help the lives of patients.

After graduating, I remained at Hopkins and immersed myself in research. I worked for two years as a graduate research student under the mentorship of Dr. Jeff Wang, PhD. I led a project with an interdisciplinary team in collaboration with an international company, DuPont Pioneer and developed a microfluidic device for high throughput genotyping. I gained a true passion for research and was intimately involved in every step of the scientific process: hypothesis formation, device development and testing, troubleshooting, data collection and analysis, presentations, and manuscript preparation (Zec H, Zheng T, et al. *Microsystems & Microengineering* 2018). These experiences formed the foundation of my

growing physician scientist career path and compelled me to pursue both a medical and scientific education at Oregon Health & Science University (OHSU).

As a doctoral student under the co-mentorship of Owen McCarty, PhD and Joseph Aslan, PhD at OHSU, I am studying the role of platelet tyrosine kinases in atherosclerosis. In my first project, I evaluated a panel of tyrosine kinase inhibitors (TKIs) targeting Spleen tyrosine kinase (Syk) and Bruton's tyrosine kinase (BTK) and their effects on platelet function. This work is published in the *American Journal of Physiology: Cell Physiology* (PMID: 33689480) and served as the foundation for my proposal in an awarded Predoctoral NRSA F30 fellowship (Impact Score: 19). Building off of my work on TKIs, I am now investigating the potential use of these inhibitors on oxidized LDL enhanced platelet procoagulant activity. This work is currently in submission in the journal *Blood Advances*. Lastly, I have also co-authored numerous publications, including proteomics study of platelet activation GPVI pathways in the journal *Blood* (PMID: 32640021) and others listed below. Upon completion of my PhD dissertation, I will finish my medical program and apply for a medical residency that will allow me to fully train as a physician scientist and translate my research to benefit patients. With this dual scientific and medical training, I hope to bridge research into the clinic and make the greatest impact on the practice of physicians and the lives of patients.

Publications

Peer Reviewed -Accepted/Completed (Chronological)

1. Zeiler SR, Hubbard R, Gibson EM, **Zheng T**, Ng K, O'Brien R, Krakauer JW. Paradoxical Motor Recovery from a First Stroke after Induction of a Second Stroke: Reopening a Postischemic Sensitive Period. Neurorehabil Neural Repair. 2016 Sep; 30(8):794-800.

2. Zec, H., **Zheng, T**, Liu, L., Hsieh, K., Rane, T., Pederson, T., Wang, T.H. "Programmable Microfluidic Genotyping of Plant DNA Samples for Marker-Assisted Selection." Microsystems & Nanoengineering 2018; 4:17097.

3. Babur Ö, Melrose AR, Cunliffe JM, Klimek J, Pang J, Sepp AI, Zilberman-Rudenko J, Tassi Yunga S, **Zheng T**, Parra-Izquierdo I, Minnier J, McCarty OJT, Demir E, Reddy AP, Wilmarth PA, David LL, Aslan JE. Phosphoproteomic quantitation and causal analysis reveal pathways in GPVI/ITAM-mediated platelet activation programs. Blood. 2020 Nov 12; 136(20):2346-2358.

4. **Zheng TJ**, Lofurno ER, Melrose AR, Lakshmanan HHS, Pang J, Phillips KG, Fallon ME, Kohs TCL, Ngo ATP, Shatzel JJ, Hinds MT, McCarty OJT, Aslan JE. Assessment of the effects of Syk and BTK inhibitors on GPVI-mediated platelet signaling and function. Am J Physiol Cell Physiol. 2021 Mar 10.

5. Parra-Izquierdo I, Lakshmanan HHS, Melrose AR, Pang J, **Zheng TJ**, Jordan KR, Reitsma SE, McCarty OJT, Aslan JE. The Toll-like receptor 2 ligand Pam2CSK4 activates platelet nuclear factor κB and Bruton's tyrosine kinase signaling to promote platelet-endothelial cell interactions. Frontiers in Immunology (2021): 3492.

6. Kohs TCL, Olson SR, Pang J, Jordan KR, **Zheng TJ**, Xie A, Hodovan J, Muller M, McArthur C, Johnson J, Sousa BB, Wallisch M, Kievit P, Aslan JE, Seixas JD, Bernardes GJL, Hinds MT, Lindner JR, McCarty OJT, Puy C, Shatzel JJ. Ibrutinib inhibits BMX-dependent endothelial VCAM-1 expression in vitro and pro-atherosclerotic endothelial activation and platelet in vivo. Journal of Cellular and Molecular Bioengineering. (2022): 1-13.

7. Lakshmanan HHS, Estonilo A, Reitsma SE, Melrose AR, Subramanian J, **Zheng TJ,** Maddala J, Gruber A, Gailani D, McCarty OJT, Jurney PL, Puy C. Revised model of the tissue factor pathway of thrombin generation: role of feedback activation of FXI. Journal of Thrombosis and Hemostasis. (2022).

Peer Reviewed – In Submission

8. **Zheng TJ**, Kohs TCL, Pang J, Reitsma SE, Parra-Izquierdo I, Melrose AR, Larson MK, Williams CD, Hinds MT, McCarty OJT, Aslan JE. Effect of antiplatelet agents and tyrosine kinase inhibitors on oxLDL-mediated procoagulant platelet activity. Blood Advances. Submitted January 2022. Response to Reviewers.

9. **Zheng TJ,** Parra-Izquierdo I, Reitsma SE, Heinrich MC, Larson MK, Shatzel JJ, Aslan JE, McCarty OJT. Platelets and tyrosine kinase inhibitors: clinical features, mechanism of action and effects on physiology. American Journal of Physiology – Cell Physiology. Submitted January 2022. Response to Reviewers.

Conferences – Posters & Talks (Chronological)

10. **Zheng, T.,** Zec, H., Hsieh, K., Kaushik, A., Axt, B., Hsieh, Y., Wang, T.H. (2016). "Silicone Oil Improves Small Molecule Retention for Droplet-Based Bioassays." Presented at Twentieth International Conference on Miniaturized Systems for Chemistry and Life Sciences, Dublin, Ireland.

11. Axt, B., Hsieh, Y., Zec, H., Hsieh, K., **Zheng, T.,** Kaushik, A., Wang, T.H. (2016). "Fully Automated Operation of Microfluidic Device with Impedance Based Valve Control." Presented at Twentieth International Conference on Miniaturized Systems for Chemistry and Life Sciences, Dublin, Ireland.

12. **Zheng, T.**, Lofurno, E., Elgamal, S., Melrose, A., Pang, J., Shatzel, J., McCarty O., Aslan, J. (2019). "Tyrosine Kinase Inhibitors (TKIs) Targeting Syk and BTK Signaling Differentially Affect PI3K Signalosome Organization and Platelet Function." Presented at American Society of Hematology (ASH) Conference, Orlando, Florida.

13. **Zheng, T.**, Lofurno, E., Melrose, A., Pang, J., Shatzel, J., McCarty, O., Aslan, J. (2020). "Tyrosine Kinase Inhibitors (TKIs) Targeting Syk and BTK Signaling Differentially Affect PI3K Organization and Inhibit Platelet Function." Presented at International Society of Thrombosis and Hemostasis (ISTH) Conference, Milan, Italy (Virtual).

14. **Zheng TJ**, Lofurno ER, Melrose AR, Lakshmanan HHS, Pang J, Phillips KG, Fallon, ME, Kohs TCL, Ngo ATP, Shatzel JJ, Hinds MT, McCarty OJT., Aslan JE (July 2021). "Assessment of the effects of Syk and BTK inhibitors on GPVI-mediated platelet signaling and function." Presented at

International Society of Thrombosis and Hemostasis (ISTH) Conference, Philadelphia, Pennsylvania (Virtual).

15. Lakshmanan HHS, Reitsma SE, **Zheng TJ**, Melrose AR, Estonilo A, Maddala J, Gailani D, Shatzel JJ, Gruber A, Jurney PL, McCarty OJT., Puy C (July 2021). "Refine and validate a model of FXI activation and activity in thrombin generation and blood coagulation." Presented at International Society of Thrombosis and Hemostasis (ISTH) Conference, Philadelphia, Pennsylvania (Virtual).

16. Nguyen NDQ, Melrose AR, Parra-Izquierdo I, **Zheng TJ**, Lakshmanan HHS, Pang J, McCarty OJT, Aslan JE (July 2021). "Expression and localization of Rab GTPase proteins in platelets." Presented at International Society of Thrombosis and Hemostasis (ISTH) Conference, Philadelphia, Pennsylvania (Virtual).

17. Kohs TCL, **Zheng TJ**, Parra-Izquierdo I, Olson SR, Xie A, Hodovan J, Muller M, McArthur C, Johnson J, Wallisch M, Lorentz C, Verbout N, Kievit P, Larson M, Aslan J, Puy C, Lindner J, McCarty O, Shatzel J (July 2021). "The Role of TEC Family Kinases in oxLDL-mediated Platelet Activity in vitro and Platelet and Endothelial Dysfunction in vivo" Presented at International Society of Thrombosis and Hemostasis (ISTH) Conference, Philadelphia, Pennsylvania (Virtual).

18. Lakshmanan HHS, Reitsma SE, **Zheng TJ**, Subramanian J, Melrose AR, Estonilo A, Maddala J, Gruber A, Gailani D, Jurney PL , Puy C McCarty OJT (October 2021). "An integrative biology approach to study the role of long-chain polyphosphate in catalyzing thrombin generation." Presented at PolyP Day at University of Georgia (Virtual).

19. **Zheng TJ**, Kohs TCL, Pang J, Reitsma SE, Parra-Izquierdo I, Melrose AR, Larson MK, Williams CD, Hinds MT, McCarty OJT, Aslan JE. Effect of antiplatelet agents and tyrosine kinase inhibitors on oxLDL-mediated procoagulant platelet activity. Talk awarded at Vascular Discovery: From Genes to Medicine Scientific Sessions 2022.

20. **Zheng TJ,** Kohs TCL, Pang J, Reitsma SE, Parra-Izquierdo I, Melrose AR, Larson MK, Williams CD, Hinds MT, McCarty OJT, Aslan JE. P2Y receptor antagonists and tyrosine kinase inhibitors reduce oxLDL-mediated procoagulant activity (July 2022) Presented at International Society of Thrombosis and Hemostasis (ISTH) Conference, London, UK.

Grants Awarded

NIH/NHLBI, F30 HL 158079 Jul 1, 2021 – June 30, 2025
Title: "Role of Platelet Bruton's Tyrosine Kinase in Atherosclerosis"
Direct costs, annual budget: $51,036